THESIS

DAM OVERTOPPING AND FLOOD ROUTING WITH THE TREX WATERSHED MODEL

Submitted by

Andrew Steininger

Department of Civil and Environmental Engineering

In partial fulfillment of the requirements

For the Degree of Master of Science

Colorado State University

Fort Collins, Colorado

Spring 2014

Master's Committee:

Advisor: Pierre Y. Julien

Jeffrey Niemann
Stephanie Kampf

ABSTRACT

DAM OVERTOPPING AND FLOOD ROUTING

WITH THE TREX WATERSHED MODEL

Modeling dam overtopping and flood routing downstream of reservoirs can provide basic information about the magnitudes of flood events that can be beneficial in dam engineering, emergency action planning, and floodplain management. In recent years there has been considerable progress in computer model code development, computing speed and capability, and available elevation, vegetation, soil type, and land use data which has led to much interest in multi-dimensional modeling of dam failure, overtopping, and flood routing at the watershed scale.

The purpose of this study is to ascertain the capability of the Two-dimensional, Runoff, Erosion and Export (TREX) model to simulate flooding from dam overtopping as the result of large scale precipitation events. The model has previously been calibrated for the California Gulch watershed near Leadville Colorado and was used for all of the simulations preformed for this study. TREX can simulate the reservoir filling and overtopping process by inserting an artificial dam into the digital elevation model (DEM) of a watershed.

To test the numerical stability of the model for large precipitation events, point source hydrographs were input to the model and the Courant-Friedrichs-Lewy (CFL) condition was used to determine the maximum numerically stable time steps. Point sources as large as 50,000 m^3/s were stably routed utilizing a model time step as small as

0.004 seconds. Additionally the effects of large flows on the flood plain were analyzed using point source hydrographs. The areal extent of floodplain inundation was mapped and the total areal extent of flooding was quantified.

The attenuation of watershed outlet discharge due to upstream dams was analyzed. Three probable maximum precipitation (PMP) events and three estimated global maximum precipitation (GMP) events (the 1 hour, 6 hour, and 24 hour duration events), were simulated. Larger duration rainstorms had lower rainfall intensities but larger runoff volumes. A series of artificial dams ranging from 5 to 29 meters high were inserted into the DEM in sequential simulations and the attenuation of the downstream flood wave was quantified. The maximum attenuation of the peak discharge at the outlet of the watershed was 63% for an 18 meter high rectangular dam for the 1 hour PMP event, 58 % for a 20 meter high dam for the 6 hour PMP event, and 46% for a 29 meter high dam for the 24 hour duration PMP event. The same analysis was done using estimated global maximum precipitation (GMP) events. The maximum attenuation of the peak discharge at the outlet of the watershed was 59% for a 23 meter high rectangular dam for the 1 hour GMP event, 21 % for a 29 meter high dam for the 6 hour GMP event, and 9% for a 29 meter high dam for the 24 hour duration GMP event.

ACKNOWLEDGMENTS

I would like to thank everyone who helped me both directly and indirectly with my thesis work that is presented here. The support that I've received in both a scholarly sense and in my personal life has greatly helped me in my pursuit of a civil engineering degree from Colorado State University.

Thanks firstly to my advisor Dr. Pierre Julien who allocated the necessary funding for my research and provided me with direction and advice to accomplish this research work. Thanks also to my peers within the civil engineering department and specifically within Dr. Julien's group. Thanks to Jazuri Abdullah and Jaehoon Kim for their routine help with my research. Thanks also to Mark Velluex for the help I received while learning to operate the model used for my research.

Thanks also to the Department of Defense Center for Geosciences and Atmospheric Research (CGAR) for the funding that was provided for this research and for the opportunities granted within this research group.

Finally thanks to those of my friends and family who helped me along the way with words of wisdom and motivation. This support provided much needed perspective and inspiration along the way.

TABLE OF CONTENTS

ABSTRACT II

ACKNOWLEDGMENTS IV

TABLE OF CONTENTS V

LIST OF TABLES VIII

LIST OF FIGURES IX

CHAPTER I. INTRODUCTION 1

SECTION 1.1 OVERVIEW 1

1.1.1 DAM BREACH AND OVER TOPPING (THE PROBLEM) 2

1.1.2 MODELING DAM OVERTOPPING AND FLOOD ROUTING 4

SECTION 1.2 OBJECTIVES 4

CHAPTER II. LITERATURE REVIEW 5

SECTION 2.1 DAM BREACH MODELING TECHNIQUES OVERVIEW 5

2.1.1 DAM BREACH EMPIRICAL MODELS 5

2.1.2 DAM BREAK ANALYTICAL MODELS 9

2.1.3 DAM BREACH COMPUTER MODELS 11

2.1.4 WATERSHED COMPUTER MODELS 13

CHAPTER III. THE TWO-DIMENSIONAL RUNOFF EROSION AND EXPORT MODEL 17

SECTION 3.1 TREX CONCEPTUAL MODEL 17

SECTION 3.2 HYDROLOGIC PROCESS DESCRIPTIONS 18

3.2.1 PRECIPITATION AND INTERCEPTION 18

3.2.2 Infiltration and Transmission Loss 20
3.2.3 Storage 21
3.2.3 Overland and Channel Flow 22
Section 3.3 Numerical Method 25
CHAPTER IV. CALIFORNIA GULCH MODEL CONFIGURATION 27
Section 4.1 Overview and Site Description 27
Section 4.3 Digital Elevation Model 29
Section 4.4 Land Use 32
Section 4.5 Soil and Sediment Types 33
Section 4.6 Overview of Work Done at California Gulch 34
Section 4.7 Calibration and Validation 35
CHAPTER V. FLOOD ROUTING, POINT SOURCE SIMULATION 38
Section 5.1 Overview of Work 38
Section 5.2 Model Stability and Time Step Analysis Methods 39
Section 5.3 Empirical Relationships and Examples 47
Section 5.4 Areal Extent of Flood Plain Inundation 50
Section 5.5 Discussion of Results 56
CHAPTER VI. OVERTOPPING MODELING 60
Section 6.1 Overview of Work 60
Section 6.2 Dam Possibilities and Locations 60
Section 6.3 Effects of Dams on Outlet Hydrographs 63
6.3.1 Probable Maximum Precipitation Simulation Analysis Methods 63

6.3.2 GLOBAL MAXIMUM PRECIPITATION SIMULATION ANALYSIS METHODS 70

SECTION 6.4 DISCUSSION OF RESULTS 76

CHAPTER VII. CONCLUSIONS 78

SECTION 7.1 CONCLUSIONS ABOUT TREX OVERTOPPING MODELING AND FLOOD ROUTING 78

REFERENCES 81

APPENDICES 84

APPENDIX 1.0 PROBABLE MAXIMUM PRECIPITATION MAPS 84

APPENDIX 2.0 COMPARISON OF POPULAR HYDROLOGIC MODELS 87

LIST OF TABLES

Table 1.1: Selected dam failures (Association of Dam Safety Officials) 2

Table 2.1: Summary of dam breach hydrograph empirical relationships (Thornton et al. 2011) 7

Table 2.2: Physically-based embankment breach parameters (Wahl 1998) 11

Table 5.1: Multi-watershed time step stability data 46

Table 6.1: Summary of PMP simulation results 70

Table 6.2: Summary of GMP simulation results 76

LIST OF FIGURES

Figure 1.1: Relative number of dam failures due to a variety of mechanisms 3

Figure 2.1: Dam failure data sets (Thornton et al. 2011) 7

Figure 2.2: Predicted time of failure vs. observed time of failure 9

Figure 3.1: TREX conceptual model structure and simulated processes 18

Figure 4.1: Study site location, California Gulch, Colorado (Velleux 2005) 27

Figure 4.2: California Gulch watershed and Leadville Colorado 28

Figure 4.3: California Gulch digital elevation model 30

Figure 4.4: California Gulch aspect map 31

Figure 4.5: California Gulch slope map 31

Figure 4.6: California Gulch link map 32

Figure 4.7: California Gulch land use type map 33

Figure 4.8: California Gulch soil type map 34

Figure 4.9: California Gulch gaging stations 35

Figure 4.10: California Gulch hydrologic calibration 36

Figure 4.11: California Gulch hydrologic validation 37

Figure 5.1: Typical approximated point source hydrograph 38

Figure 5.2: Numerical model domains (Schär 2014) 40

Figure 5.3: TREX, California Gulch point source stability 41

Figure 5.4: Model stability watershed comparison (Kim 2012) (Abdullah 2013) 45

Figure 5.5: 5 meter high dam breach simulation. 50

Figure 5.6: 4,000 m^3/s point source 52

Figure 5.7: 4,000 m^3/s point source (zoom 1) 53

Figure 5.8: 4,000 m^3/s point source (zoom 2) 54

Figure 5.9: 4,000 m^3/s point source floodplain inundation at selected time steps, (depth ≥ 1 meter) 55

Figure 5.10: 7,000 m^3/s point source floodplain inundation 56

Figure 6.1: Rectangular and Triangular profile dam examples as seen from above 61

Figure 6.2: California Gulch artificial dam site location 62

Figure 6.3: Three-dimensional dam representation 62

Figure 6.4: Overtopping simulation 64

Figure 6.5: Example model output 65

Figure 6.6: 1 hour duration PMP outlet discharge 67

Figure 6.7: 1 hour duration PMP peak outlet discharge vs. dam height 67

Figure 6.8: 6 hour duration PMP outlet discharge 68

Figure 6.9: 6 hour duration PMP peak outlet discharge vs. dam height 68

Figure 6.10: 24 hour duration PMP outlet discharge 69

Figure 6.11: 24 hour duration PMP peak outlet discharge vs. dam height 69

Figure 6.12: World's greatest measured precipitation 71

Figure 6.13: 1 hour duration GMP outlet discharge 73

Figure 6.14: 1 hour duration GMP peak outlet discharge vs. dam height 73

Figure 6.15: 6 hour duration GMP outlet discharge 74

Figure 6.16: 6 hour duration GMP peak outlet discharge vs. dam height 74

Figure 6.17: 24 hour duration GMP outlet discharge 75

Figure 6.18: 24 hour duration GMP peak outlet discharge vs. dam height 75

LIST OF SYMBOLS

A_c = cross sectional area of flow

A_s = surface area over which the precipitation occurs

B_x,B_y = flow width in the x- or y- direction

c =celerity

C = Courant number

D_c = dam crest height

dt = time step for numerical integration

dx = modeled raster cell size

E = evaporation rate

f = infiltration rate

F = cumulative (total) infiltrated water depth

g = gravitational acceleration

h = surface water depth

h_d = drop in reservoir surface level

H_c = capillary pressure (suction) head at the wetting front

H_d = Height of a dam

H_w = hydrostatic pressure head (depth of water in channel)

H_b = Height of the water behind the dam

i = precipitation rate

i_n = net effective precipitation rate

k_b = mean erosion rate of a dam breach

K_h = effective hydraulic conductivity

L = embankment length

n = Manning roughness coefficient

P_c = wetted perimeter of channel flow

q_l = lateral unit discharge (into or out of the channel)

q_x, q_y = unit discharge in the x- or y- direction = Q_x/B_x, Q_y/B_y

Q_x, Q_y = flow in the x- or y- direction

Q = total discharge

Q_p = peak discharge

R_h = hydraulic radius of flow = A_c/P_c

S_{fx}, S_{fy} = friction slope in the x- or y- direction

S_{0x}, S_{0y} = ground surface slope in the x- or y- direction

$s\big|_{t+dt}$ = value of the model state variable at time t + dt

$s\big|_{t}$ = value of the model state variable at time t

S_i = interception capacity of projected canopy per unit area

S_e = effective soil saturation

t = time

t_f = time of dam failure

t_l = transmission loss rate

t_p = time to peak discharge

t_r = precipitation duration

T = cumulative (total) depth of water transported by transmission loss

u = flow velocity

V_s = volume of water stored behind the dam at capacity

V_i = interception volume

V_g = gross precipitation water volume

V_n = net precipitation

W = unit discharge from/to a point source/sink

W_{ave} = average embankment width

α_x, α_y = resistance coefficient for flow in the x- or y- direction

β = resistance exponent = 5/3

$\left.\frac{\partial s}{\partial t}\right|_t$ = value of model state variable derivative at time t

Φ = total soil porosity

Θ_e = effective soil porosity = $(\phi - \theta_r)$

θ_r = residual soil moisture content

Chapter I. Introduction

Section 1.1 Overview

While dams provide the ability to control the flow of fresh water and function to simplify our lives in many ways, they also pose an inherent and inevitable threat to the environment and to public safety. Since the creation of the first dams, dams have been failing due to unpredictable environmental conditions, poor engineering, or improper management. Unfortunately, when dams fail they often do so catastrophically because of the large amount of potential energy involved. Many engineering efforts have been made to reduce the potential hazard of dams as well as to provide emergency action plans for the event of a dam failure. Modeling the dam failure and overtopping processes and routing flood waves downstream can provide basic information about flood events that can be beneficial in dam engineering, emergency action planning, and floodplain management.

Due to the complex nature of the hydraulics involved with dam overtopping and large flood routing, much of the computer modeling in these areas has been done with one-dimensional models. However, in recent years there has been considerable progress in model code development, computing speed and capability and available elevation, vegetation, soil type, and land use data. The progress in these areas has led to much interest in multi-dimensional modeling of dam failure, overtopping, and flood routing as these events are certainly multi-dimensional in nature. To date there have been several explicit dam failure models developed which simulate the dam failure mechanism and localized effects (Wahl 1998, 2010). Watershed scale models can also be very valuable in

the analysis of dam failure, overtopping and flood routing by simulating the larger scale system influences on a reservoir and downstream effects of failure and overtopping events.

1.1.1 Dam Breach and Over topping (The Problem)

As dams pose a serious threat to residents, businesses, infrastructure, landowners, crops, etc. downstream of them, it has always been important to analyze the causes and results of dam failure and dam overtopping. It is also important to understand the effect that reservoirs can have on large precipitation events within a watershed, as they can have the ability to contain upstream flooding and attenuate total peak discharge. There are currently about 80,000 dams listed in the U.S. national inventory (Altinakar 2008). 81% of these are earthen dams, and 1,595 are considered a significant hazard to a city downstream. Dam failures have proven to be quite deadly, destructive, and costly.

Table 1.1: Selected dam failures (Association of Dam Safety Officials)

Date	Name	Fatalities	Estimated Cost
May 6, 1874	Mill River Dam, Massachusetts	139	
May 31, 1889	South Fork Dam, Massachusetts	>2,200	
Feb. 26, 1972	Buffalo Creek Valley, West Virginia	125	$400 million
June 9, 1972	Canyon Lake Dam, South Dakota	Between 33 and 237	$60 million
June 5, 1976	Teton Dam, Idaho	11	$1 billion
June 19, 1977	Laurel Run Dam, Pennsylvania	>40	$5.3 million
Nov. 5, 1977	Kelly Barnes Dam, Georgia	39	$2.5 million

Historically the vast majority of dam failures have been caused by overtopping. Dam overtopping can also cause a flood pulse downstream of a dam without the dam failing due to the stage discharge relationship of the reservoir. Dam overtopping and dam failure are very difficult processes to understand, predict, analyze, or model due to the inherently complex and contextual nature of the overtopping and failure processes and the lack of existing data relevant to dam failure.

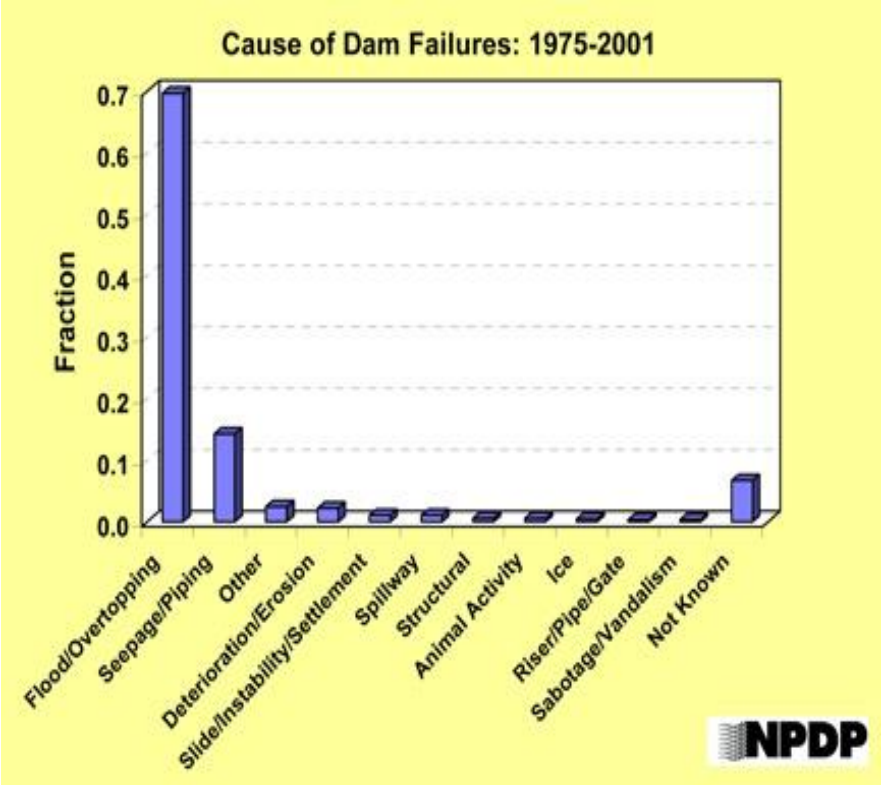

Figure 1.1: Relative number of dam failures due to a variety of mechanisms (Association of Dam Safety Officials)

At the watershed scale there are several sub-processes that make up the hydrologic response to precipitation induced flooding when a dam is involved. Each separate process of a dam overtopping or dam failure scenario (precipitation, geotechnical failure, or flood routing) can be analyzed separately or the total process analyzed as one event. Analyses of particular process aspects of these events can be especially beneficial when combined with

other similarly developed analyses to create an understanding of the entire process and consequence of these events. Processes such as the retention of flood flows by reservoirs with available capacity and the downstream routing of flows that overtop a dam lend themselves well to watershed scale numerical modeling analysis techniques.

1.1.2 Modeling Dam Overtopping and Flood Routing

Section 1.2 Objectives

The objectives of this research are as follows:

1). Ascertain the necessary model time step required to maintain numerical stability for routing a large range, in peak discharge magnitude, of point source hydrographs.

2). Simulate the inundation of the flood plain below a reservoir due to a dam failure by introducing flood wave simulating hydrographs into the watershed at a point. Map the areal extent of the downstream flooding. Quantify the areal extent of flood plain inundation. Create enhanced graphical and animation representations of simulation results to improve interpretation and visualization of simulation results.

3). Simulate the dam overtopping process as the result of extreme precipitation events. Quantify the attenuation of flood hydrograph peak discharge at the outlet of a watershed due to upstream dams.

Chapter II. Literature Review

Section 2.1 Dam Breach Modeling Techniques Overview

Dam failure modeling can generally be sorted into three categories of analysis techniques. The first technique is regression analysis utilizing the available dam failure data. This data includes outflow hydrograph data and dam geometry. The second category involves analytically modeling the dam failure process by characterizing the physical processes involved with the failure process to make predictions. The third technique is numerically modeling dam failure, overtopping, and flood wave routing with a computer model.

Dam failure and overtopping computer modeling can essentially be categorized into two major types of models, those that explicitly model the dam failure mechanism and outflow hydrograph and those that model the watershed scale hydrology and hydraulics in order to quantify the amount of water available to a reservoir and then route an outflow hydrograph from a dam. Coupling of these two types of models can also be done to simulate the entire process at a watershed scale and localized scale.

Presented in the following sections are overviews of the current and past research with each of the aforementioned techniques and examples thereof. This review is not intended to be comprehensive, but rather a general picture of the available dam failure, overtopping, and flood wave routing modeling techniques will be presented.

2.1.1 Dam Breach Empirical Models

Although there have been thousands of man-made and natural dam failures, there is not an abundance of data available concerning dam failure events due either to a lack of

downstream gaging or to downstream gages being compromised during the flood event. However, work has been done to compile the available data in order to estimate flood characteristic parameters as a function of dam geometry and reservoir geometry parameters by regression analysis. A general description of the research that has been done in dam failure regression analysis will be presented here. Additionally, the manner by which these types of empirical relationships can be applied to modeling with TREX will be discussed in Chapter V.

The magnitude of the peak discharge from a dam failure and the time to peak discharge are two important parameters due to their direct relation to downstream floodplain management. Several researchers such as Froehlieh, Pierce and Singh over the past few decades have compiled both measured and estimated flood hydrograph data and, by regression analysis, related the peak discharge and time to peak discharge to various geometric characteristics of the failed dams or associated reservoirs. Parameters such as dam crest height, dam crest width, dam crest length, and reservoir volume have been used for these regression analyses. Thornton et al. 2011 summarized the resulting empirical functions of many of these analyses and also presented a multivariate regression analysis utilizing the data sets that were used for the regression analyses. Table 2.1 shows the compiled summary of dam failure empirical relationships.

Table 2.1: Summary of dam breach hydrograph empirical relationships (Thornton et al. 2011)

	Investigator	Type	R^2	Number of case studies: Real	Number of case studies: Simulated	Equation
Height of water equations	Kirkpatrick (1977)	Best fit	0.790[a]	13	6	$Q_p=1.268(H_w+0.3)^{2.5}$
	Soil Conservation Service (SCS) (1981) for dams > 31.4 m	Envelope[b]	Not available	13		$Q_p=16.6(H_w)^{1.85}$
	U.S. Bureau of Reclamation (1982)	Envelope	0.724	21		$Q_p=19.1(H_w)^{1.85}$
	Singh and Snorrason (1982)	Best fit	0.488		8	$Q_p=13.4(H_d)^{1.89}$
	Pierce et al. (2010)—linear	Best fit	0.633	72		$Q_p=0.784(H)^{2.668}$
	Pierce et al. (2010)—curvilinear	Best fit	0.640	72		$Q_p=2.325\ \ln(H)^{6.405}$
Storage equations	Singh and Snorrason (1984)	Best fit	0.918		8	$Q_p=1.776(S)^{0.47}$
	Evans (1986)	Best fit	0.836	29		$Q_p=0.72(V_w)^{0.53}$
	Pierce et al. (2010)	Best fit	0.805	87		$Q_p=0.00919(V)^{0.745}$
Height of water and storage equations	Hagen (1982)	Envelope	Not Available	6		$Q_p=1.205(V_w \cdot H_w)^{0.48}$
	MacDonald and Langridge-Monopolis (1984)	Best fit	0.788	23		$Q_p=1.154(V_w \cdot H_w)^{0.412}$
	MacDonald and Langridge-Monopolis (1984)	Envelope	0.156	23		$Q_p=3.85(V_w \cdot H_w)^{0.411}$
	Costa (1985)	Best fit	0.745[c]	31		$Q_p=0.763(V_w \cdot H_w)^{0.42}$
	Pierce et al. (2010)	Best fit	0.844	87		$Q_p=0.0176(V \cdot H)^{0.606}$
	Froehlich (1995)	Best fit	0.934	22		$Q_p=0.607(V_w^{0.295} \cdot H_w^{1.24})$
	Pierce et al. (2010)	Best fit	0.850	87		$Q_p=0.038(V^{0.475} \cdot H^{1.09})$

[a]This R^2 value was calculated using a portion of the writer's original data set.
[b]Wahl (1998) suggested that this is an enveloping equation even though three data points plot slightly above the curve.
[c]This R^2 value was calculated without the five concrete and masonry dams included in the writer's original data set.

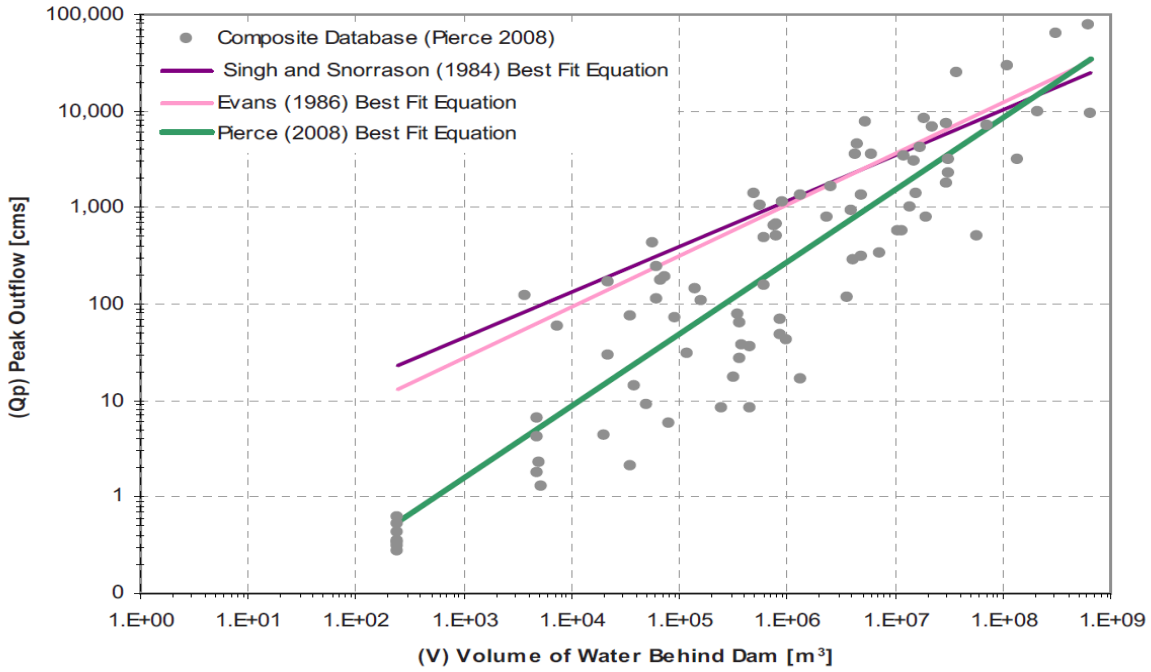

Figure 2.1: Dam failure data sets (Thornton et al. 2011)

The following relationships are the multivariate regression equations that were developed for the peak discharge from a dam breach:

$$Q_p = 0.863\left(V_s^{0.335} H_d^{1.833} W_{ave}^{-0.633}\right) \tag{2.1}$$

$$Q_p = 0.012\left(V_s^{0.493} H_d^{1.205} L^{0.226}\right) \quad (2.2)$$

In Equations 2.1 and 2.2: V_s = volume of water behind the dam

H_d = dam crest height

W_{ave} = average embankment width (perpendicular to the crest)

L = embankment length (crest length)

It was determined that when the number of pertinent dam characteristic variables increased from one to three as in these equations, the coefficient of variation increased slightly and the mean predicted error and the uncertainty bandwidth decreased (Thornton 2011).

Similar regression analyses have been done to develop equations for the time to failure of a breach outflow. Figure 2.2 was taken from the 1998 Department of the Interior Bureau of Reclamation Dam Safety Office report entitled "Prediction *of Embankment Dam Breach Parameters*". This figure details predicted versus observed time of failure values as determined by Froehlich 1995, Von Thun and Gillette 1990, MacDonald and Langridge-Monopolis 1984, and Reclamation 1988.

The relationships that have been developed by regression analyses of these data sets are tools for rough estimation of flood characteristics which can be helpful in emergency response and flood plain management. These relationships can also be used in conjunction with computer models. These methods will be discussed in chapter **V**.

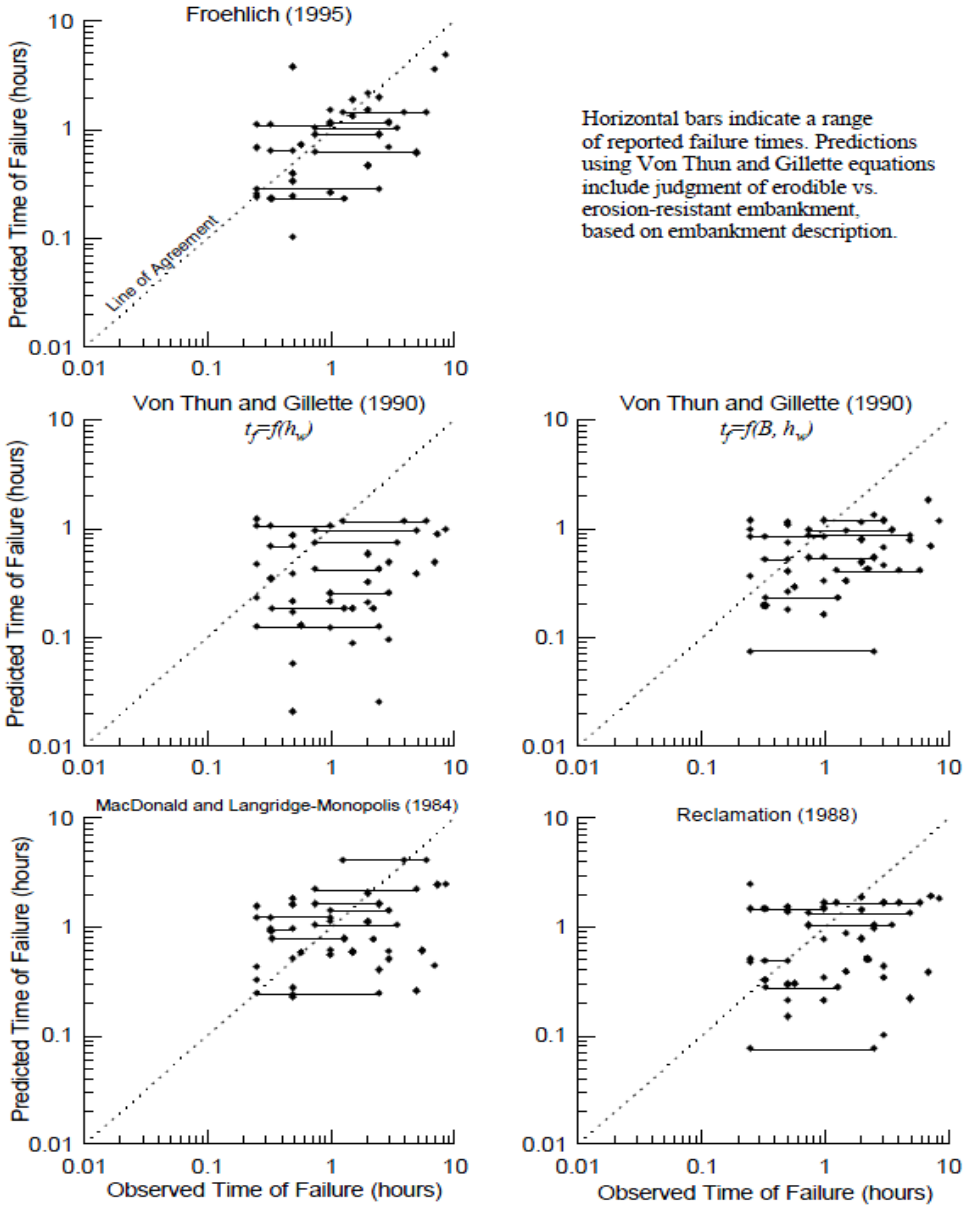

Figure 2.2: Predicted time of failure vs. observed time of failure (Wahl 1998)

2.1.2 Dam Break Analytical Models

While the water flow and erosional physical processes involved in dam failure are well known, they are still difficult to analytically model and quantify due to complex turbulence and rapidly varying characteristics. However, several analytical models have

been developed that determine the discharge from a dam breach from mathematical formulations of the physics of the breach process.

Cristofano, in 1965, related the erosion of a breach channel to the discharge though the breach using the shear strength of the dam material and the force of the flowing water (Wahl 2010). Several assumptions were made about the shape of the breach and an empirical coefficient was used to calibrate the model (Wahl 2010). Walder and O'Connor, in 1997, developed a model for the peak discharge from a breach as a function of the material erosion rate, the reservoir size, a breach shape parameter, the breach side slope angle, a reservoir shape factor, and the breach depth-to-dam height ratio (Wahl 2010). The following "benchmark case" relationships were developed for the peak discharge (Q_p) from a natural or constructed earthen dam breach and the time to peak discharge (t_p) (Walder and O'Connor 1997).

$$Q_p = 1.51\left(g^{1/2} h_d^{5/2}\right)^{0.06}\left(\frac{k_b V_s}{h_d}\right)^{0.94}, t_p \approx 1.24\left(\frac{V_s}{k_b^{\,2}(gh_d)^{1/2}}\right)^{1/3} \ldots for\left(\frac{k_b}{(gh_d)^{1/2}}\right)\left(\frac{V_s}{h_d^{\,3}}\right) <\sim 0.6 \quad (2.3)$$

$$Q_p = 1.94\left(g^{1/2} h_d^{5/2}\right)\left(\frac{D_c}{h_d}\right)^{3/4}, t_p = \frac{h_d}{k_b} \ldots for\left(\frac{k_b}{(gh_d)^{1/2}}\right)\left(\frac{V_s}{h_d^{\,3}}\right) >> 1 \quad (2.4)$$

In Equations 2.3 and 2.4: g = gravitational acceleration

h_d = water level drop in reservoir

k_b = mean erosion rate of the breach

V_s = volume of water stored behind the dam

D_c = dam crest height

The first equation applies to reservoirs where the volume stored to dam height ratio is small and the second equation applies to reservoirs where the volume stored to dam

height ratio is large. These formulations apply to average reservoir conditions for all parameters that are not present in the equations. This method recognizes the difference in dam failure processes between large and small reservoirs. Table 2.2 summarizes several popular physically based dam breach models that have been developed.

Table 2.3: Physically-based embankment breach parameters (Wahl 1998)

Model and Year	Sediment Transport	Breach Morphology	Parameters	Other Features
Cristofano (1965)	Empirical formula	Constant breach width	Angle of repose	
Harris and Wagner (1967); BRDAM (Brown and Rogers, 1977)	Schoklitsch formula	Parabolic breach shape	Breach, dimensions, sediments	
DAMBRK (Fread, 1977)	Linear predetermined erosion	Rectangular, triangular, or trapezoidal	Breach dimensions, others	Tailwater effects
Lou (1981); Ponce and Tsivoglou (1981)	Meyer-Peter and Muller formula	Regime type relation	Critical shear stress, sediment	Tailwater effects
BREACH (Fread 1988)	Meyer-Peter and Muller modified by Smart	Rectangular, triangular, or trapezoidal	Critical shear stress, sediment	Tailwater effects; dry slope stability
BEED (Singh and Scarlatos, 1985)	Einstein- Brown formula	Rectangular or trapezoidal	Sediments, others	Tailwater effects, saturated slope stability
FLOW SIM 1 and FLOW SIM 2 (Bodine, undated)	Linear predetermined erosion; Schoklitsch formula option	Rectangular, triangular, or trapezoidal	Breach dimensions, sediments	

2.1.3 Dam Breach Computer Models

The National Weather Service (NWS) dam-break forecasting model FLDWAV was developed by D. L. Fread to model the dam breach process and the downstream flooding process. FLDWAV took over for the popular DAMBRK model which has been used since the

nineteen seventies (Fread 1984, 1993). FLDWAV utilizes a finite-difference numerical method to solve the complete one dimensional Saint Venant equations for unsteady flow. The model will compute the outflow hydrograph from a dam resulting from spillway flow, overtopping, and/or dam breach and then route the flood wave downstream. Internal boundary conditions can be input to represent man-made control structures such as dams, weirs, and bridges. The flow may be subcritical, supercritical, or mixed and can also vary from Newtonian to non-Newtonian (Fread and Lewis 1998).

The BREACH dam breach model predicts the outflow hydrograph from an earthen dam using a physically based approach which takes into account various geometric, geotechnical, erosional, and flow characteristics (Fread 1988). The model uses information about the constituent materials of a dam along with the Meyer-Peter and Müller sediment transport equation and a quasi-steady uniform flow (manning equation) to define the breach opening evolution in time. Subsequently the outflow hydrograph can be determined. The BREACH model code is free.

The United States Army Corps of Engineers (USACE) Hydrologic Engineering Center (HEC) developed the HEC-RAS Hydraulic channel flow model as part of their suite of hydrologic and hydraulic modeling tools (Brunner 2010). While primarily used as a flow routing model, a dam breach module has been added to the model to simulate the breach process. HEC-RAS can simulate steady or unsteady one-dimensional flow by solving the full one dimensional Saint-Venant equations. Also subcritical, supercritical, or mixed flow regimes can be simulated.

2.1.4 Watershed Computer Models

Over the past several decades, many watershed scale computer models have been developed within government agencies, academia, and the private sector. Watershed models are often categorized into lumped parameter, semi-distributed parameter, and distributed parameter models. Lumped parameter models are those which assign one parameter value to the whole watershed. Semi-distributed models are those which distribute parameter values by sub-catchments within a watershed. Distributed parameter models divide a watershed into a grid of cells and assign a parameter value to each cell within the watershed domain. Several in-depth comparative reviews of watershed models have been done. The World Meteorological Organization (WMO) has sponsored comparative studies of watershed models in 1975, 1986, and 1992. Singh et al. have written comparisons as well (Singh et al. 2002). The National Weather Service (NWS) sponsored a review of distributed models called the distributed model inter-comparison project (DIMP) (Smith et al. 2004). In the interest of providing context for the research presented here regarding modeling with the TREX watershed model, several popular models will be described here. An inter-comparison table taken from Singh et al. 2002 is presented in Appendix 2.0. A more detailed review of the TREX model will be presented in Chapter III.

The United States Army Corps of Engineers (USACE) has developed a series of lumped parameter watershed models. The most recent version is the Hydrologic Engineering Center (HEC) Hydrologic Modeling System (HEC-HMS) (Feldman 2010). This model simulates watershed scale processes using empirical equations. This model and similar lumped parameter models are simple to use and require far less set up time and

field data to run than distributed models. In many cases they can be as accurate as a more sophisticated physically based model. However, they do not represent the runoff characteristics of complex watersheds which have highly varied soil types or land uses as well as distributed parameter models. They will not provide information about the distribution of flow within a watershed. Also they always require calibration, which essentially limits their utility to cases where calibration and validation data are available.

An example of a semi-distributed parameter model is the Hydrologic Simulation Program-Fortran (HSPF) (Bicknell et al. 1997). This model has its roots in one of the oldest watershed models, the Stanford Watershed Model (Crawford and Linsley, 1966). This model simulates many hydrologic, sediment transport, and chemical transport processes. The hydrologic processes are represented as stored water and flow is routed between storages (Velleux et al. 2010). Flow is simulated with the one-dimensional kinematic wave approximation of the Saint Venant equation.

The Kinematic Runoff and Erosion (KINEROS) is another example of a semi-distributed parameter model (Woolhiser et al. 1990). This model is an example of an "open book" model whereby a watershed is represented by planes which route flow into channels. KINEROS simulates rainfall, interception, infiltration, surface runoff, and erosion. Flow is calculated by the one-dimensional kinematic wave approximation of the Saint Venant equation.

The Soil and Water Assessment Tool (SWAT) is another example of a physically based semi-distributed parameter model which simulates rainfall, infiltration, surface flow, groundwater flow, and transmission losses (Neistch et al. 2002). SWAT has been linked

with the Arc/Info geographic information system (GIS) (Velleux et al. 2010). All three of these semi-distributed parameter models have publicly available source code.

System Hydrologique European Fortran (SHETRAN) is a fully-distributed parameter, physically based model which simulates interception, infiltration, surface runoff, groundwater flow, evapotranspiration, sediment transport, and chemical transport (Ewen et al. 2000). Surface flow is calculated with the diffusive wave approximation of the Saint Venant equation. This model is two-dimensional in the overland plane and one dimensional in channels. Groundwater flow is three-dimensional. While SHETRAN is not commercially available, there is a commercially available package called MIKE SHE (DHI 2005).

FLO-2D is a two-dimensional physically based model which simulates rainfall, surface flow, interception, and infiltration (O'Brien 2006). FLO-2D uses the full dynamic wave Saint-Venant equation to route flow in two dimensions. This software is commercially available and there is a free basic version.

Several features of a computer model are necessary or highly desirable when modeling dam overtopping and large magnitude flood events at the watershed scale. A model must be a fully distributed parameter type in order to analyze the interactions between the floodplain and the channel and to map the distribution of flow within a watershed in time. Floodplain interactions are complex due to highly varied roughness and many possible flow directions. Fully distributed models best capture this detail. Also location specific events like overtopping and dam failure must be modeled with a fully distributed model in order to accurately represent the localized detail at a dam site. A model should also route flow in two dimensions in the flood plain. Large scale flood flows

are very multi-dimensional in nature as the flows are not confined by channel walls. Modeling floods that originate from a point within a watershed requires a model that is capable of accepting a user defined point source hydrograph as input. The incorporation of a GIS program into the pre-processing of model input data and post-processing of model calculated, distributed flow depths and velocities is crucial for this type of modeling. It allows for easy modification of watershed elevations for dam representations. It also provides a vehicle for visually interpreting model outputs in the form of maps and animations.

The TREX model is a fully distributed parameter, physically based, two dimensional model that is easily integrated with a GIS program such as the Environmental Systems Research Institute (ESRI) ArcGIS suite of GIS tools. TREX is also an open source model that is free to the public. For these reasons TREX is well suited to watershed scale modeling of dam overtopping and flood routing. These attributes and other aspects of the TREX model are discussed in chapter III.

Chapter III. The Two-Dimensional Runoff Erosion and Export Model

Section 3.1 TREX Conceptual Model

The Two-Dimensional Runoff Erosion and Export (TREX) watershed model is composed of three distinct components which are hierarchical in their dependence on one another. The first and most basic component of the model is the hydrologic group of processes which simulates precipitation, infiltration, storage, and overland and channel flow. These processes are controlled by the governing equations of water flow and input parameters that describe the geography and roughness of the watershed, namely the Digital Elevation Model and land use types. The second component is the sediment transport group of processes which governs aggradation, degradation, and sediment advection in the overland plane and in the channel. These processes are all dependent on the hydrologic governing equations and various soil characteristic input parameters. The third component controls the transport and fate of chemicals within the watershed. The constituent processes of this component are dependent on those of the first two model components.

The hydrologic model component can be run alone, or sediment transport can be modeled with hydrology, or chemical fate and sediment transport can be modeled with hydrology. Only the hydrologic process descriptions and governing equations will be detailed here, as the other two model components were not utilized for the dam failure and dam overtopping simulations presented.

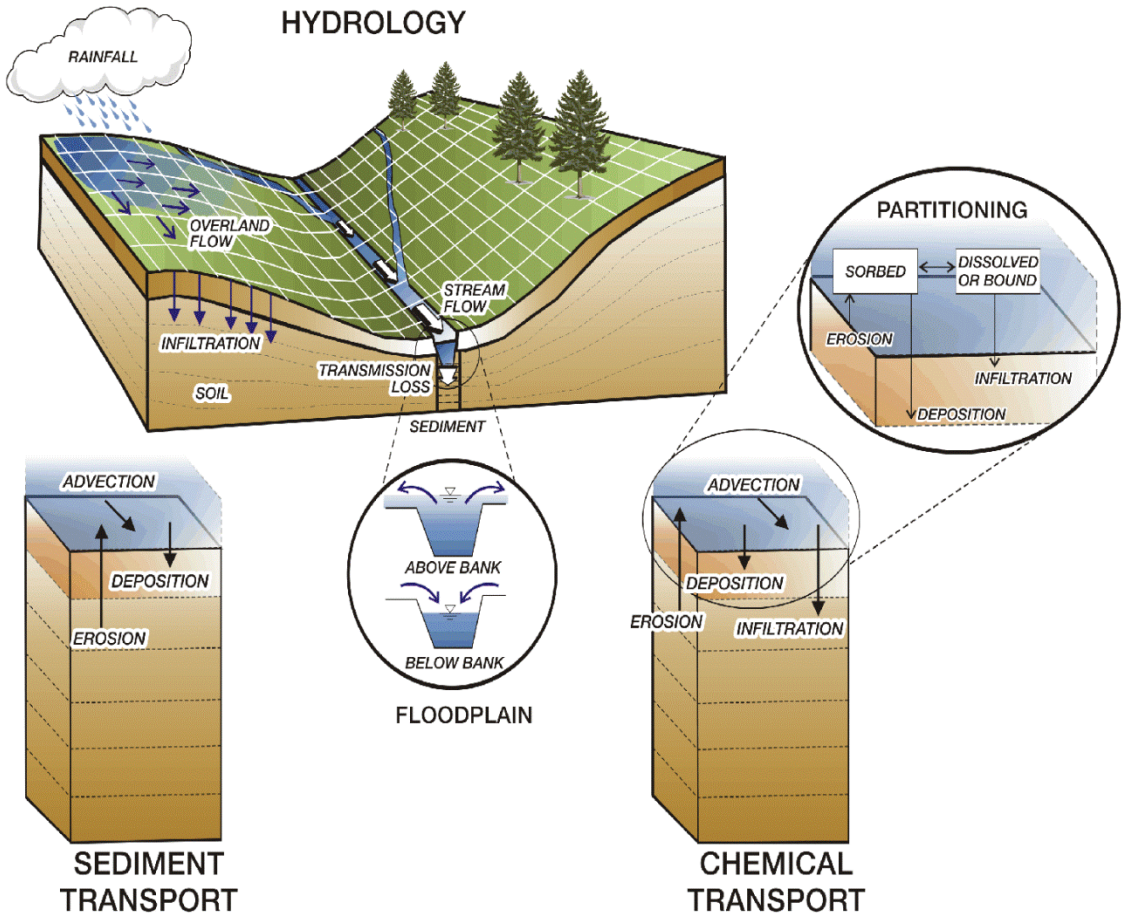

Figure 3.1: TREX conceptual model structure and simulated processes (Velleux 2005)

Section 3.2 Hydrologic Process Descriptions

The main hydrologic processes incorporated into the hydrologic model component are precipitation and interception, infiltration and transmission loss, surface storage, and overland and channel flow (Velleux 2005). Much of the notation and description presented for the hydrologic sub-model are taken from the TREX user manual (Velleux et al. 2011).

3.2.1 Precipitation and Interception

The precipitation that effectively reaches the land or water surface can be represented as a depth or volume of water. The representation of continuity which reflects this is the following:

$$\frac{\partial V_g}{\partial t} = i_g A_s \tag{3.1}$$

In Equation 3.1: V_g = gross precipitation water volume

i_g = gross precipitation rate

A_s = surface area over which the precipitation occurs

t = time

Surface vegetation effectively reduces the total amount of water available for infiltration or run off by trapping water by surface tension with the foliage. Intercepted water can be stored by the vegetation or can evaporate. Intercepted precipitation can be represented as a depth or volume.

$$V_i = (S_i + Et_R)A_s \tag{3.2}$$

The net precipitation available for infiltration or run off can then be represented as the gross precipitation volume minus the intercepted volume.

$$V_n = V_g - V_i \tag{3.3}$$

In Equations 3.2 and 3.3: V_i = interception volume

S_i = interception capacity of projected canopy per unit area

E = evaporation rate

t_R = precipitation duration

V_n = net precipitation

When gross precipitation volume is greater than the intercepted volume, then the excess precipitation volume can be represented as a net effective precipitation rate as follows:

$$i_n = \frac{1}{A_s}\frac{\partial V_n}{\partial t} \tag{3.4}$$

In Equation 3.4: i_n = net effective precipitation rate

3.2.2 Infiltration and Transmission Loss

Infiltration is the transport of surface water into the subsurface due to gravity and capillary action. Many parameters affect a soil's ability to convey water such as hydraulic conductivity, capillary suction head, and degree of saturation. The Green and Ampt infiltration process description is incorporated by TREX where any infiltrated water is considered to be a loss from the surface water. This relationship assumes that a sharp wetting front exists at the interface of the infiltration zone and the initial water content. When the pressure head due to surface ponding is neglected, that is to say that it is much smaller than the suction head, the Green and Ampt relationship can be expressed as the following (Julien, 2002):

$$f = K_h\left(1+\frac{H_c(1-S_e)\theta_e}{F}\right) \tag{3.5}$$

In Equation 3.5:
- f = infiltration rate
- K_h = effective hydraulic conductivity
- H_c = capillary pressure (suction) head at the wetting front
- Θ_e = effective soil porosity = (Φ-θ_r)
- Φ = total soil porosity

Θ_r = residual soil moisture content

S_e = effective soil saturation

F = cumulative (total) infiltrated water depth

Water can infiltrate in channels similarly to how it does in the overland plane. Transmission loss in channels is also modeled with the Green and Ampt relationship in TREX. However ponded surface water and the associated hydrostatic pressure head are accounted for. The transmission rate can be expressed as the following:

$$t_l = K_h\left(1+\frac{(H_w+H_c)(1-S_e)\theta_e}{T}\right) \tag{3.6}$$

In Equation 3.6: t_l = transmission loss rate

K_h = effective hydraulic conductivity

H_w = hydrostatic pressure head (depth of water in channel)

H_c = capillary pressure (suction) head at the wetting front

Θ_e = effective soil porosity = (Φ-θ_r)

Φ = total soil porosity

Θ_r = residual soil moisture content

S_e = effective sediment saturation

T = cumulative (total) depth of water transported by transmission loss

3.2.3 Storage

Water that is stored in surface depressions both in the overland plane and within channels is represented within TREX as an equivalent total volume or when normalized by the raster cell area, as a depth. A threshold depth in surface depressions creates a

condition for the initiation of water flow. The stored water in overland and channel cells is subject to infiltration and evaporation.

3.2.3 Overland and Channel Flow

Water flow will occur in overland and channel cells when the surface water depth exceeds the depression storage threshold depth. Flow can generally be described by conservation of mass (continuity) and conservation of momentum. Within TREX water can flow in two dimensions. The two-dimensional (vertically integrated) equation of continuity for gradually varied flow in the overland plane in rectangular coordinates is the following (Julien et al. 1995; Julien, 2002):

$$\frac{\partial h}{dt} + \frac{\partial q_x}{dx} + \frac{\partial q_y}{dy} = i_n - f + W = i_e \qquad (3.7)$$

In Equation 3.7:

h = surface water depth

q_x, q_y = unit discharge in the x- or y- direction = Q_x/B_x, Q_y/B_y

Q_x, Q_y = flow in the x- or y- direction

B_x, B_y = flow width in the x- or y- direction

i_n = net effective precipitation rate

f = infiltration rate

W = unit discharge from/to a point source/sink

i_e = excess precipitation rate

The momentum of overland and channel flow can be represented by the Saint-Venant equations. These equations can be simplified to the diffusive wave approximation if the relatively small terms that describe the local and convective acceleration are neglected (Julien et al. 1995; Julien, 2002):

$$S_{fx} = S_{0x} - \frac{\partial h}{dx} \tag{3.8}$$

$$S_{fy} = S_{0y} - \frac{\partial h}{dy} \tag{3.9}$$

In Equations 3.8 and 3.9:

S_{fx}, S_{fy} = friction slope in the x- or y- direction

S_{0x}, S_{0y} =ground surface slope in the x- or y- direction

To solve continuity and momentum equations for flow in the overland plane, five hydraulic variables can be defined which describe flow resistance in terms of a depth-discharge relationship. Flow resistance can be described by the manning equation, assuming that is turbulent. The depth discharge relationships for two-dimensional flow in the overland plane are the following (Julien et al. 1995; Julien, 2002):

$$q_x = \alpha_x h^{\beta} \tag{3.10}$$

$$q_y = \alpha_y h^{\beta} \tag{3.11}$$

$$\alpha_x = \frac{S_{fx}^{1/2}}{n} \tag{3.12}$$

$$\alpha_y = \frac{S_{fy}^{1/2}}{n} \tag{3.13}$$

In Equations 3.10, 3.11, 3.12 and 3.13:

α_x, α_y = resistance coefficient

for flow in the x- or y- direction

S_{fx}, S_{fy} = friction slope in the x- or y- direction

β = resistance exponent = 5/3

n = Manning roughness coefficient

If channel flow is simplified to a one-dimensional approximation (vertically and laterally integrated) in the direction parallel to the channel thalweg, the equation for continuity can be expressed as follows (Julien et al. 1995; Julien, 2002):

$$\frac{\partial A_c}{dt} + \frac{\partial Q}{dx} = q_l \tag{3.14}$$

In Equation 3.14: A_c = cross section al area of flow

Q = total discharge

q_l = lateral unit discharge (into or out of the channel)

The diffusive wave approximation of the full Saint-Venant equation can once again be used to describe conservation of momentum for one-dimensional channel flow, assuming that the local and convective acceleration terms of the Saint-Venant equations are relatively small and can be neglected (Equations 3.8 and 3.9). The Manning equation to represent channel flow resistance is the following (Julien et al. 1995; Julien, 2002):

$$Q = \frac{1}{n} A_c R_h^{2/3} S_f^{1/2} \tag{3.15}$$

In Equation 3.15: Q = total discharge

A_c = cross section al area of flow

R_h = hydraulic radius of flow = A_c/P_c

P_c = wetted perimeter of channel flow

n = Manning roughness coefficient

S_f = friction slope

Section 3.3 Numerical Method

The TREX model solves the governing equations for all of the state variables involved with the hydrologic, sediment transport, and chemical transport sub-models. The model uses a finite difference, first order numerical integration scheme to solve the flow equations for every raster cell in the watershed domain as individual control volumes. Euler's method for numerical integration is used as the technique to solve the governing equations at every time step.

$$s\big|_{t+dt} = s\big|_t + \left.\frac{\partial s}{\partial t}\right|_t dt \tag{3.16}$$

In Equation 3.16: $s\big|_{t+dt}$ = value of the model state variable at time t + dt

$s\big|_t$ = value of the model state variable at time t

$\left.\frac{\partial s}{\partial t}\right|_t$ = value of model state variable derivative at time t

dt = time step for numerical integration

This numerical method requires that model stability is highly dependent on the magnitude of the simulation time step, *dt*. The model accepts as input a series of user specified time steps, or a model option can be selected whereby the Courant-Freidrichs-Lewy (CFL) condition is employed by the model to determine the maximum stable time step at each simulated iteration (Velleux et al. 2011).

$$\frac{udt}{dx} \le C \tag{3.17}$$

In Equation 3.17: c = celerity

dt = model time step

dx = modeled raster cell size

C = Courant number

Chapter IV. California Gulch Model Configuration

Section 4.1 Overview and Site Description

California gulch is a watershed which drains into the upper Arkansas River near the town of Leadville in central Colorado (Figure 4.1).

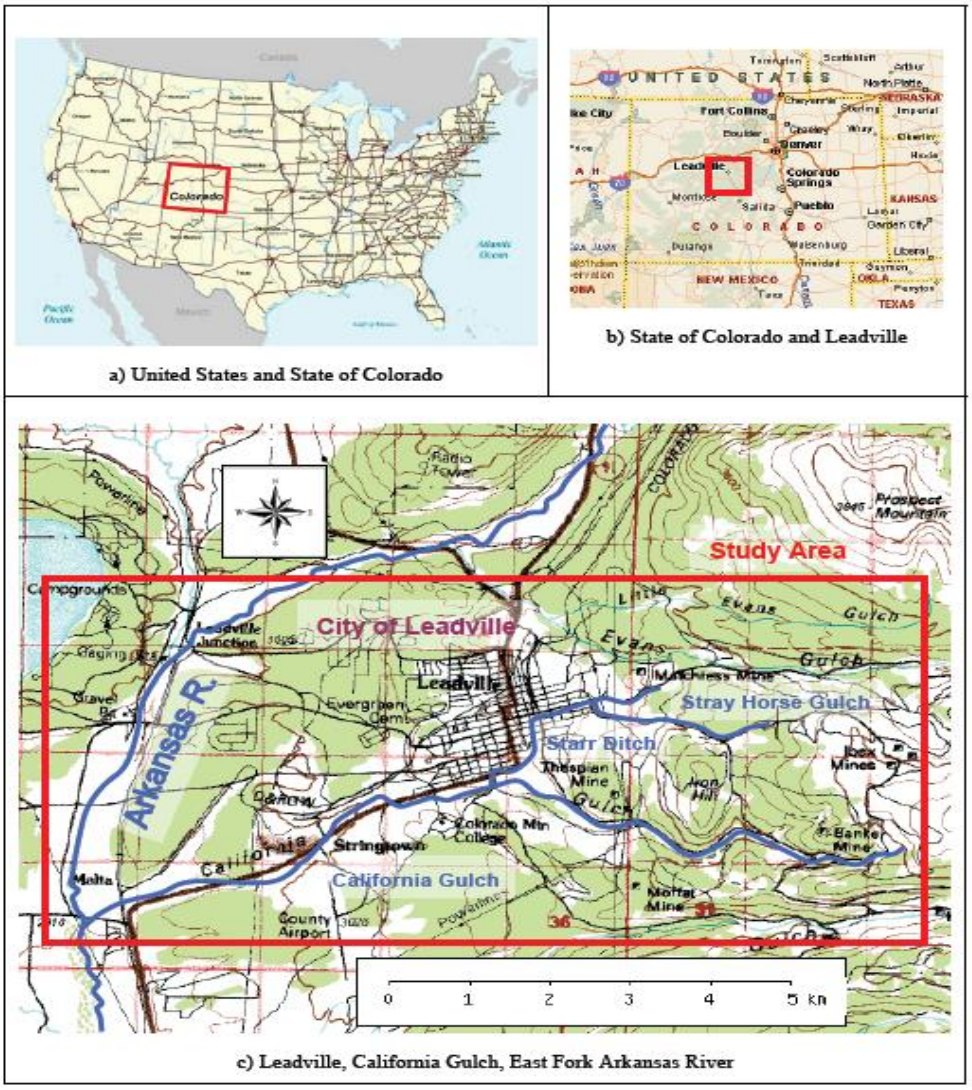

Figure 4.1: Study site location, California Gulch, Colorado (Velleux 2005)

The California Gulch watershed encompasses most of the city of Leadville and the uplands east of the city. California Gulch has several tributaries, the largest of which is

Stray Horse Gulch which joins California Gulch within the city of Leadville (Figures 4.1 and 4.2).

Figure 4.2: California Gulch watershed and Leadville Colorado

A portion of the watershed is urbanized and more impervious than the rest of the drainage area. The headwaters of the watershed are at and above tree line and much of this region was heavily mined in the late 1800's and early 1900's. The hard rock mining techniques of this era have led to a reduction in vegetation and considerable sediment instability and heavy metal contaminant drainage. This change in the land use has significantly changed the hydrology and ecology of the area and as such, the Environmental Protection Agency (EPA) established a superfund project site in California Gulch and Stray Horse Gulch. Several flow paths have been altered by diversions and settling ponds. Much of the rest of

the watershed is evergreen forested. Figure 4.7 shows the full detail of the land use representation.

Section 4.3 Digital Elevation Model

The area of California Gulch is 30.6 km^2. The elevation within the watershed varies between 3654 meters and 2910 meters (Figure 4.3). A Digital Elevation Model (DEM) was created for California Gulch with Geographic Information System (GIS) software and elevation data from the United States Geological Survey (USGS). 30 meter by 30 meter resolution elevation data was used to create the grid elevation representation of the watershed. The DEM contains 34,002 cells.

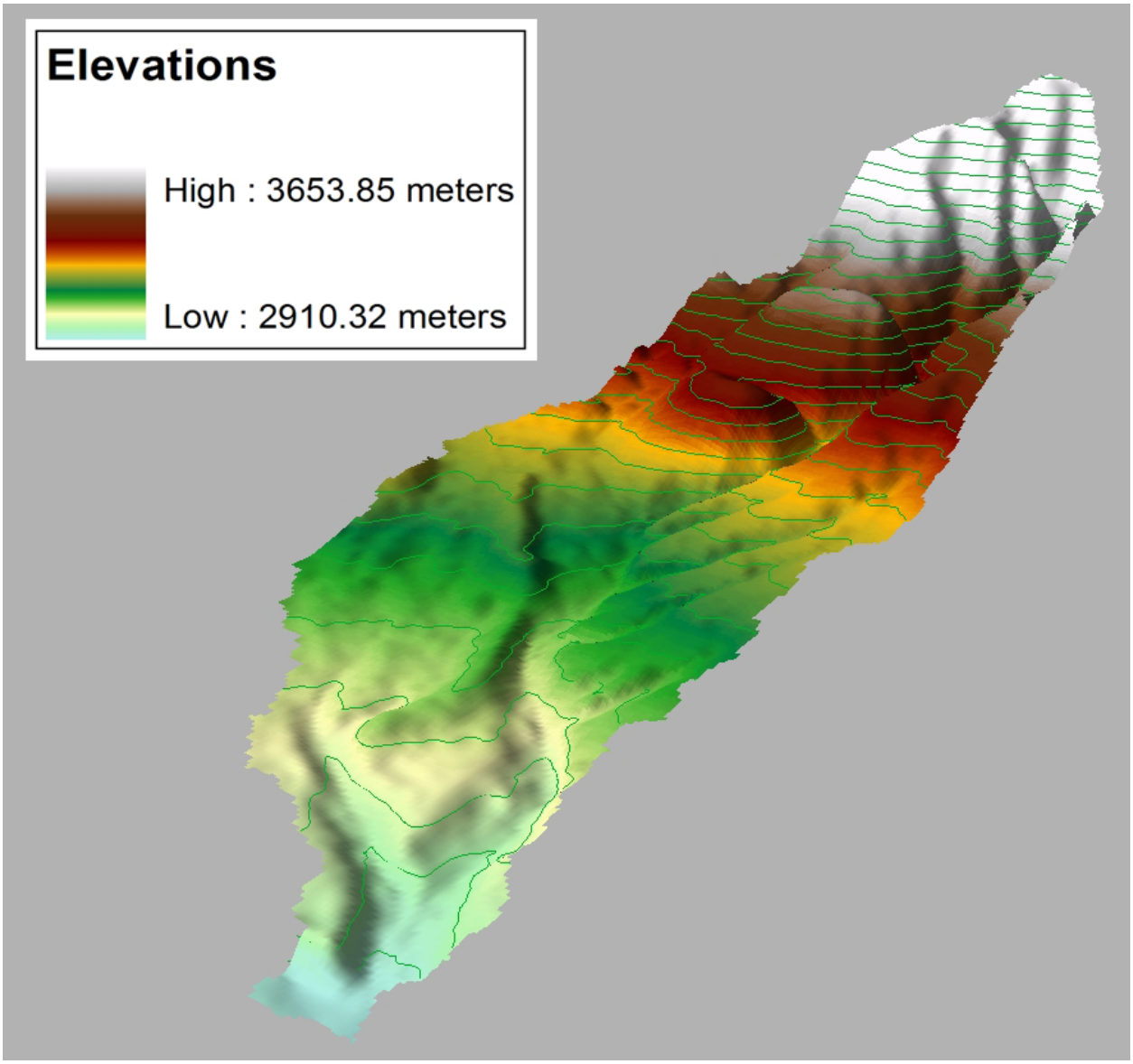

Figure 4.3: California Gulch digital elevation model

Slope and aspect maps were also created to delineate the watershed and create a flow network during the DEM processing of the watershed. These processes were utilized during the original model set up creation for the California Gulch watershed.

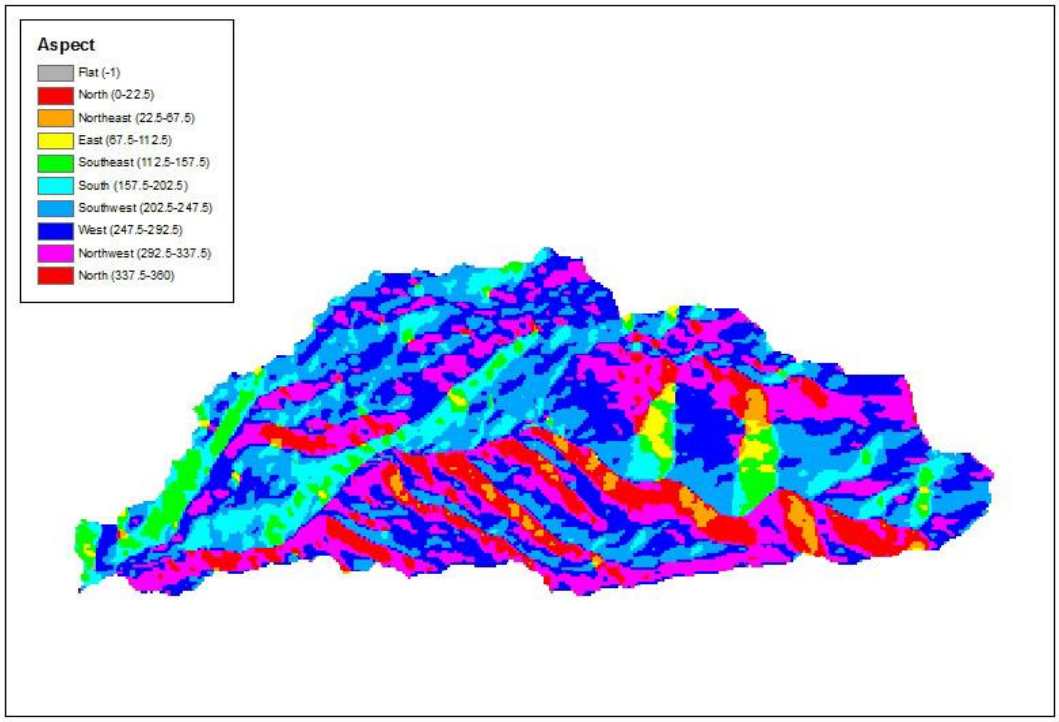

Figure 4.4: California Gulch aspect map

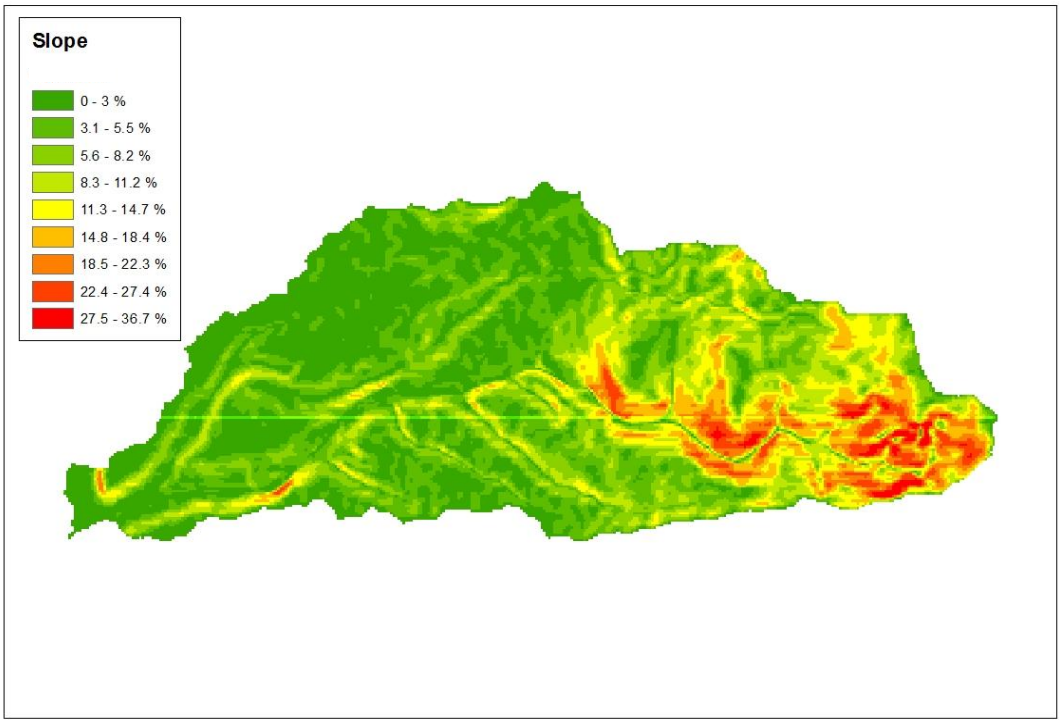

Figure 4.5: California Gulch slope map

A stream network was created with 25 links and 1395 nodes. 42 km of total stream length was created to distinguish between channel flow and overland flow.

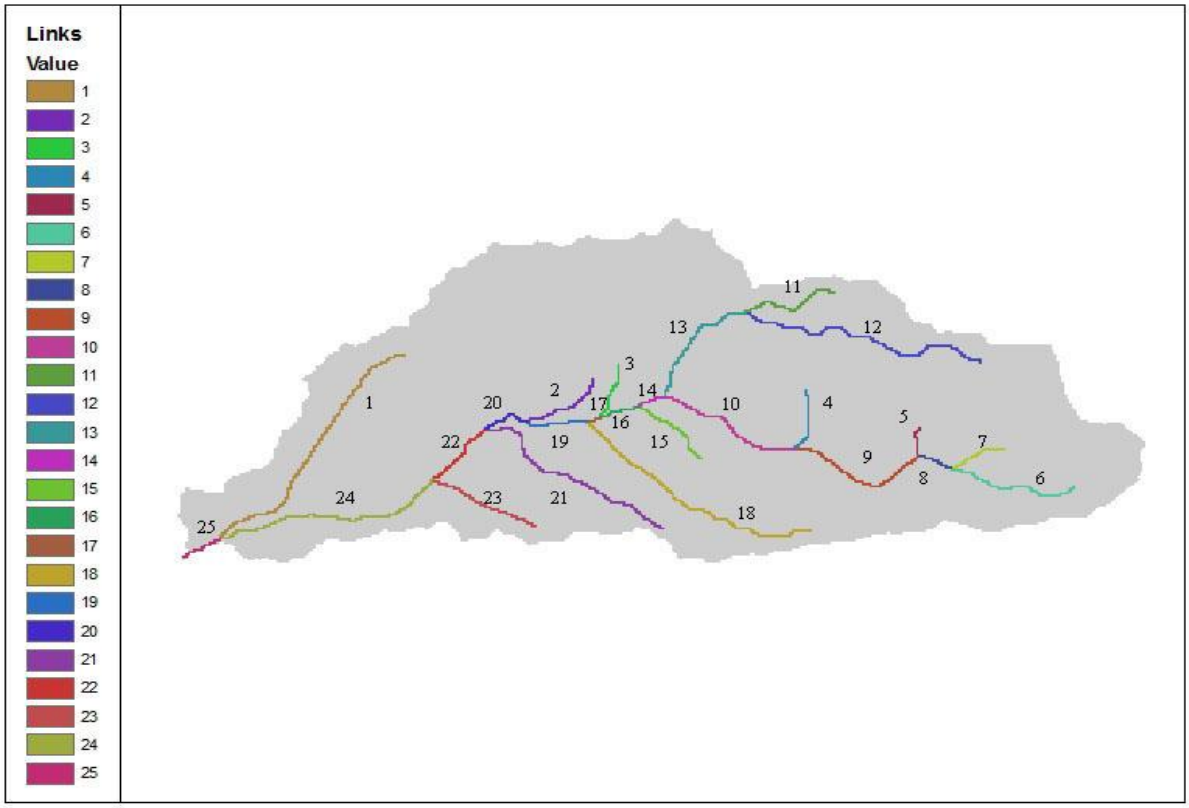

Figure 4.6: California Gulch link map

Section 4.4 Land Use

Land use data were also obtained from the USGS. A land use map was created to represent the surface roughness of the watershed for model calculations. Values for parameters such as ground cover factor, surface roughness, vegetative interception depth, grain size, and erodibility were assigned to each land use type (Velleux 2005).

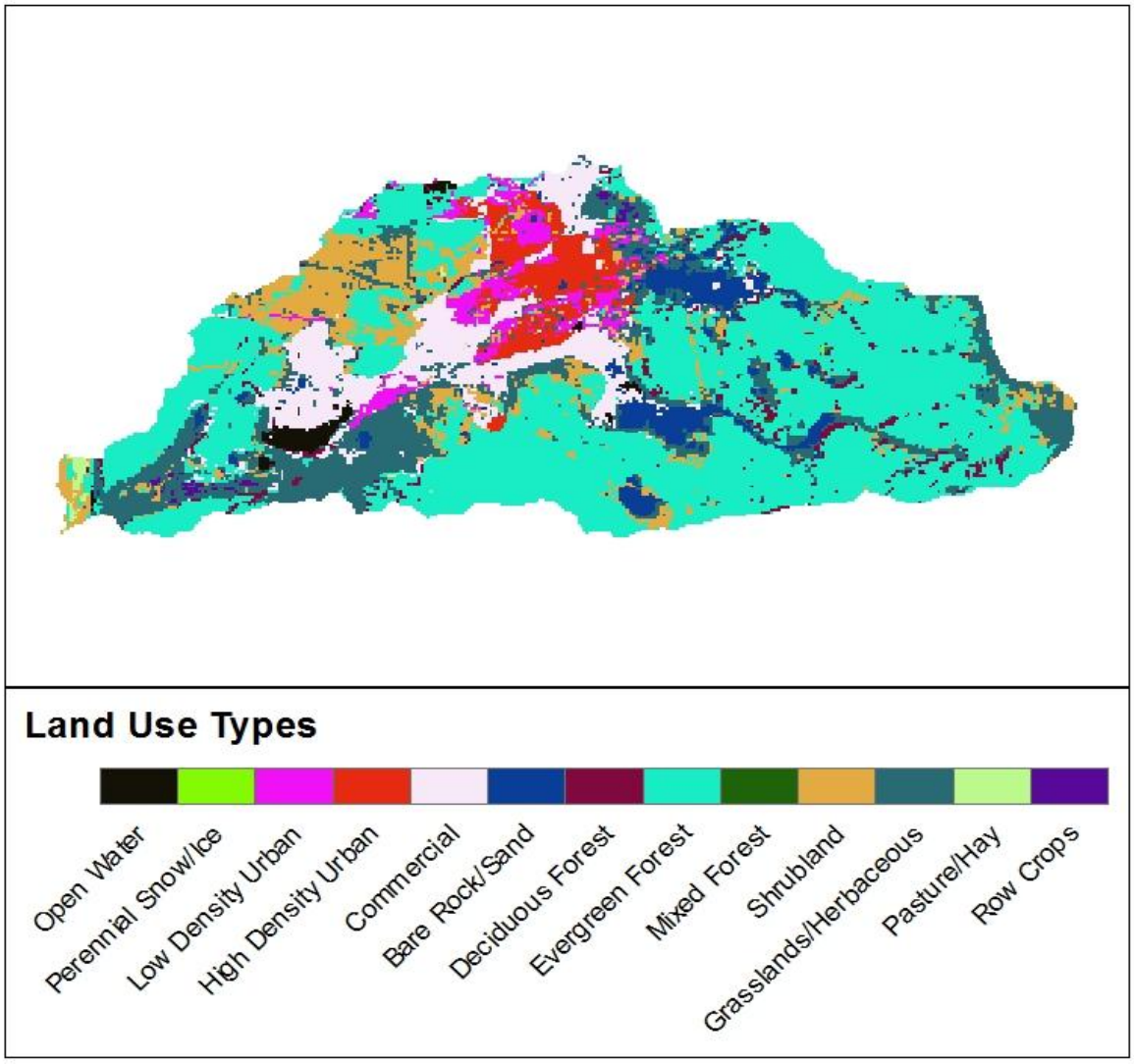

Figure 4.7: California Gulch land use type map

Section 4.5 Soil and Sediment Types

Soil survey data was obtained from the U.S. Department of Agriculture (USDA) and the Natural Resources Conservation Service (NRCS). These data provided characterizations of the soils of the watershed such as hydraulic conductivity, porosity, and grain size distribution. Additional soil data was acquired from EPA superfund project reports. Values for parameters such as grain size, hydraulic conductivity, and porosity

were assigned to each soil type (Velleux 2005).

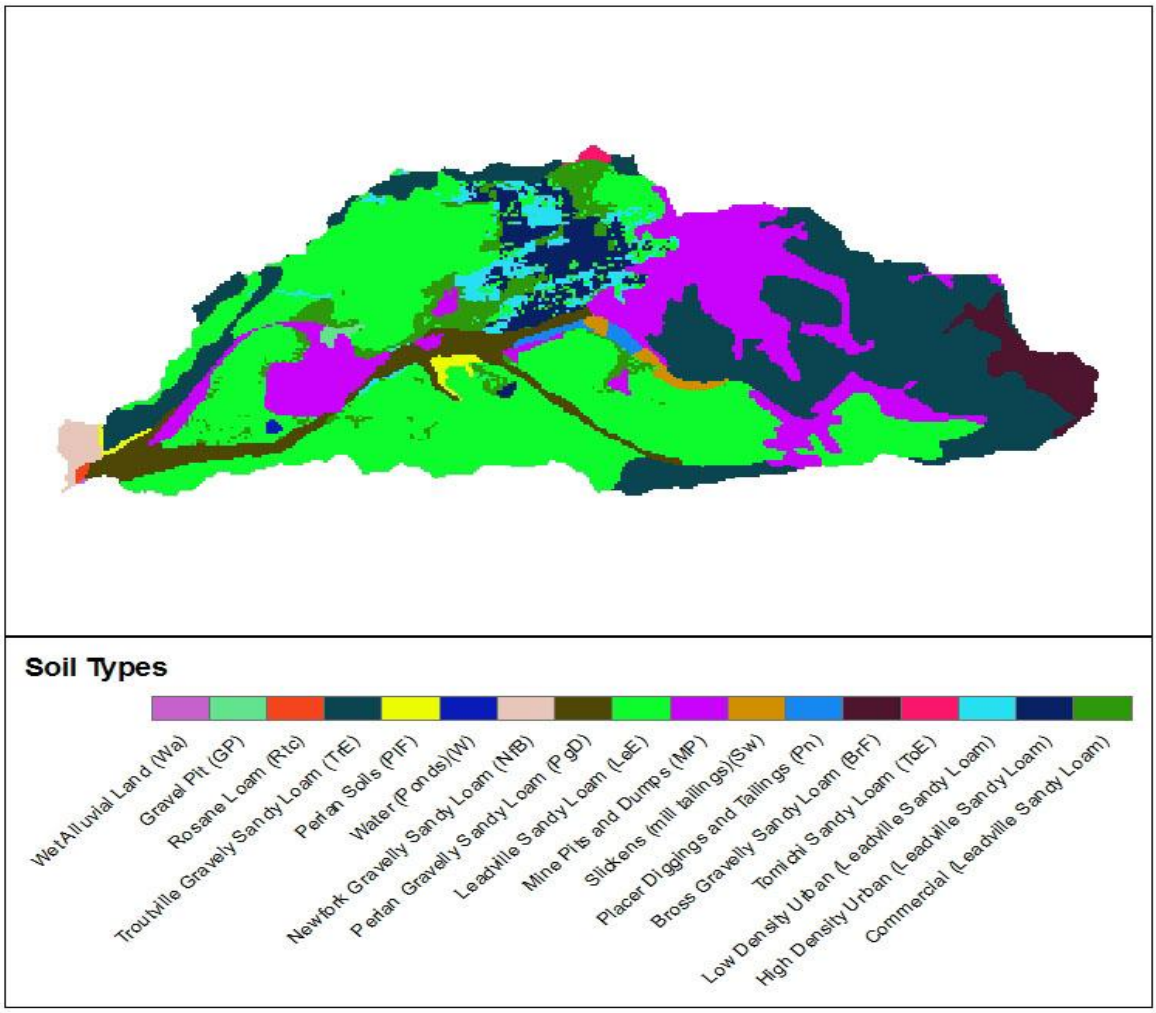

Figure 4.8: California Gulch soil type map

Section 4.6 Overview of Work Done at California Gulch

Much work has been done in past years collecting a comprehensive dataset which has been compiled to develop the California Gulch TREX model set up. Data collected for the EPA, Resurrection Mining Company, American Smelting and Refining Company (ASARCO), Denver and Rio Grande Railroad Company, and Colorado Department of Public Health and Environment (CDPHE) was used for this model set up. Additionally, data from

the USGS and the USDA was extracted from databases for use in the model setup. While much of this data collected was for the part of the model setup which characterizes the sediment and chemical transport of the watershed, the data pertaining to soil type, land use, elevation, soil moisture, and precipitation was integral to the model simulations preformed for this analysis.

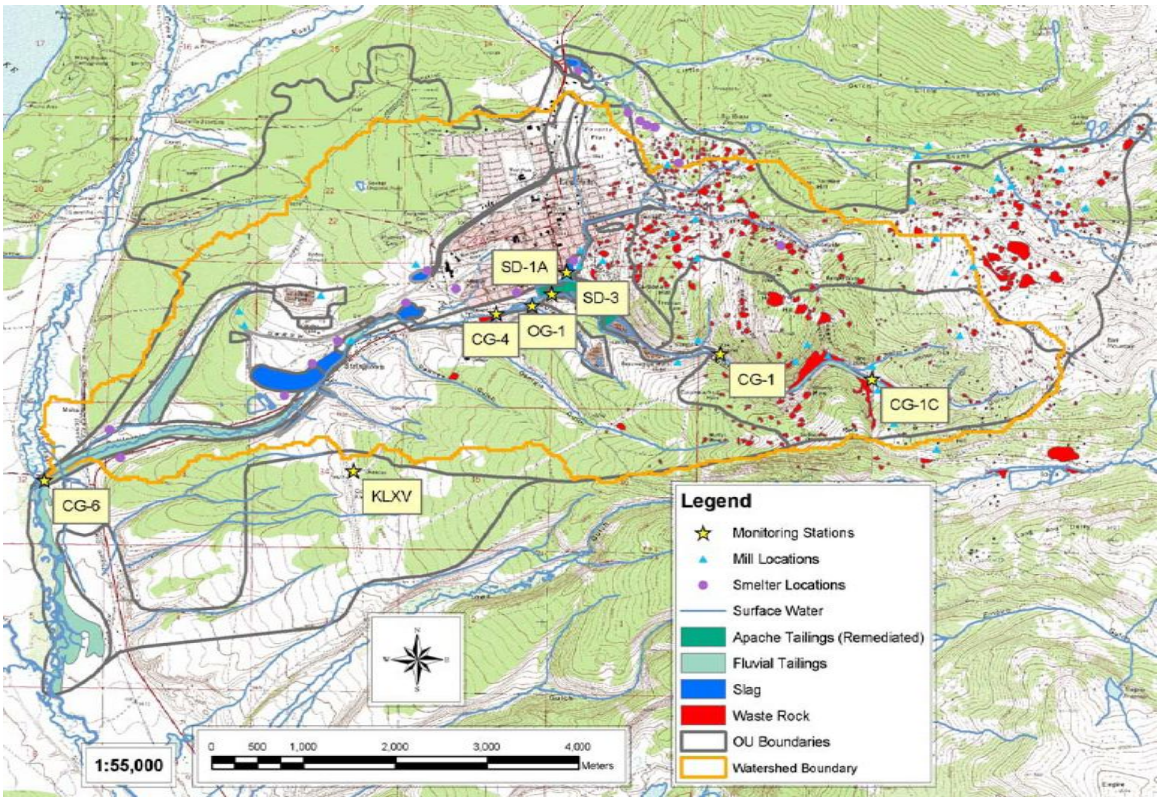

Figure 4.9: California Gulch gaging stations (Velleux 2005)

Section 4.7 Calibration and Validation

The calibration event used for the California Gulch model set up was on June 12-23, 2003 (Velleux 2005). The validation event used was on September 5 – 8, 2003. Figure 4.9 shows the gaging station locations within the California Gulch watershed and Figures 4.10 and 4.11 show the results of the calibration and validation simulations. The details about

the model performance are available from Velleux 2005.

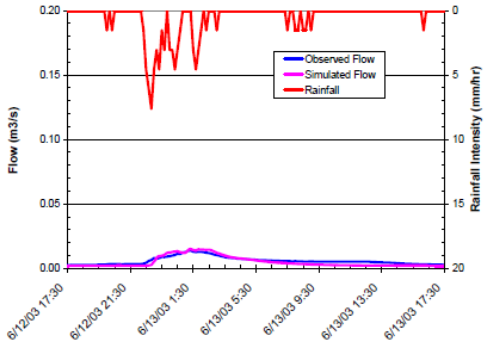

Figure 5-2. Hydrologic calibration at Station CG-1 (June 12-13, 2003).

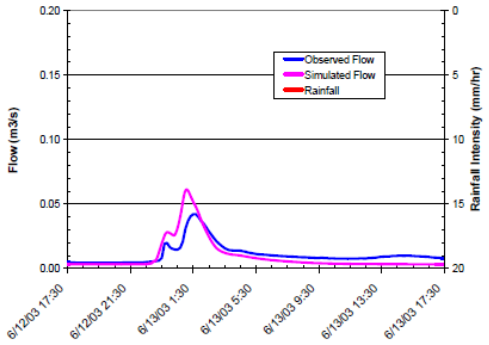

Figure 5-3. Hydrologic calibration at Station SD-3 (June 12-13, 2003).

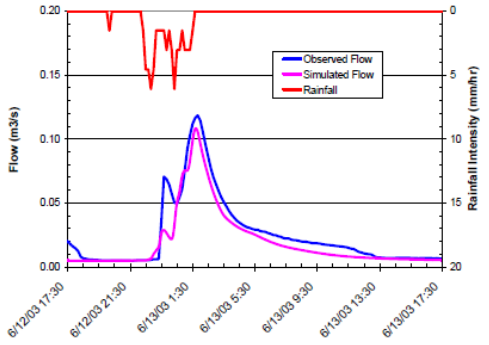

Figure 5-4. Hydrologic calibration at Station CG-4 (June 12-13, 2003).

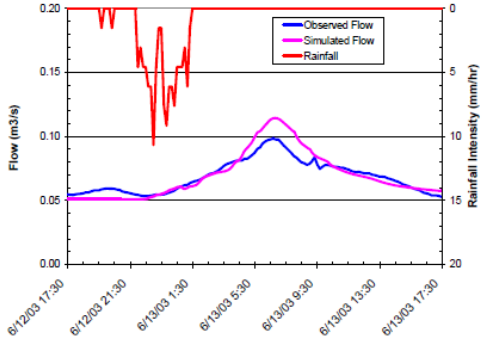

Figure 5-5. Hydrologic calibration at Station CG-6 (June 12-13, 2003).

Figure 4.10: California Gulch hydrologic calibration (Velleux 2005)

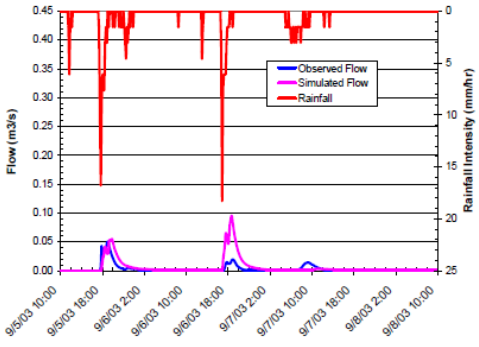

Figure 5-6. Hydrologic validation at Station CG-1 (September 5-8, 2003).

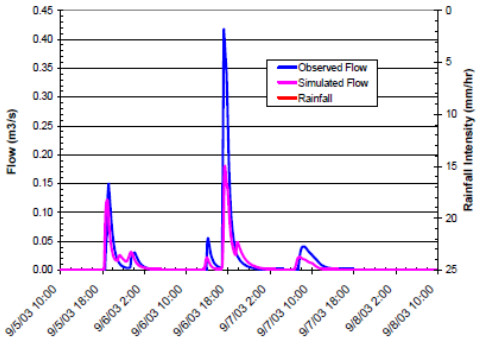

Figure 5-7. Hydrologic validation at Station SD-3 (September 5-8, 2003).

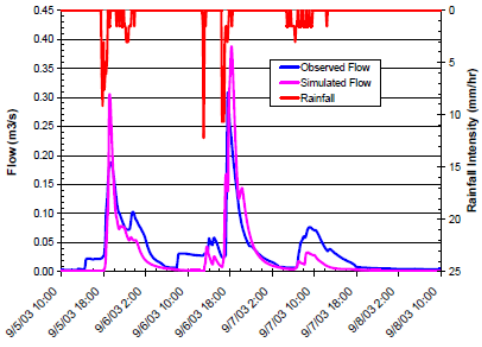

Figure 5-8. Hydrologic validation at Station CG-4 (September 5-8, 2003).

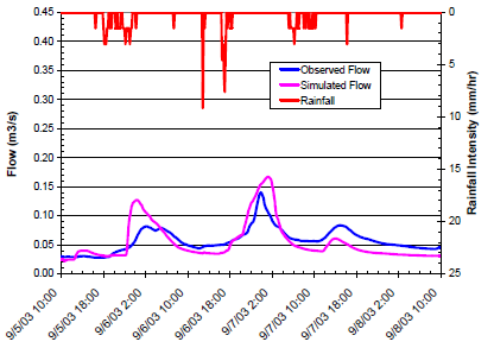

Figure 5-9. Hydrologic validation at Station CG-6 (September 5-8, 2003).

Figure 4.11: California Gulch hydrologic validation (Velleux 2005)

Chapter V. Flood Routing, Point Source Simulation

Section 5.1 Overview of Work

A point source hydrograph can be inserted into the DEM of a TREX simulation at a specified raster cell. In this way flood routing can be done in order to analyze the characteristics of the flood progression through a watershed. Particularly the inundation of the flood plain as a function of time and downstream distance can be simulated.

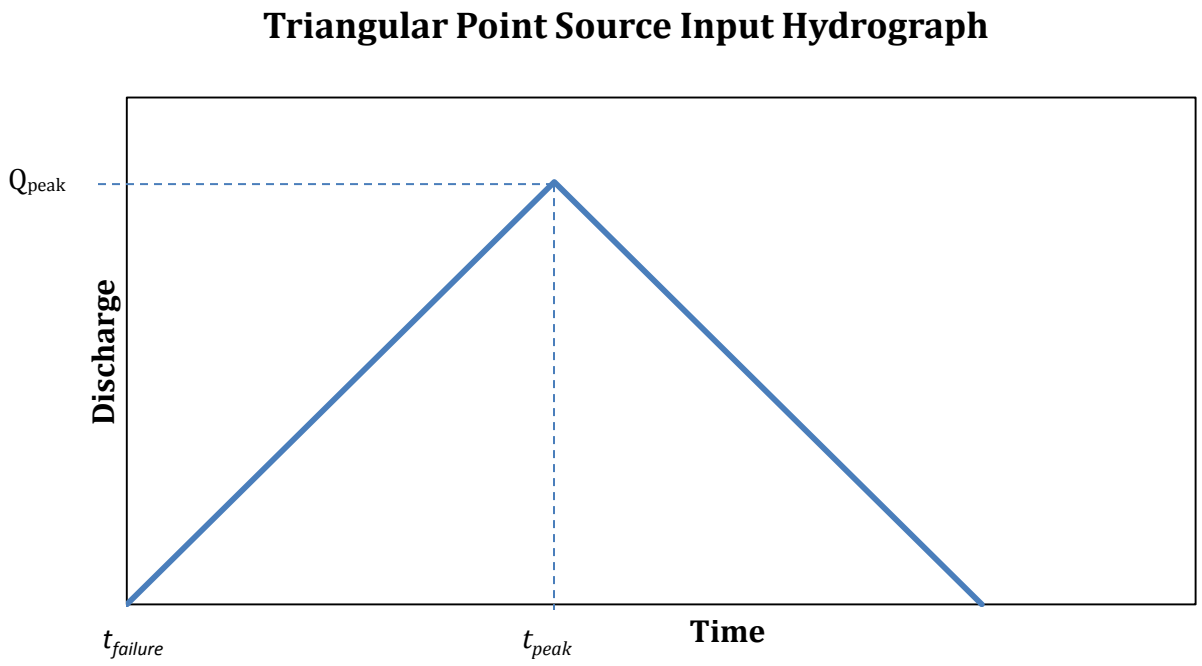

Figure 5.1: Typical approximated point source hydrograph

The outflow from a dam failure can be routed within the TREX model without simulating the localized failure mechanism. A user defined hydrograph can be introduced to a point in the watershed. In this way a known dam failure hydrograph can be routed downstream and through the flood plain. Also a dam failure can be simulated with an

empirical, an analytical, or an explicit dam breach numerical model and the determined outflow can be input into TREX to be routed through the watershed.

Section 5.2 Model Stability and Time Step Analysis Methods

In order to route dam failure magnitude flood flows within the TREX model a time step must be determined which is suitably small as to establish model numerical stability. The explicit scheme, finite difference numerical solving method employed by TREX will remain stable as long as a suitably short time step is used for the model calculations. TREX has a time step mode in which the model calculates the maximum time step allowed at every iteration that maintains numerical stability. This mode determines a time step which satisfies the Courant-Friedrichs-Lewy (CFL) condition.

$$\frac{cdt}{dx} \leq C \tag{5.1}$$

In Equation 5.1: c = wave celerity

dt = model time step

dx = modeled raster cell size

C = Courant number

A finite differencing numerical model scheme has a physical domain of dependence which consists of a spatial dimension and a temporal dimension. The domain of dependence within a numerical model is the set of all points in the past from which information can propagate at or slower than the wave celerity (Julien 2002). The differencing domain, or numerical domain of dependence, consists of the set of state variable values used to determine the value of the next numerical solution. In order for a

forward marching numerical scheme to be stable, the numerical domain must be wider in the spatial dimension than the domain of dependence.

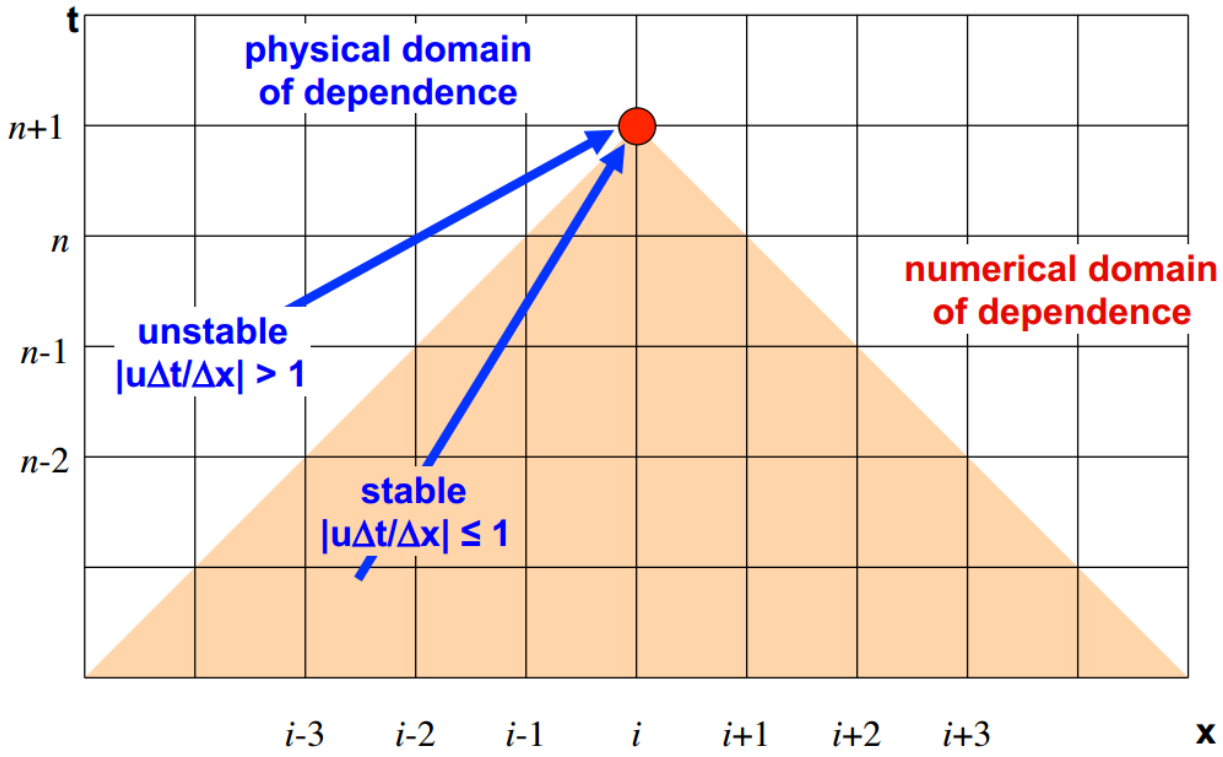

Figure 5.2: Numerical model domains (Schär 2014)

The Courant number can be thought of as the ratio of physical wave celerity to grid celerity. The Courant number effectively limits the total distance that wave energy can travel within every cell of a simulated domain to a percentage of the cell size for a simulated flow.

When the CFL model option is used within TREX, a Courant number is specified by the user as input. The unique model output of a simulation using this option is a file report of the model determined maximum stabile time steps for every iteration of the simulation. Point source hydrographs were introduced to the California Gulch Watershed of varying peak discharge magnitudes while using the CFL option in order to determine the maximum time step required to maintain numerical stability as a function of input discharge. Courant

numbers of 0.2, 0.5, 0.8 and 1.0 were used as constraints for four different groups of simulations. Triangular input hydrographs with peak discharges ranging from 1 m^3/s to 50,000 m^3/s were routed though the watershed to the outlet. The lowest value of the stable time steps for each simulation was recorded. In this way a graphical representation of the model's stability dependence upon peak discharge and Courant number was created.

As seen in Figure 5.3, the stable time steps are sequentially reduced as Courant number is reduced. This result should be expected as the stable time step is directly proportional to the Courant number (Equation 5.1).

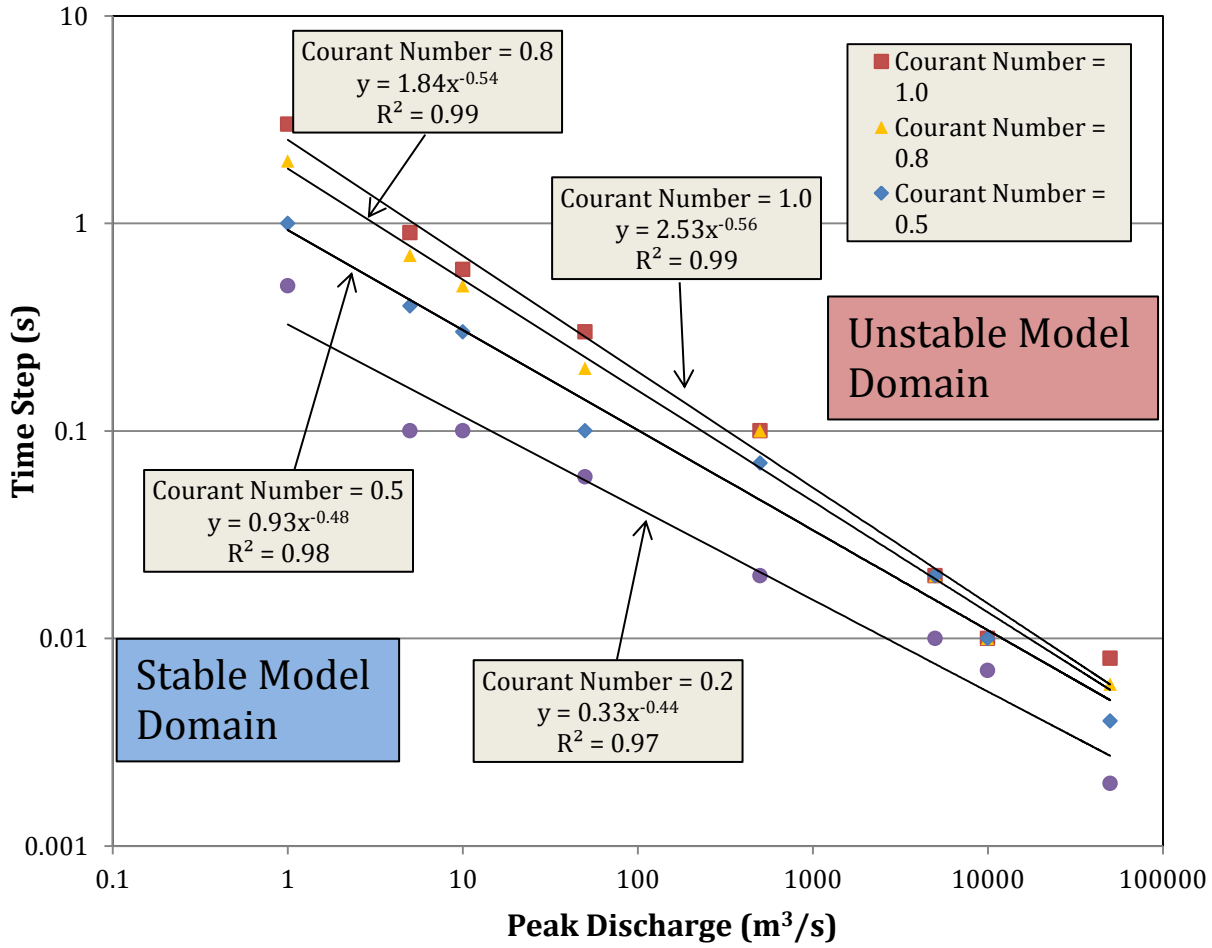

Figure 5.3: TREX, California Gulch point source stability

Also celerity should be expected to increase with increasing discharge as it is directly proportional to velocity (Equation 5.7). The stable time step also decreases as a power function of discharge.

A flood wave discharge can be approximated by an unsteady, one-dimensional flow in a wide rectangular impervious channel. The unit discharge (q), and flow velocity (V) can be approximated by a power functions of depth (Julien 2012).

$$q = \alpha h^{\beta} \tag{5.2}$$

$$V = \alpha h^{\beta-1} \tag{5.3}$$

Therefore, using the Manning coefficients for channel roughness,

$$V = \alpha\left(\frac{q}{\alpha}\right)^{\left(\beta-1/\beta\right)} = \alpha^{0.6} q^{0.4} = \frac{(S_0)^{0.3}}{n^{0.6}} q^{0.4} \tag{5.4}$$

In Equation 5.4: $\alpha = \frac{S_0^{1/2}}{n}$ = Manning resistance coefficient for flow in the downstream direction

β= 5/3 = Manning resistance exponent

q = Unit discharge

V = flow velocity

h = flow depth

S_0 = Bed slope

n = Manning roughness coefficient

The Kleitz-Seddon relationship for floodwave celerity is the following (Julien 2012):

$$c = \frac{\partial Q}{\partial A} \tag{5.5}$$

The floodwave celerity equation then reduces to the following (Julien 2012):

$$\frac{\partial h}{\partial t} + c\frac{\partial h}{\partial x} = 0 \tag{5.6}$$

$$c = \frac{\partial q}{\partial h} = \beta\alpha h^{\beta-1} = \beta V = \frac{5(S_0)^{0.3}}{3n^{0.6}} q^{0.4} \tag{5.7}$$

When this equation for celerity is inserted into the CFL equation, the following relationship between stable time step and discharge is obtained.

$$dt \le \left[\frac{3C(dx)n^{0.6}}{5(S_0)^{0.3}} \right] q^{-0.4} \tag{5.8}$$

In Equation 5.8: c = wave celerity

dt = model time step

dx = modeled raster cell size

C = Courant number

Substituting in the relationship between total discharge (Q) and unit discharge (q),

$$dt \le \left[\frac{3C(dx)n^{0.6}W^{0.4}}{5(S_0)^{0.3}} \right] Q^{-0.4} \tag{5.9}$$

In Equation 5.9: W = Channel width

Q = total discharge

Equation 5.9 provides a general theoretical description of the dependence of stable model time steps upon discharge. This relationship is very generalized and simplified. Also for high discharge flood flows there is no easy way to determine or assume a value for either the width of the flow, or for the Manning roughness coefficient (n). For these reasons it is not possible to make a direct comparison between model simulated stable time steps and theoretical values. However, what is noteworthy here is that the power of -0.4 by which the time step varies with discharge in Equation 5.9 is in decent agreement

with the powers yielded by the point source CFL simulations plotted in Figure 5.3. These powers ranged from; -0.44 for a Courant number of 0.2, to -0.56 for a Courant number of 1.0. This result provides some evidence of a general agreement between the shape of the theoretical time step dependence and the modeled dependence.

The TREX model has been applied to other watersheds for the purpose of modeling extreme precipitation and flood events. Time step and discharge data were compiled from TREX flood simulations in watersheds in Korea and in Malaysia to compare stable flood simulations from other watersheds with the simulation results from California Gulch. The Duksan Creek and Naerin Creek watershed simulations from Korea were used (Kim 2012). Also the Lui, Semenyih and Kota Tinggi watershed simulations from Peninsular Malaysia were used (Abdullah 2013). These 5 watersheds all have very different hydrologic characteristics. Watershed areas vary from 33 km^2 to 1,635 km^2. Also variables such as slope, land use, soil type and vegetative cover vary widely between these watersheds and between these watersheds and the California Gulch watershed.

High return period rainfall-runoff events, up to magnitudes as extreme as PMP and GMP, were modeled in these watersheds. These simulations yielded peak outlet discharges for several rainfall events as well as stable time steps for these simulations. These time steps were not calculated by the model to be the maximum stable time steps, however, in the interest of establishing the fastest possible model run times for these simulations an iterative trial and error process was used to find stable time steps that were as large as possible while maintaining model numerical stability. So, these time steps can be assumed to be relatively close to the maximum stable time steps. These model setups incorporated a variety of spatial grid resolutions. They varied from 30m by 30m grid cell size to 230m

by 230m grid cell size. In order to compare all of these simulations and the simulations from California Gulch the model time step divided by the grid resolution was plotted against peak outlet discharge for each simulated event (Figure 5.4).

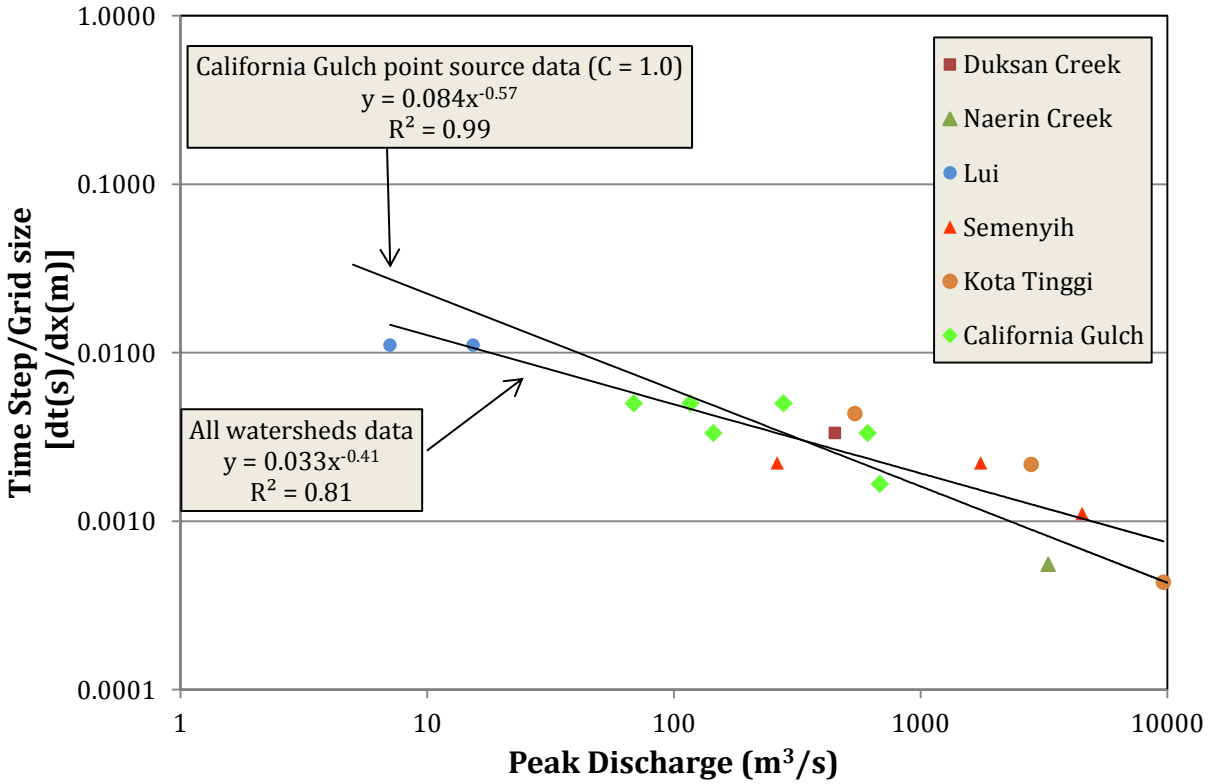

Figure 5.4: Model stability watershed comparison (Kim 2012) (Abdullah 2013)

In Figure 5.4 a trend line was plotted for all of the rainfall-runoff simulations. Also the data from the California Gulch point source simulations with the Courant number of 1.0 was plotted. The trend line plotted for all of the watersheds proved to fit the data fairly well even given the wide range of modeled hydrologic variables between the different watersheds and different precipitation events. While the Courant trend line didn't establish a boundary for the stable time steps, it did show general agreement with the multi-watershed data. Table 5.1 details the model input and output used for this analysis.

Table 5.1: Multi-watershed time step stability data

Rainfall-Runoff Simulations Watershed Name	Watershed Area, A(km²)	Peak Outlet Discharge, Q(m³/s)	Precipitation Event Duration (hr)	[Rainfall Intensity(mm/hr), Time(hr)]	Grid Resolution, dx (m)	Time Step, dt (s)	dt/dx (s/m)
Duksan Creek	33	452	3	62	30	0.1	0.0033
Naerin Creek	1000	3300	3	76	180	0.1	0.0006
Lui	68	15	6	[(39.5, 1.0),(16.5,2.0),(8.6,3.0),(4.4,4.0),(3.8,5.0),(2.1,6.0)]	90	1	0.0111
Lui	68	7	2	[(42.1,1.0),(4.0,2.0)]	90	1	0.0111
Semenyih	236	263	4	38	90	0.2	0.0022
Semenyih	236	1756	12	43.2	90	0.2	0.0022
Semenyih	1635	4527	10	85.7	90	0.1	0.0011
Kota Tinggi	1635	2820	168	7.6	230	0.5	0.0022
Kota Tinggi	1635	9664	120	25.8	230	0.1	0.0004
Kota Tinggi	1635	543	48	7	230	1	0.0043
California Gulch	30	279	1	203	30	0.15	0.0050
California Gulch	30	685	6	106	30	0.05	0.0017
California Gulch	30	613	24	79	30	0.1	0.0033
California Gulch	30	117	1	101	30	0.15	0.0050
California Gulch	30	145	6	30	30	0.1	0.0033
California Gulch	30	69	24	16	30	0.15	0.0050
Point Source Simulations Watershed Name	**Watershed Area, A(km²)**	**Peak Input Discharge, Q (m³/s)**			**Grid Resolution, dx (m)**	**Time Step, dt (s)**	**dt/dx**
California Gulch	30	1			30	3	0.1000
California Gulch	30	5			30	0.9	0.0300
California Gulch	30	10			30	0.6	0.0200
California Gulch	30	50			30	0.3	0.0100
California Gulch	30	500			30	0.1	0.0033
California Gulch	30	5000			30	0.02	0.0007
California Gulch	30	10000			30	0.01	0.0003
California Gulch	30	50000			30	0.008	0.0003

Section 5.3 Empirical Relationships and Examples

While certainly limited, some data about dam breach flood flows has been collected over the past century. Most commonly the peak discharge may be known or be accurately estimated. Also the time to peak, or breach formation time, might be known. These data sets, while not forming a comprehensive picture of the dam breach outflow hydrograph, do lend some critical and useful information. The peak discharge from a dam breach can reveal much about the total extent of flooding downstream of a dam. The time to peak and breach formation time parameters can lend insight into early notification capabilities. Peak discharge data has allowed researchers to empirically relate peak discharge data with various geometric parameters of dams. Some parameters that have been used in these types of regression analyses are: the maximum height of a dam, the depth of the water behind a dam, the volume of water behind a dam, and the crest length of a dam. Recently the results of many of the regression analyses that have been done over the past few decades were compiled for comparison and review (Thornton et al. 2011). These results can be found in Table 2.1 and Figure 2.2.

These empirical relationships can be incorporated into TREX simulations by using the model in conjunction with a GIS to determine the necessary parameter values for a certain precipitation event to create a dam breach outflow hydrograph, and then in turn inserting this hydrograph back into a simulation as a point source to be routed downstream.

The steps in this type of analysis are as follows:

1. Watershed input data must be collected, and the model must be calibrated and validated for the watershed of concern.

2. The dam of interest is constructed digitally in the Digital Elevation Model, DEM.
3. A precipitation event, the return period of which is of interest, is simulated on the new DEM.
4. The results of this simulation can be post processed in a GIS program to determine quantities such as the volume of water behind the dam at capacity. Also the simulation results can be used to determine the time to fill the reservoir.
5. Using one of the aforementioned empirical relationships, peak discharge and breach formation time can be estimated.
6. Using the estimated peak discharge, breach formation time, and breach initiation time, a triangular dam breach outflow hydrograph can be inserted into the model to simulate the dam breach flood.
7. This process can be repeated for any precipitation event and any type of dam or dam location.

This process could be used to analyze dam failures retrospectively or to create a set of failure scenario data for planning and forecasting pertaining to prospective dams. An example of this process was performed for the California Gulch site. The two hour duration, 100 year return period precipitation event was used as the input, and a 5 meter high earthen rectangular dam was used to create the reservoir. The volume of water stored behind the 5 meter high dam was calculated using a GIS. The empirical equation formulated by Pierce et al. 2010 was used to determine the peak discharge.

$$Q_p = 0.038\left(V_s^{0.475} H_d^{1.09}\right) \tag{5.10}$$

In Equation 5.10: V_s = volume of water stored behind the dam at capacity

H_d = height of the dam

The empirical equation formulated by Froehlich 1995 was used for the time of failure.

$$t_f = 0.00254\left(V_s^{0.53} H_b^{-0.90}\right) \tag{5.11}$$

In Equation 5.11: V_s = volume of water stored behind the dam at capacity

H_b = height of the water behind the dam

The time to initiation of the breach was determined from a simulation run which filled the reservoir. Assuming a triangular outflow hydrograph, which is most common, and a peak outflow occurring at the full formation of the breach, a hydrograph was created and input into TREX as a point source at the dam site during a simulation with precipitation. It was introduced to the simulation at the previously determined time at which overtopping began. This time was assumed to correspond to the time at which a breach formation would begin.

Figure 5.5 shows the results of the 100 year return period precipitation event simulation with the incorporated dam breach. Discharge was recorded and plotted for channel locations just downstream of the dam and at the outlet of the watershed.

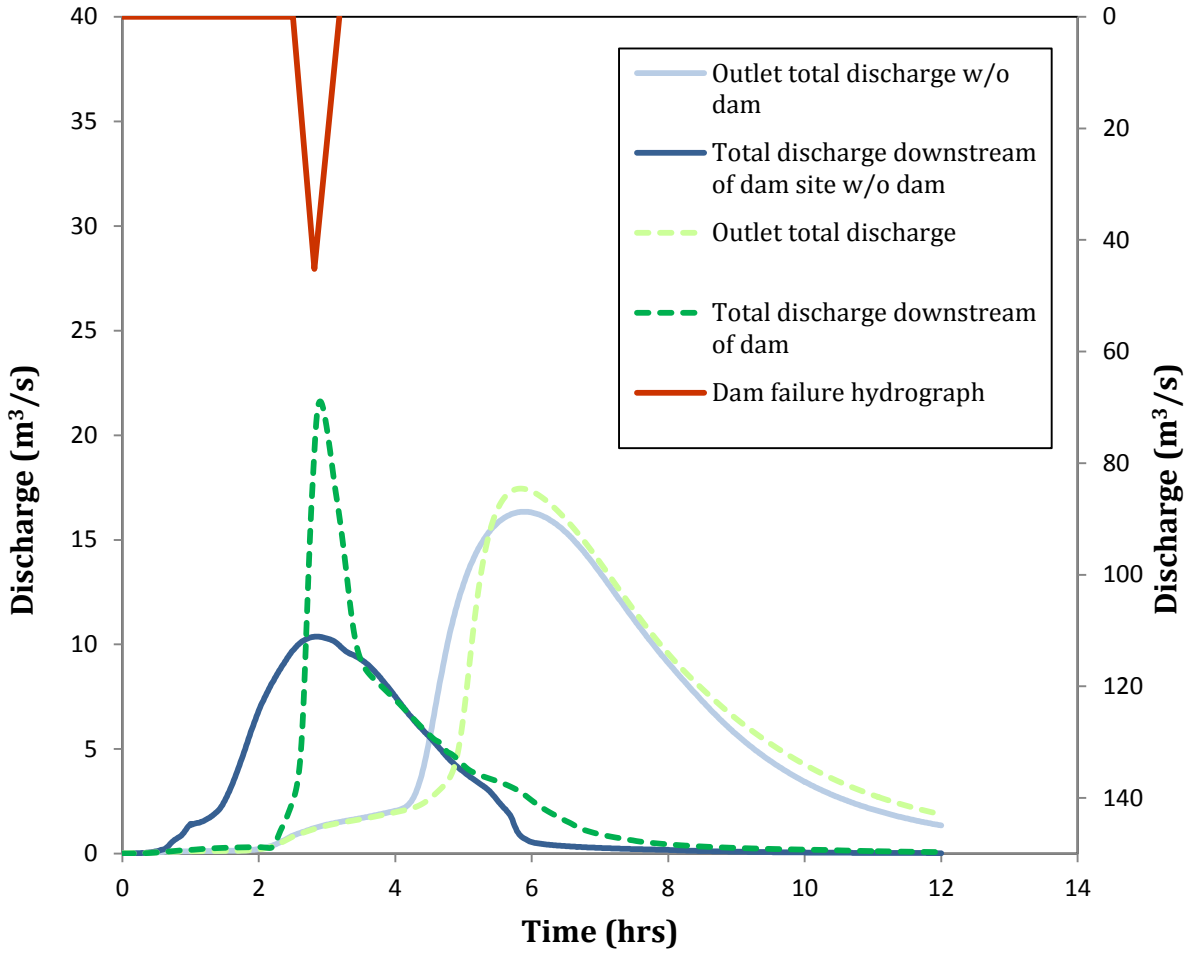

Figure 5.5: 5 meter high dam breach simulation. Input hydrograph and output hydrographs recorded just downstream of the dam site and at the outlet of the watershed for two conditions. First with no dam in place, and second with the 5 meter high dam across the channel.

Section 5.4 Areal Extent of Flood Plain Inundation

The areal extent of flooding due to a dam breach or large precipitation event has always been of interest in hydrologic engineering. The ability to estimate the areal extent of flooding near a stream can provide very useful information for structure design and floodplain property management. TREX has the ability to route flow into and out of the floodplain from the channel and to record gridded depths at a defined time interval. When the simulated output depths are input to a GIS program, the areal extent of flooding can be

visualized and quantified. The areal extent can be correlated to the return period of a storm or to the size of a dam failure.

Within a GIS program the model simulated depths up to a critical value can be displayed for any time step. This provides maps of the flooding up to a certain depth as the flood wave progresses downstream. This visualization could allow flood management programs to relate the areal extent of flood inundation with time. Additionally the total area inundated up to a critical value can be calculated to plot and analyze the magnitude of the areal extent of flooding relative to the size and timing of the input hydrograph.

Figures 5.6 through 5.8 show the results of a 4000 m^3/s peak discharge, one hour duration triangular input hydrograph as it is routed downstream. This point source was input to the model at the dam site described in Chapter VI and shown in Figure 6.2 and routed to the watershed outlet. These maps, which portray the flood plain area inundated to a depth of over 1 meter 45 minutes after the introduction of the flood wave to the watershed, were created in ESRI ARC Globe.

Figure 5.6: 4,000 m^3/s point source floodplain inundation at 45 minutes after flood wave introduction, (depth ≥ 1 meter)

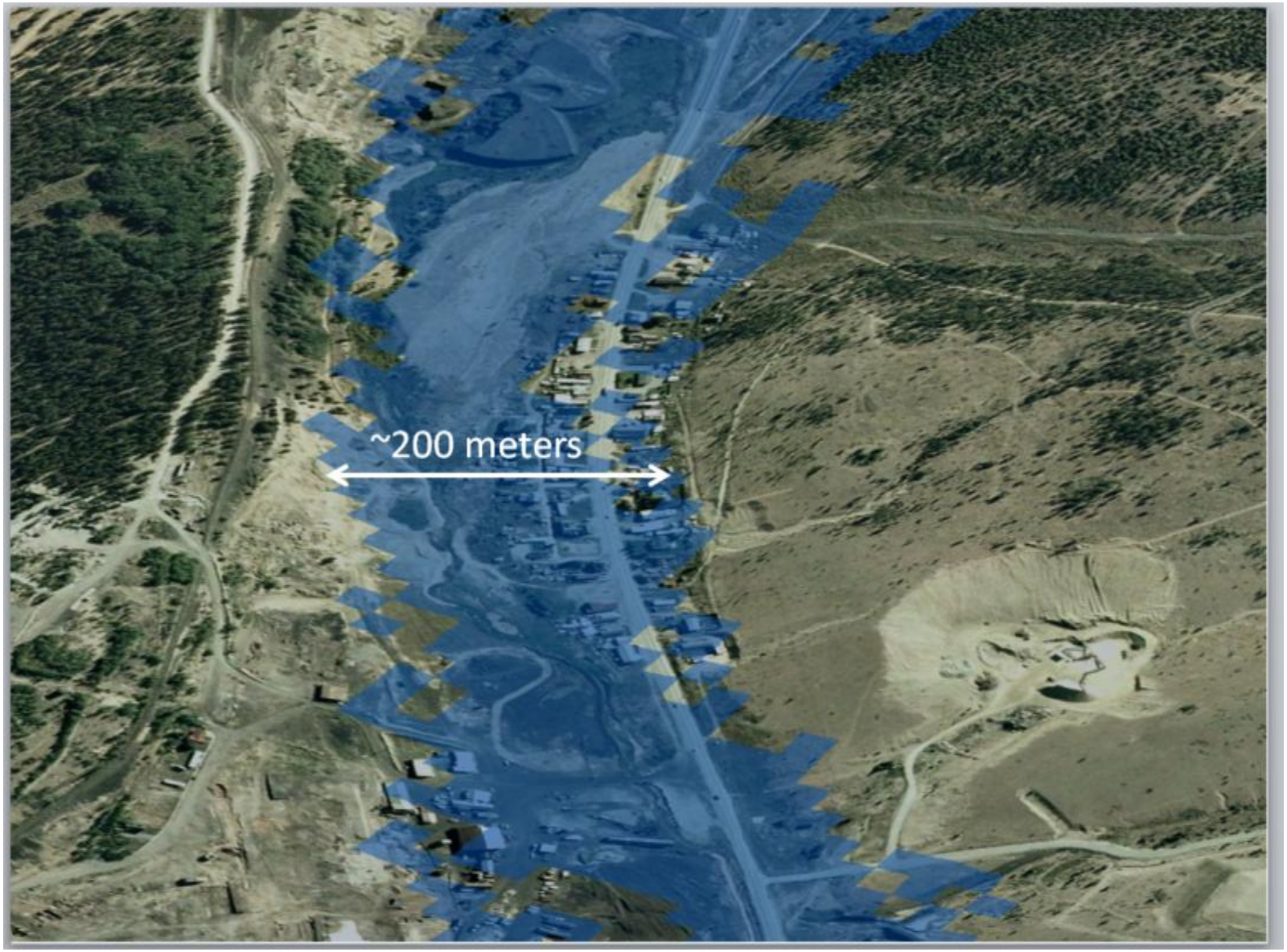

Figure 5.7: 4,000 m^3/s point source (zoom 1) floodplain inundation at 45 minutes after flood wave introduction, (depth ≥ 1 meter)

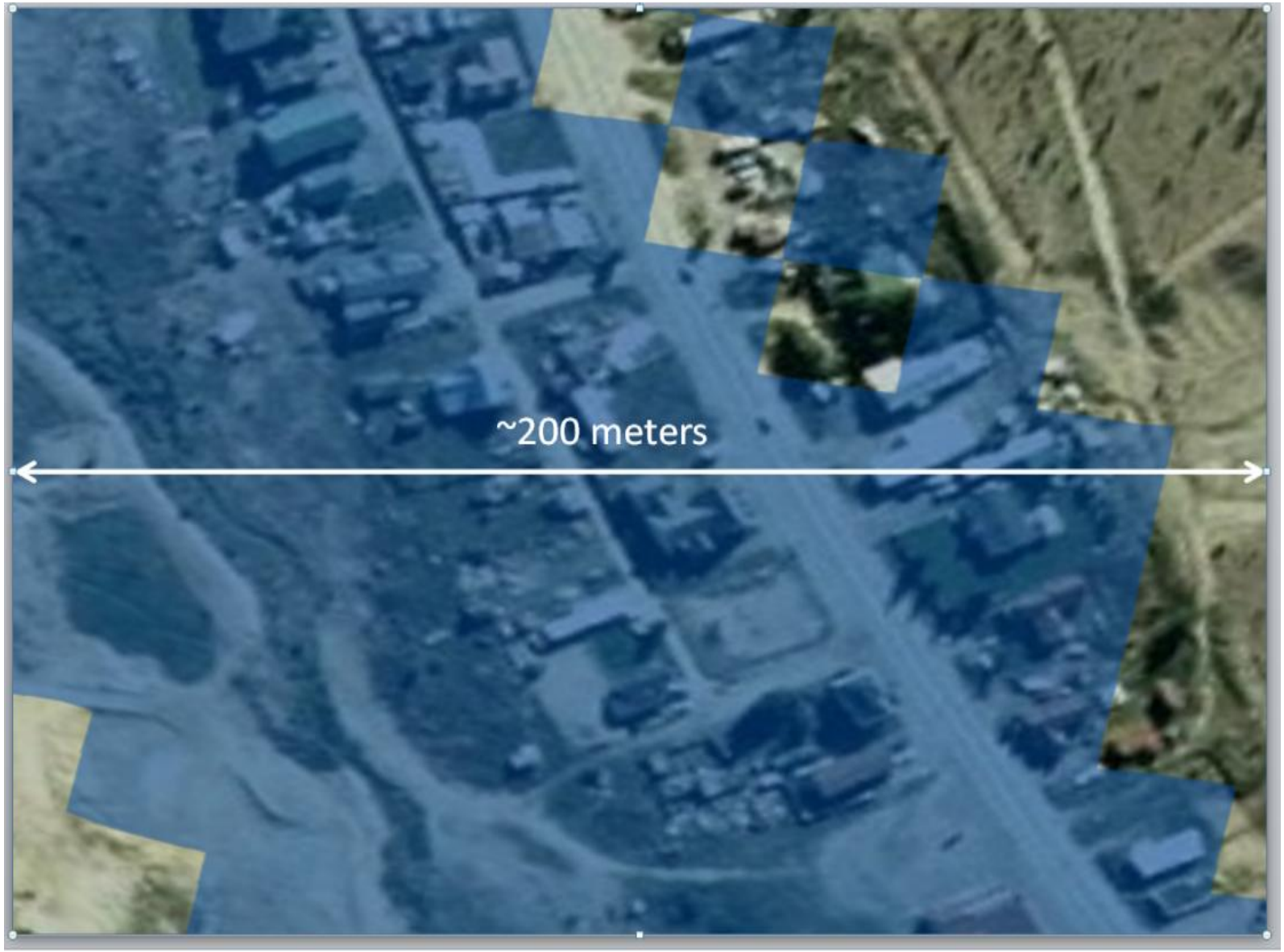

Figure 5.8: 4,000 m^3/s point source (zoom 2) floodplain inundation at 45 minutes after flood wave introduction, (depth ≥ 1 meter)

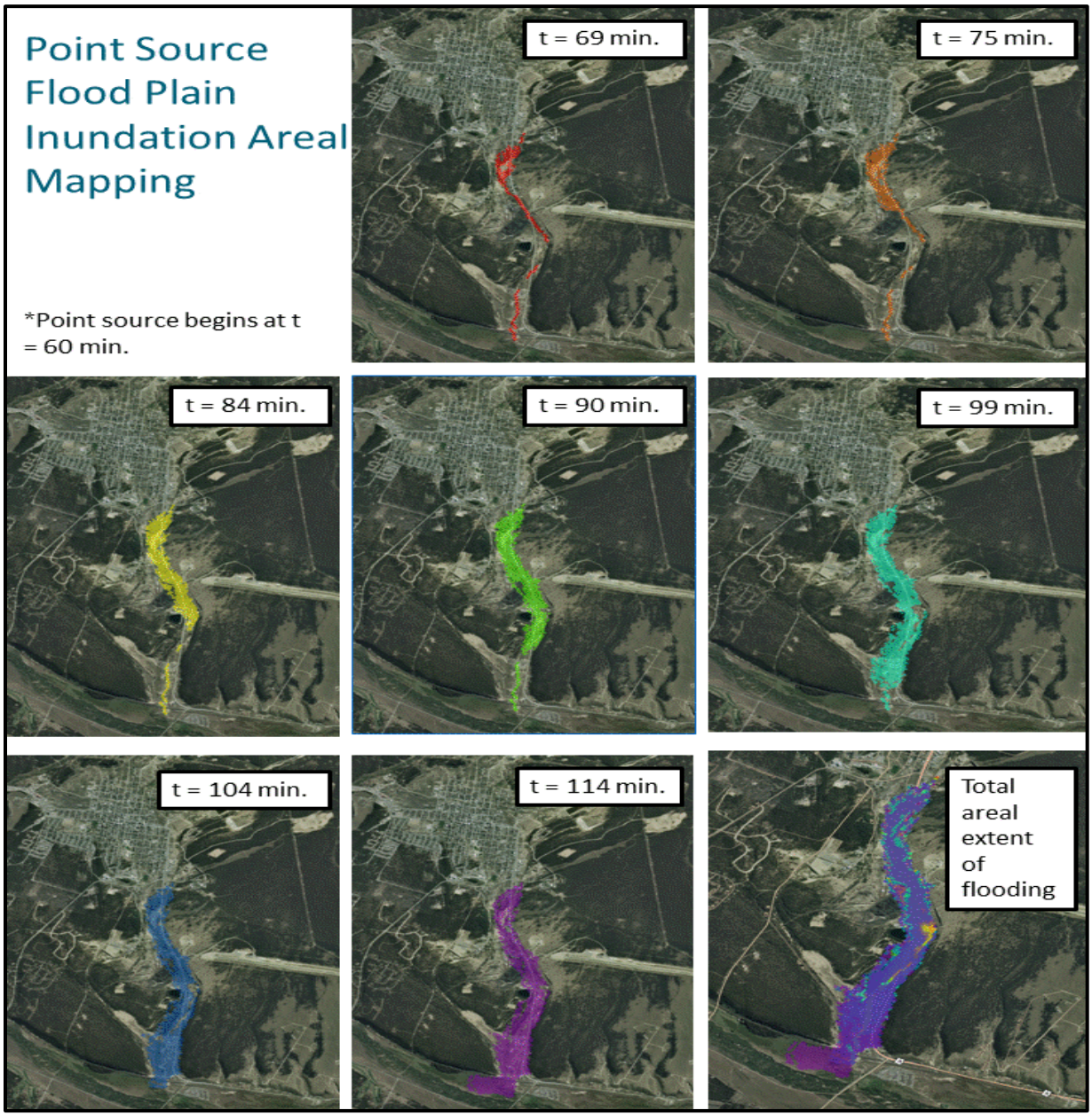

Figure 5.9: 4,000 m^3/s point source floodplain inundation at selected time steps, (depth ≥ 1 meter)

Through a GIS program the total flooded area downstream of an input point source can be calculated at every model time step. Figure 5.10 shows the total area flooded to a depth of over 1 meter downstream of the dam site for a 7,000 m^3/s peak discharge input hydrograph.

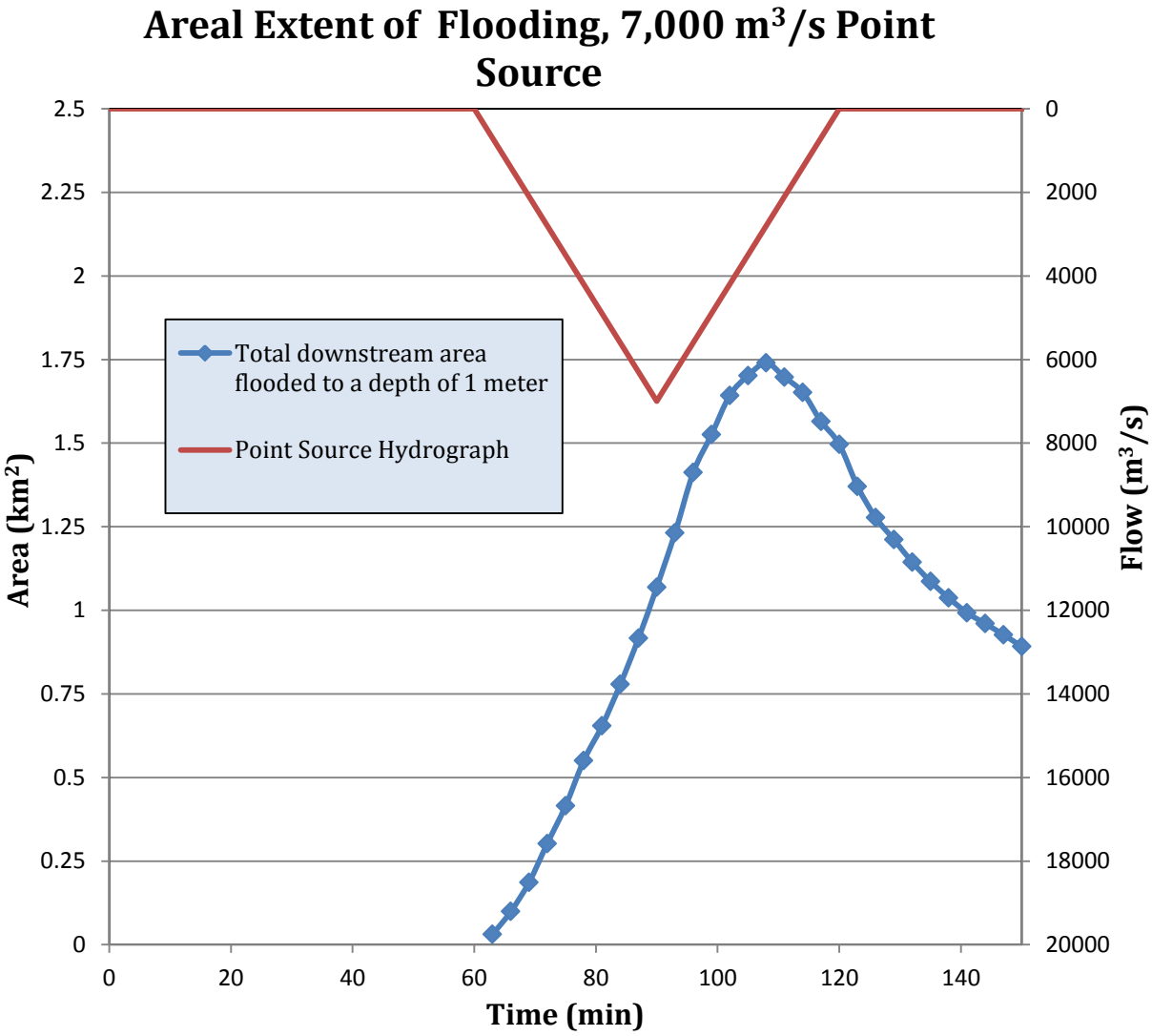

Figure 5.10: 7,000 m³/s point source floodplain inundation

Section 5.5 Discussion of Results

Point sources of varying magnitudes were input to the California Gulch watershed to determine the maximum permissible time step required to maintain numerical stability. The model stably routed flows of up to 50,000 m³/s peak discharge through the watershed. The CFL condition model time step option was employed to determine stable time steps given Courant numbers of 0.2, 0.5, 0.8, and 1.0. Simulations were run for a variety of peak discharge point source hydrographs and a plot was created showing the dependence of the

stable model time step on peak discharge in California Gulch (Figure 5.3). These stability plots create a time step stability threshold for floodwave routing. The CFL simulations with a Courant number of 1.0 yielded the following trendline.

$$dt = 2.35Q^{-0.56} \qquad C = 1.0 \tag{5.12}$$

In order to compare this resultant time step stability condition with stable simulations from other watersheds, TREX rainfall-runoff simulation data were taken from 5 other watersheds. These data, along with stable simulation data from California Gulch, were plotted with the CFL stability threshold trendline with C = 1.0 (Figure 5.4). The rainfall-runoff simulations all had different grid resolutions, so in order to compile them onto one plot, the time step value of each simulation was divided by the grid cell size (dx) and plotted against peak outlet discharge.

A trend line was plotted for these data with an R^2 value of 0.81. This shows that there seems to be similarity across different watersheds between stabile grid celerity and peak discharge. The CFL trend line did not create a boundary for all of the rainfall-runoff data. However the CFL power function had a similar power to that of the rainfall-runoff data and it appeared to plot through the centroid of the rainfall-runoff data fairly well. This function could be used as a first order estimation technique for determining stable model time steps for large scale and extreme rainfall runoff events and flood routing when a peak outlet discharge is known or can be estimated. If a peak outlet discharge is not known, a model simulation could be run using very conservative time steps in order to obtain a simulated peak outlet discharge. This peak outlet discharge could then be inserted in to the stable time step function to obtain a stable time step that is close to the threshold for

stability, and could be used for a series simulations. These methods could streamline the process of stable time step selection and reduce simulation run times which can be quite long for extreme events.

An example dam breach simulation was performed in the California Gulch watershed to demonstrate the ability of the TREX model to simulate dam failure events. An artificial dam was created within the California Gulch watershed and the 100 year return period magnitude storm was simulated. The volume of the reservoir and the time required to fill it were determined by a simulation with the reservoir initially empty. These values along with the input geometry of the artificial dam were input into empirical equations to determine the magnitude and timing of a simulated dam breach outflow hydrograph. This created hydrograph was then input into a simulation of the 100 year event to simulate the scenario wherein an empty reservoir fills completely and then fails due to overtopping.

The discharge was gaged just below the dam and at the outlet of the watershed to analyze the attenuation and lag of the flood wave. As expected, the hydrographs both downstream of the dam and at the outlet had sharper rising limbs and a greater peak discharge for the dam breach scenario than with no dam in place. Just downstream of the dam, the discharge was approximately 48% greater with the dam failure than with no dam in place. At the outlet, the peak discharge was approximately 5% greater with the dam breach than with no dam in place. This example dam overtopping and breach simulation was done to formalize and structure a process for dam breach simulation within the TREX model framework. This process could be used as a tool to analyze the downstream effects of prospective dams or to assess the potential downstream hazards of existing dams.

A point source of 7,000 m^3/s was used to create floodplain inundation maps through the use of a geographic information system. GIS was also used to quantify the total area of the floodplain that was flooded to a depth of over 1 meter. These mapping techniques demonstrate the ability to enhance model output visualization and interpretation through the use of GIS.

Chapter VI. Overtopping Modeling

Section 6.1 Overview of Work

Flooding from the overtopping of dams due to extreme precipitation events was simulated in California Gulch. Artificial dams were created in the California Gulch watershed DEM by modifying the elevations of cells in an arrangement across the channel. 14 dams of different heights up to 29 meters (as measured from the thalweg of the channel to the crest of the dam), and of lengths up to 780 meters (as measured across the crest), were created. Probable maximum precipitation (PMP) events were simulated as were even more extreme (global maximum precipitation, GMP) events. The GMP events precipitation intensities were estimated from an empirical relationship of the world's greatest measured precipitation events (Jennings 1950). Discharge was recorded in the channel just downstream of the dam and also at the outlet of the watershed in order to analyze the effect of dams, or empty reservoirs, on discharges within the watershed. Time series of water depths for each cell within the watershed were also recorded.

Section 6.2 Dam Possibilities and Locations

The method for constructing artificial dams within a watershed involves using a GIS program to locate the dam site and determine the raster cell elevation values within the DEM that should be modified to simulate the desired dam geometry across a channel. Any combination of raster cell elevations that can represent a digital dam can be created. Rectangular or triangular profile dams can be created. Spillways can be simulated by the dimensions of the channel through the dam crest cell or by lowering a cell along the crest of the dam. Figures 6.1 and 6.3 display examples of the dams simulated.

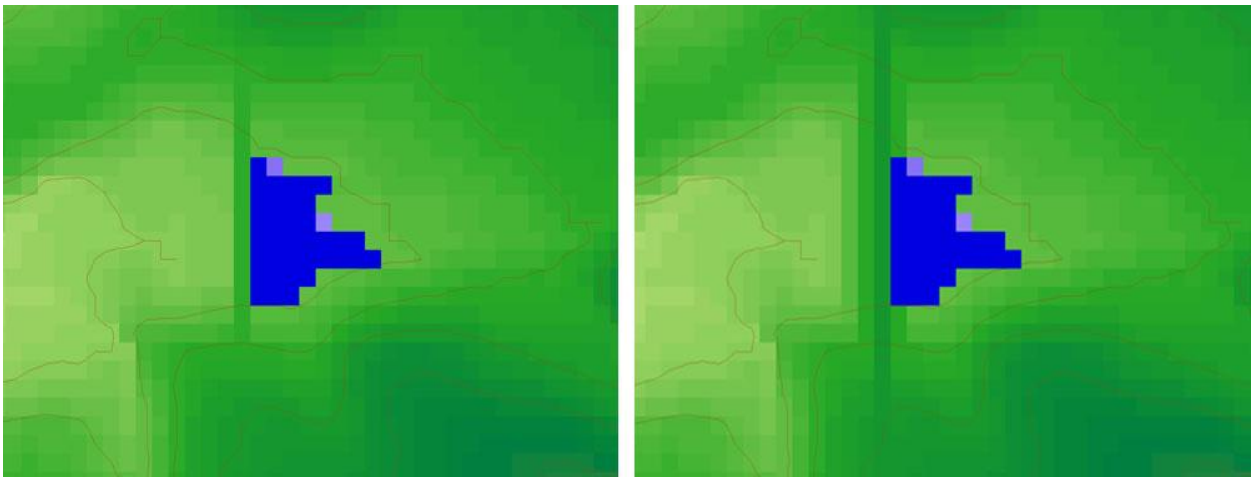

Figure 6.1: Rectangular and Triangular profile dam examples as seen from above

Dams of triangular and rectangular profile were created at a location within the California Gulch watershed for this analysis. Dam height was simulated from 1 meter to 29 meters as measured from the channel thalweg. A site was chosen within the California Gulch watershed which would be the most conducive to creating a variety of artificial digital dams within the watershed. The chosen location is on the main stem within the watershed, and just downstream of the city of Leadville.

The dam site shown in Figure 6.2 was used as the location for all of these simulations. The height of simulated dams was geographically restricted to no more than 29 meters. Any dam taller than 29 meters would be taller than the valley walls. This would force stored water out of the dammed valley at full reservoir capacity.

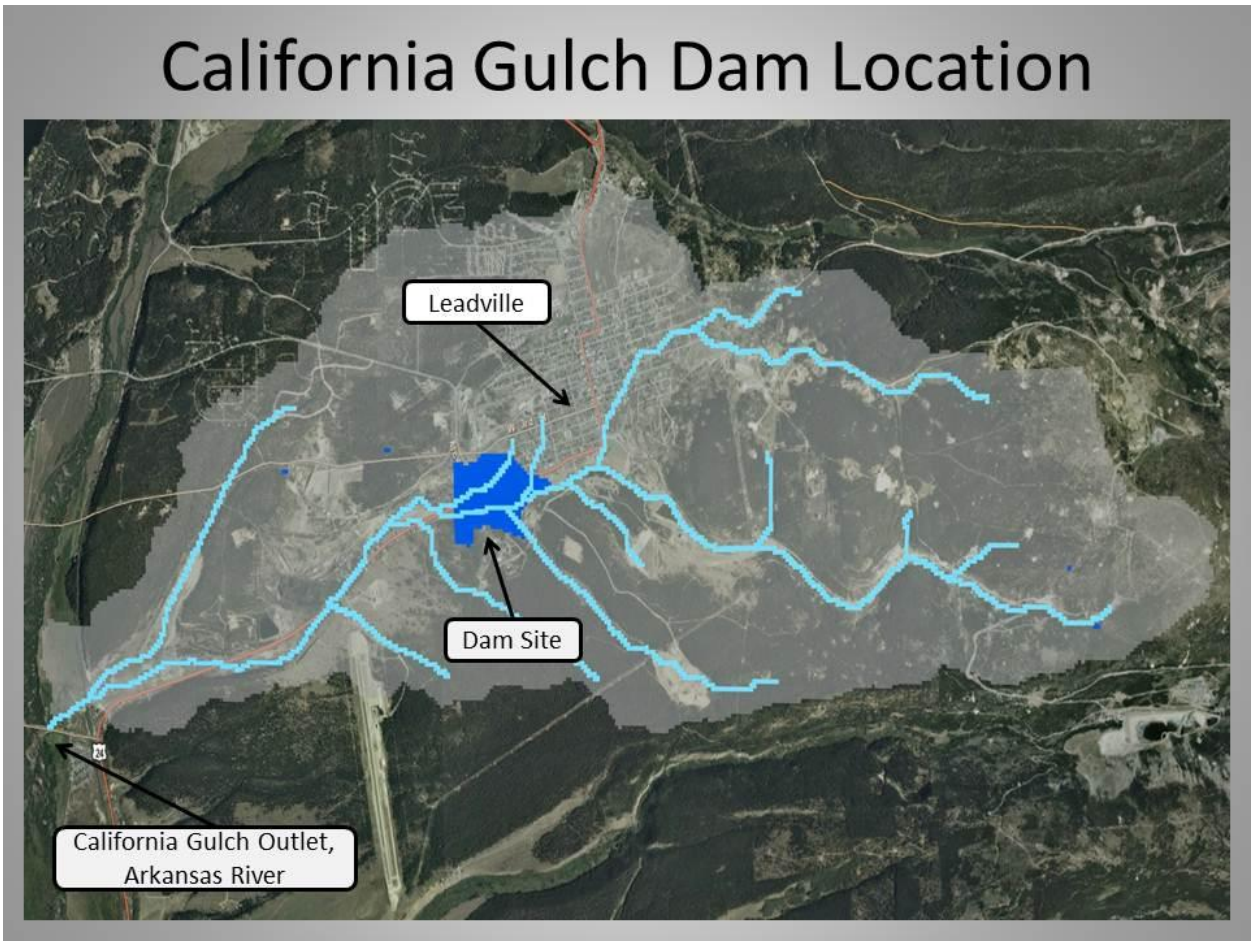

Figure 6.2: California Gulch artificial dam site location

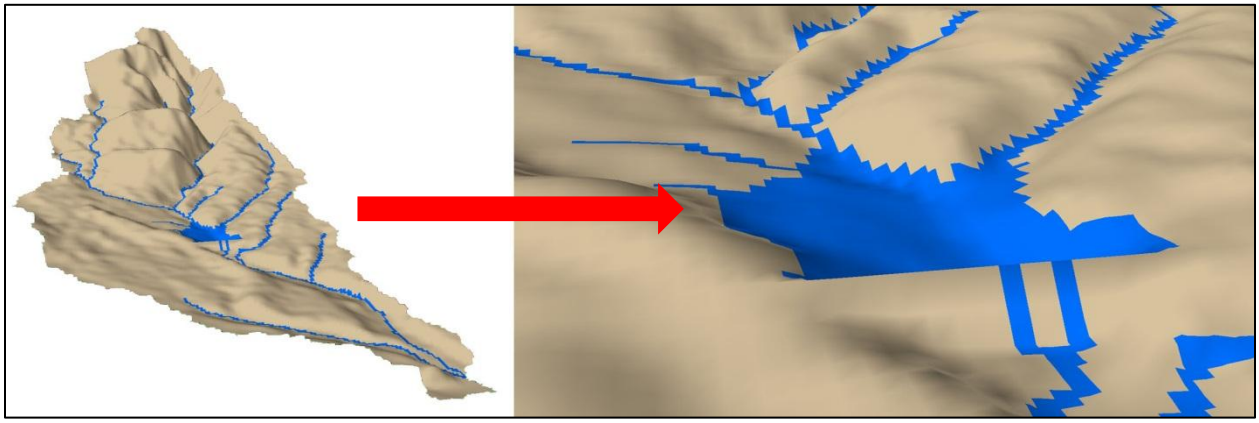

Figure 6.3: Three-dimensional dam representation

Section 6.3 Effects of Dams on Outlet Hydrographs

6.3.1 Probable Maximum Precipitation Simulation Analysis Methods

PMP maps for the region of Colorado containing California Gulch were located and used to determine the magnitude of the precipitation intensities for the 1, 6, and 24 hour duration rainfall events (Appendix 1.0). These storms were then simulated within the California Gulch watershed with a variety of artificial dams in place. For all of the simulations presented here the rainfall was uniformly distributed over the watershed and the hyetographs were all rectangular starting and ending abruptly. Surface water within the watershed would collect in the empty reservoirs and in some cases overtop the dams, in which case a flood pulse would continue to the outlet of the watershed.

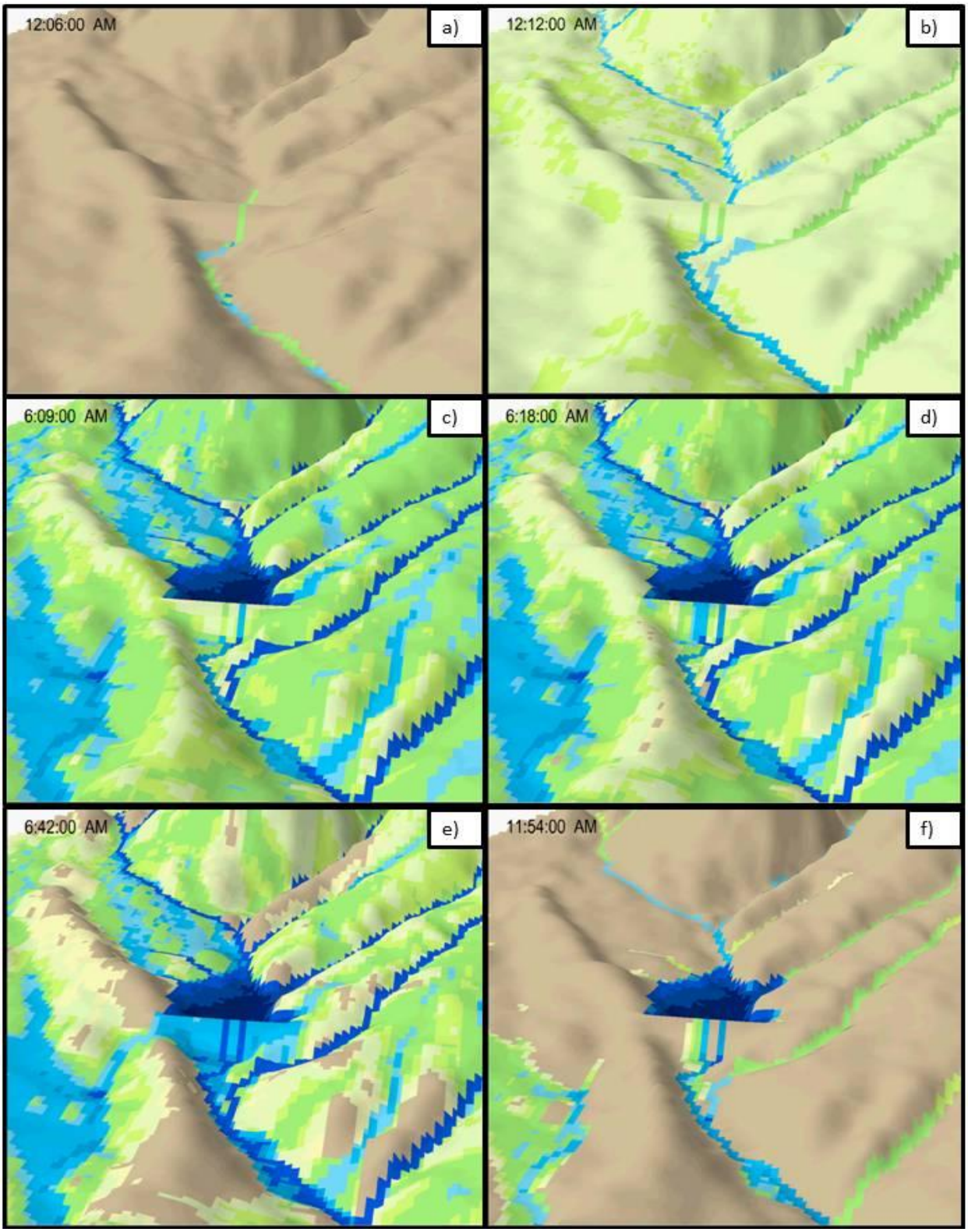

Figure 6.4: Overtopping simulation at: a) beginning of simulation, b) beginning of rainfall, c) completion of reservoir filling, d) beginning of overtopping, e) peak of overtopping flow, f) flood recession

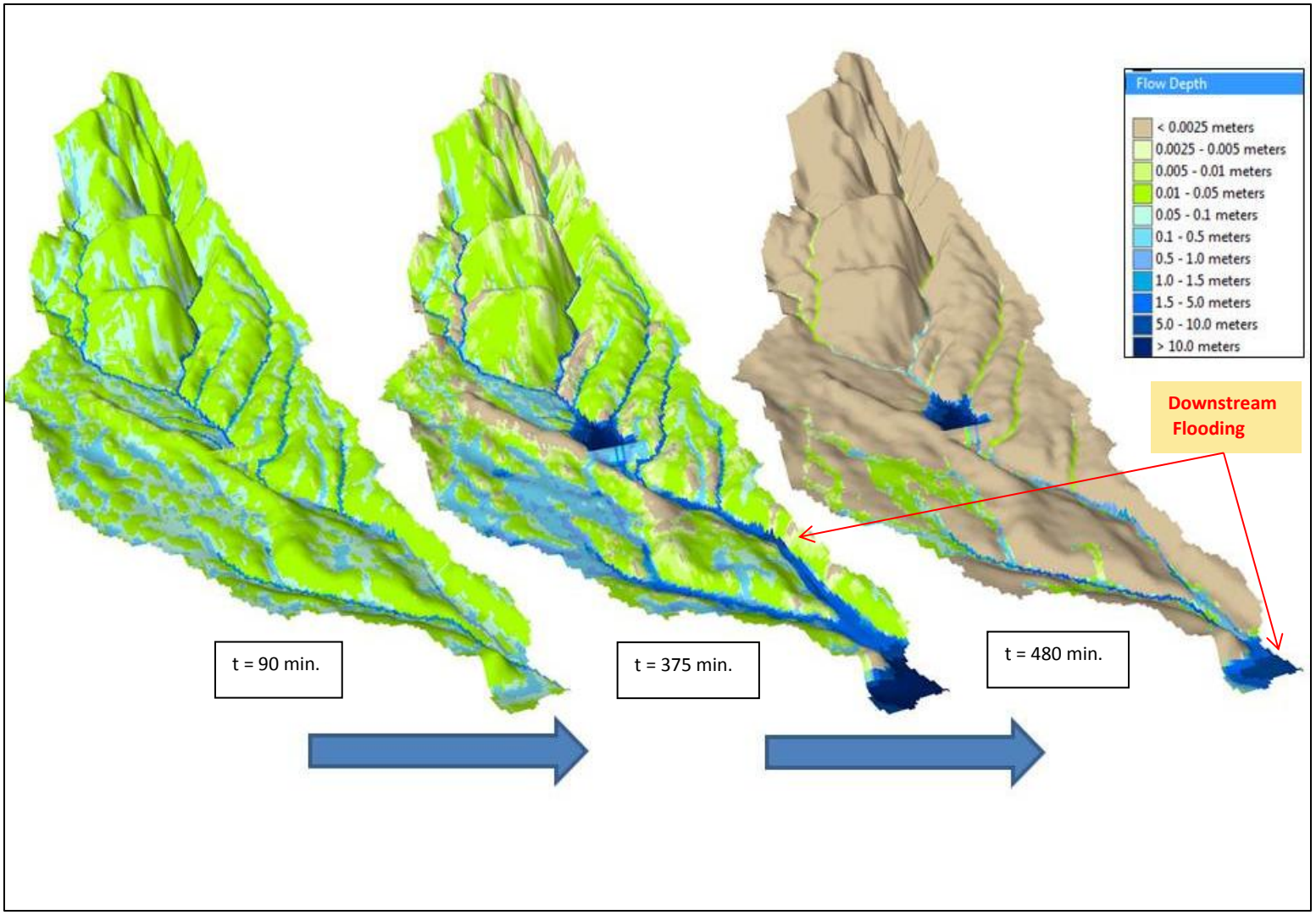

Figure 6.5: Example model output (6 hour duration GMP precipitation event dam overtopping simulation)

The 1 hour duration PMP intensity was found to be 101 mm/hr as determined through the PMP reports attained from the National Oceanographic and Atmospheric Administration (NOAA). Simulations were done with rectangular dams in place of heights: 5m, 7m, 9m, 12m, 15m, and 18m as measured from the thalweg of the channel. Also a simulation with no dam in place was done for comparison. Figure 6.6 shows the 1 hour duration PMP storm simulations for the dam site in California Gulch. A plot was also made that relates the peak outlet discharge to the height of the dams that were simulated.

Figure 6.8 shows the 6 hour duration PMP storm simulations for the dam site in California Gulch. The 6 hour duration PMP intensity was found to be 30 mm/hr also as determined from the NOAA PMP reports. Simulations were done with rectangular dams in place of heights: 5m, 7m, 9m, 12m, 15m, 18m, and 20m as measured from the thalweg of the channel and a simulation with no dam in place was done for comparison.

Finally, the 24 hour duration PMP storm event was simulated over the watershed (Figure 6.10). The 24 hour duration PMP intensity was determined to be 16 mm/hr. This precipitation intensity was simulated over the watershed with dams of heights 15m, 18m, 20m, 21m, 23m, 26m, and 29m in place. Plots were once again created of all the simulated outlet hydrographs and a plot of peak outlet discharge vs. dam height was created.

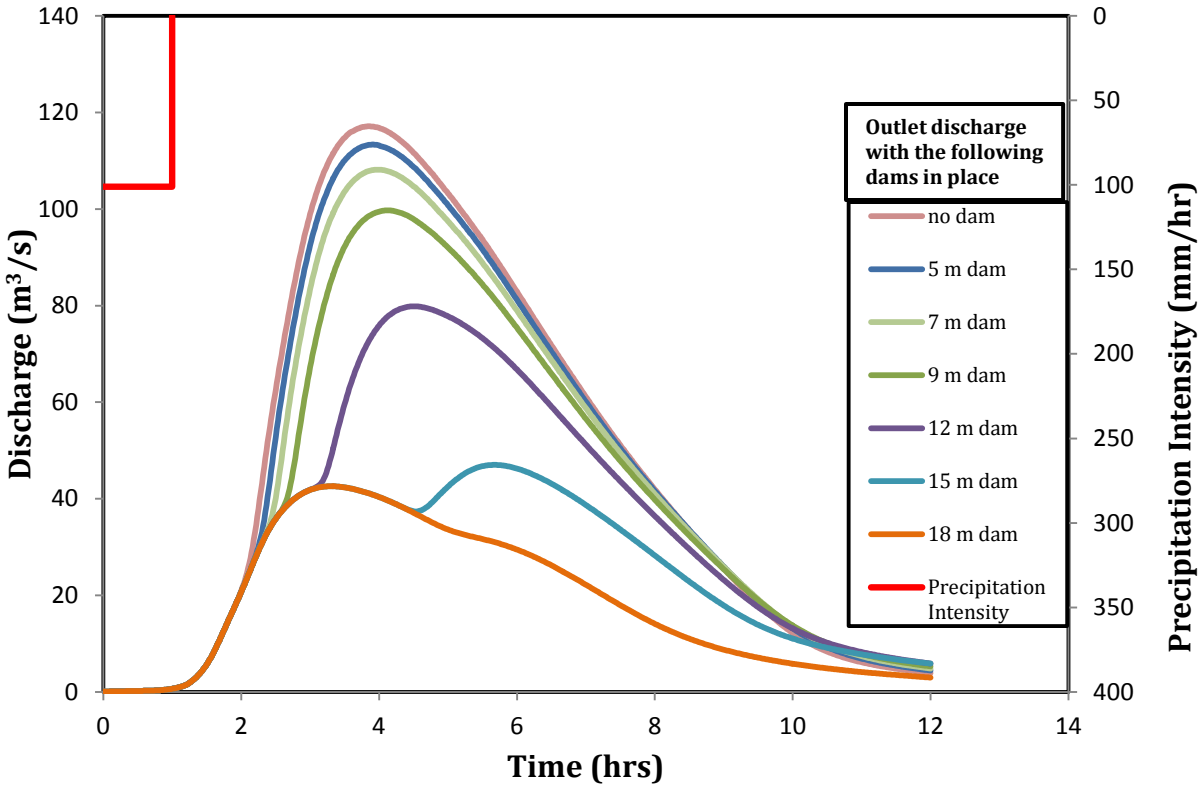

Figure 6.6: 1 hour duration PMP outlet discharge

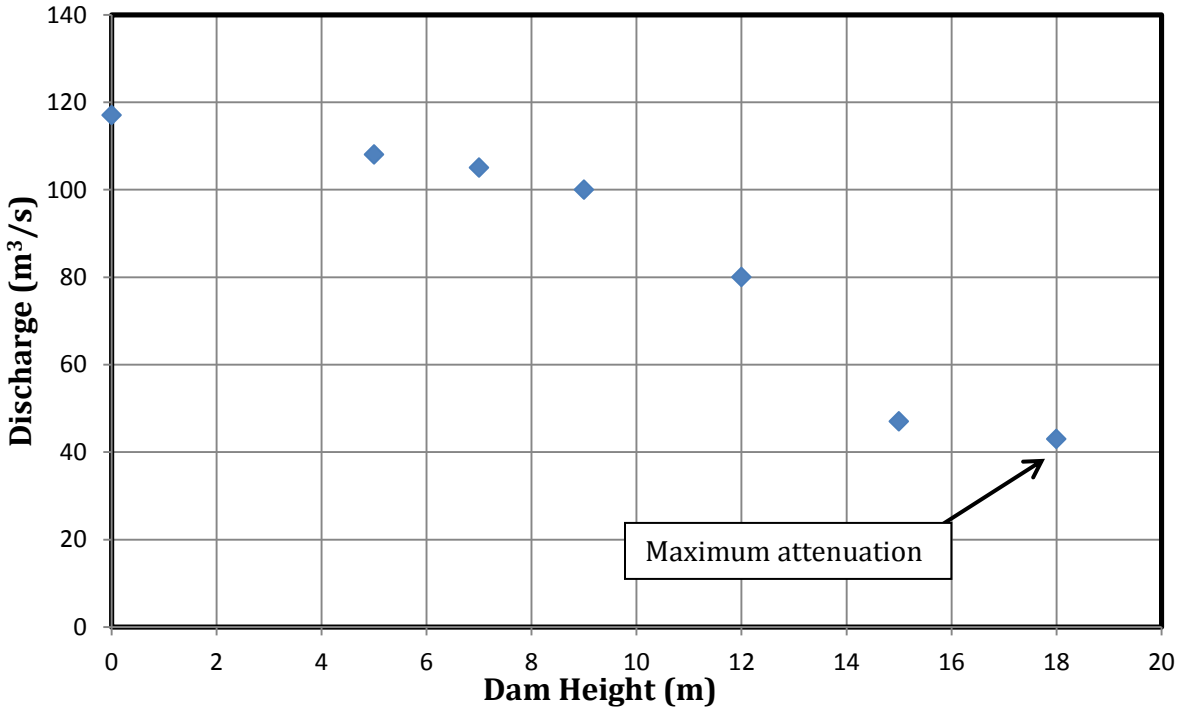

Figure 6.7: 1 hour duration PMP peak outlet discharge vs. dam height

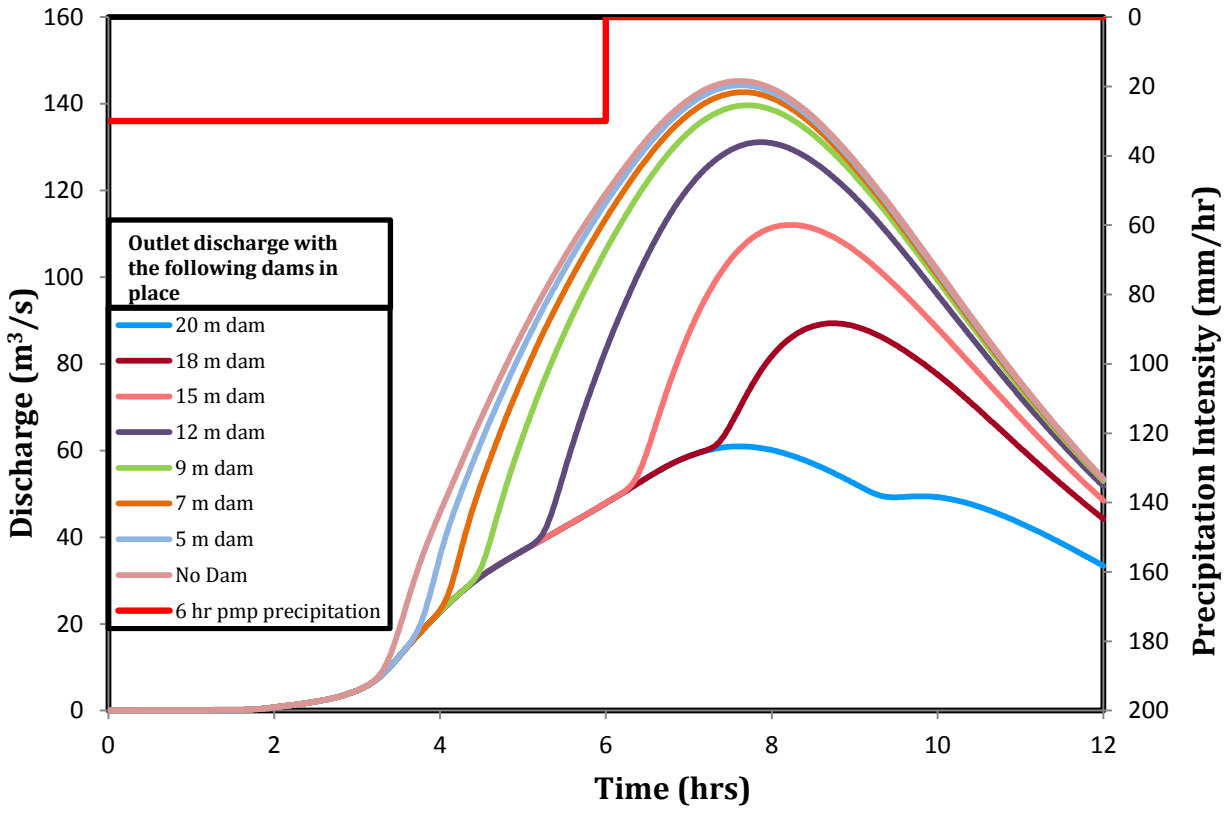

Figure 6.8: 6 hour duration PMP outlet discharge

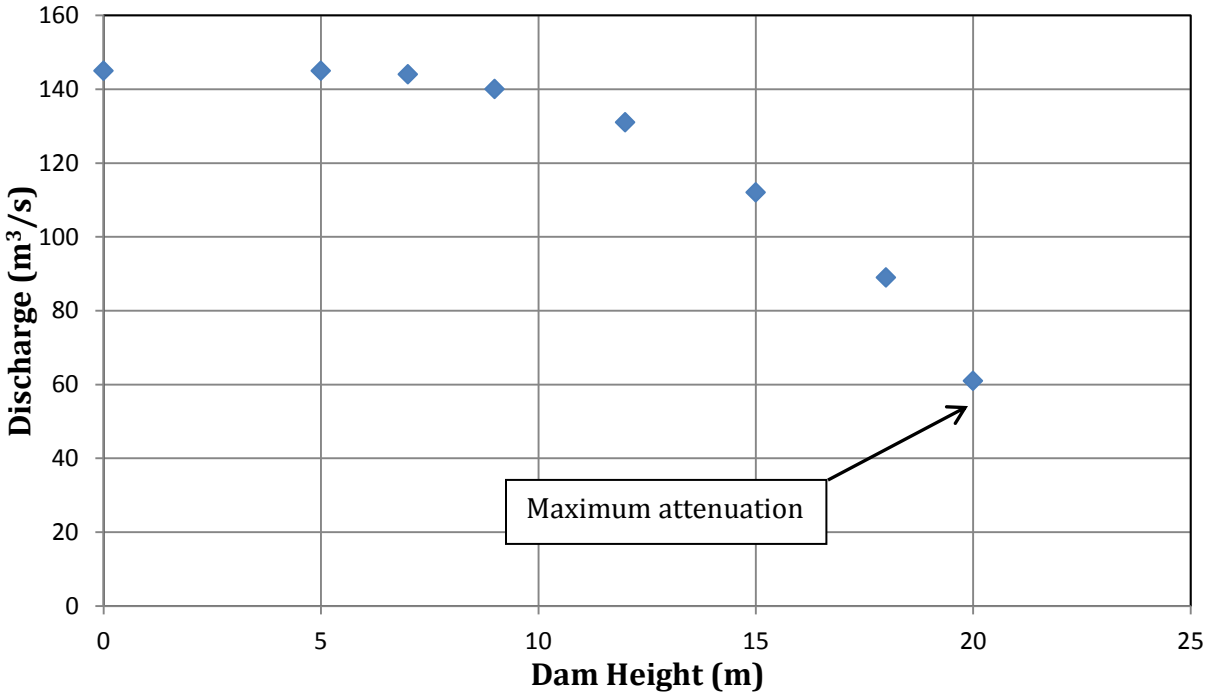

Figure 6.9: 6 hour duration PMP peak outlet discharge vs. dam height

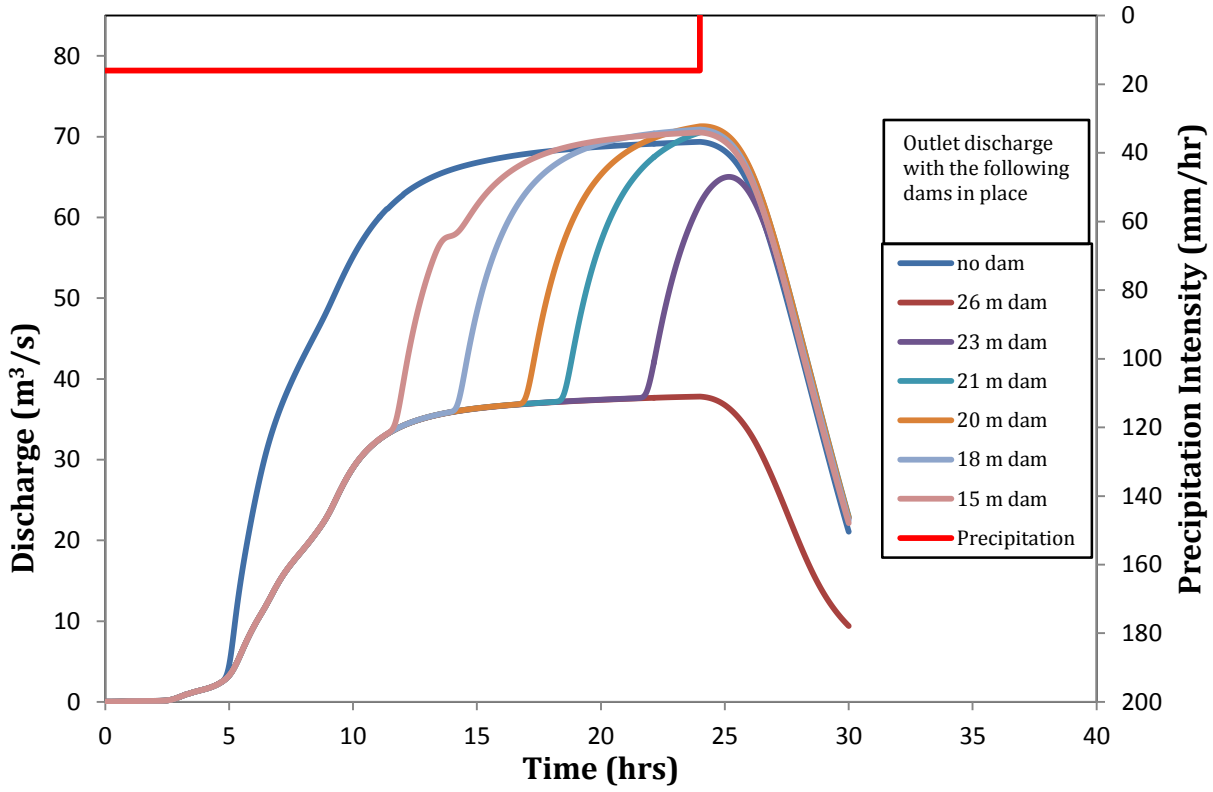

Figure 6.10: 24 hour duration PMP outlet discharge

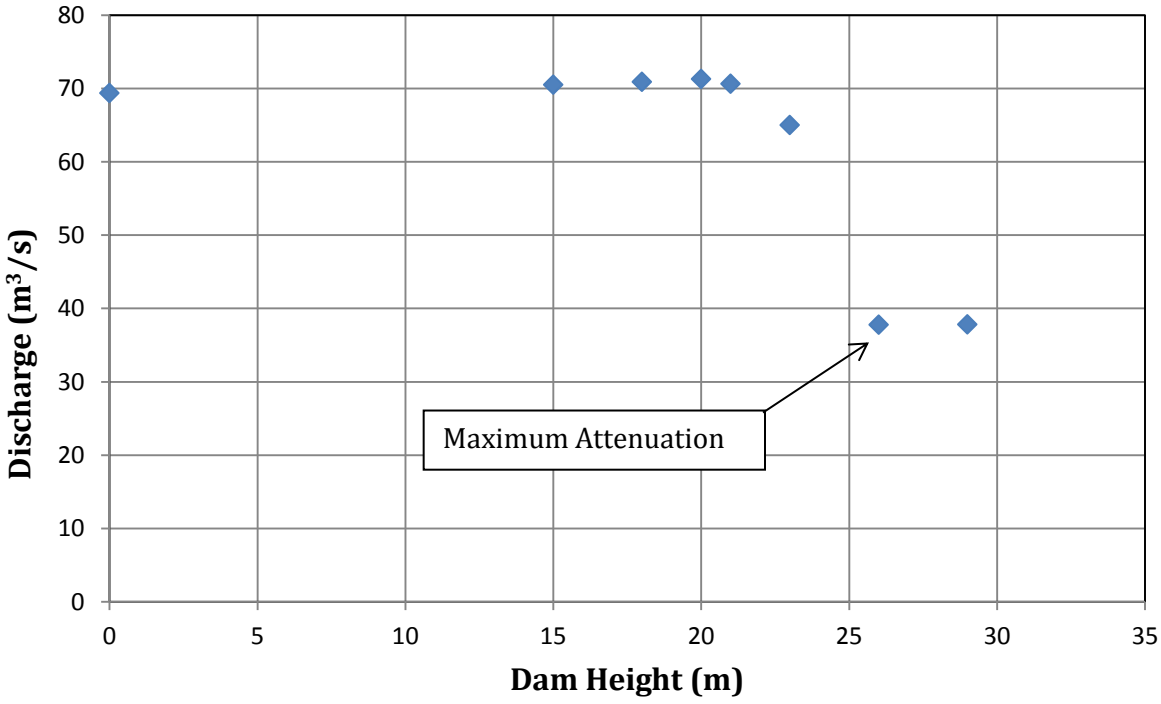

Figure 6.11: 24 hour duration PMP peak outlet discharge vs. dam height

The families of curves shown in figures 6.6, 6.8, and 6.10 represent the full range of possible outlet discharge attenuations due to dams inserted at the dam site for the 1, 6, and 24 hour duration PMP simulations respectively. The maximum attenuation of the peak discharge at the outlet of the watershed was 63% for the 18 meter rectangular dam for the 1 hour duration PMP event. The maximum attenuation of the peak outlet discharge was 58% for the 6 hour duration PMP event with the 20 meter dam in place. The maximum attenuation of the peak outlet discharge was 46% for the 24 hour duration PMP event with the 29 meter dam in place. These results are summarized in Table 6.1.

Table 6.1: Summary of PMP simulation results

PMP Event Duration	Precipitation Intensity (mm/hr)	Peak Outlet Discharge Without Dam (m^3/s)	Height of Dam causing maximum attenuation of flood (m)	Peak Outlet Discharge With Dam (m^3/s)	Attenuation (%)
1 hour	101	117	18	43	63
6 hour	30	145	20	61	58
24 hour	16	69	26	38	46

6.3.2 Global Maximum Precipitation Simulation Analysis Methods

A similar analysis to the previously described PMP analysis was done with precipitation intensities derived from a compilation of the world's largest measured precipitation events or global maximum precipitation (GMP) events (Jennings 1950). Precipitation intensities for the 1, 6, and 24 hour duration GMP events were derived from the plot in Figure 6.12 and used as TREX model input in order to quantify flood wave attenuation at the outlet of California Gulch due to dams of various crest heights. The

simulated hyetographs were rectangular and the rainfall was uniformly distributed over the watershed.

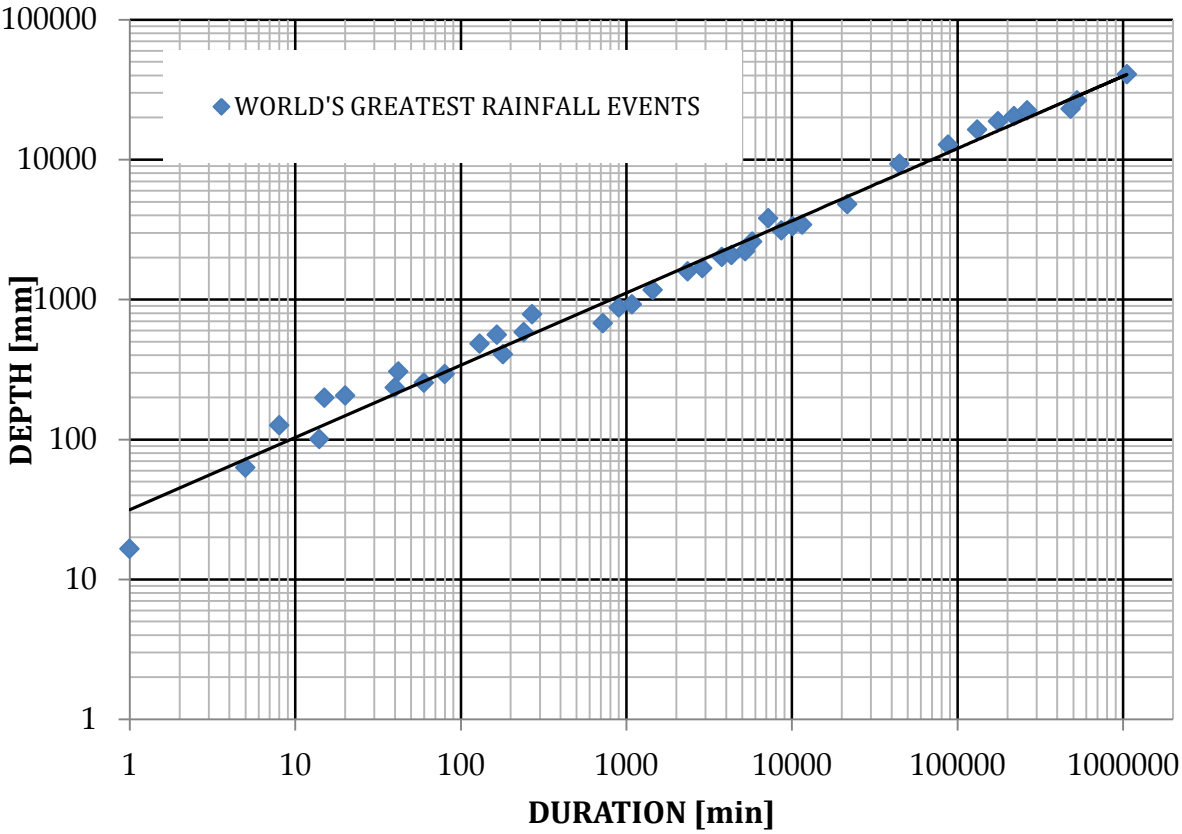

Figure 6.12: World's greatest measured precipitation

Figure 6.13 shows the family of curves describing the possible outlet flood wave attenuation due to dams when the 1 hour duration, 203 mm/hr intensity GMP event is introduced to the watershed. Dams of heights 7m, 9m, 12m, 15m, 18m, 20m, 21m, 23m, and 26m were introduced to the watershed.

A 23 meter high dam achieved the maximum flood wave attenuation of 59 %. Discharge was also plotted versus dam height for this event for a better interpretation of the dependence of peak outlet discharge on dam height. This same analysis technique was done for the 6 hour duration GMP event (Figure 6.15). A precipitation intensity of 106 mm/hr was used. Dams of heights 12m, 18m, 21m, 23m, 26m, and 29m were introduced to

the watershed. With the 29 meter high maximum height dam in place, overtopping began at approximately hour 4 and the flood wave reached the outlet in just under 1 hour. The maximum attenuation of the outlet discharge from the 6 hour duration event was determined to be 21%. This was accomplished by the 29 meter high dam. Finally, the 24 hour duration GMP event was simulated (Figure 6.17). A rainfall intensity of 79 mm/hr was simulated over the watershed and dams of heights 18m, 21m, 23m, 26m, and 29m were introduced to the dam site. The maximum attenuation of the outlet discharge for the 24 hour GMP event was determined to be 9 %. This was the attenuation due to the 29m dam. Table 6.2 is a compilation of all of the GMP results.

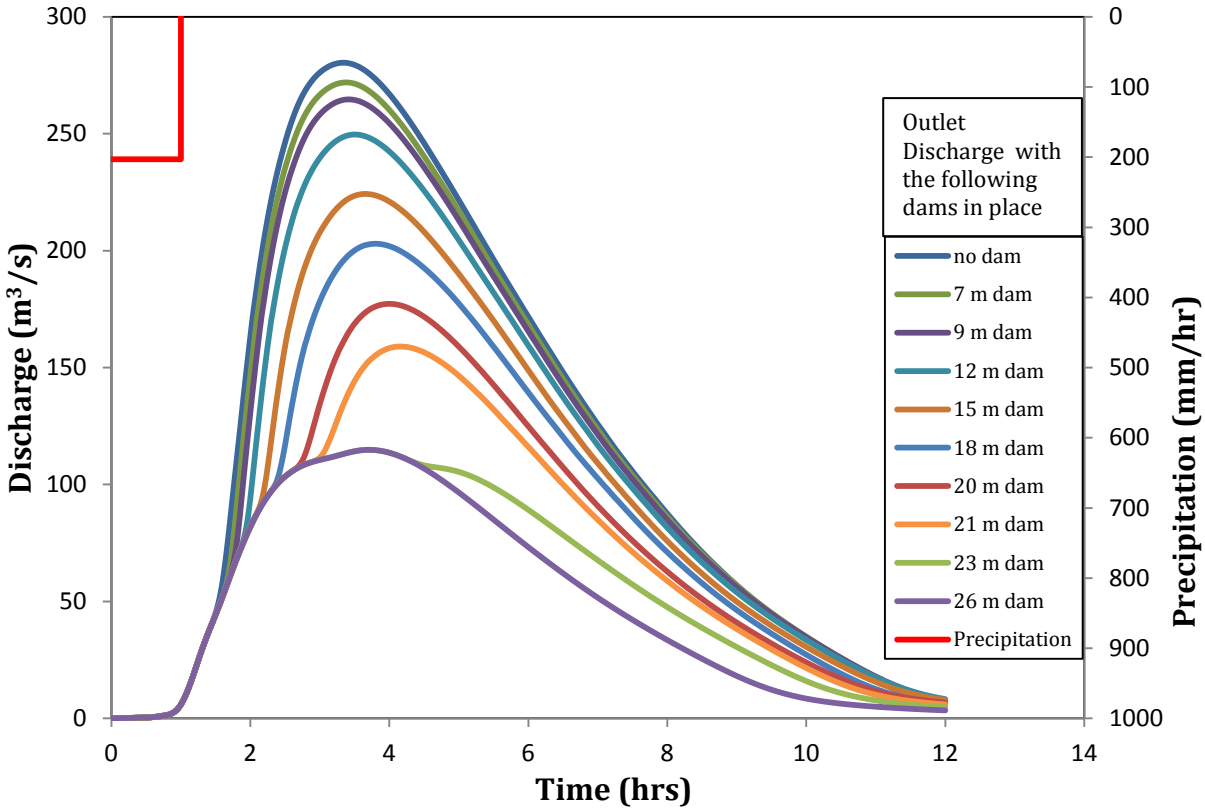

Figure 6.13: 1 hour duration GMP outlet discharge

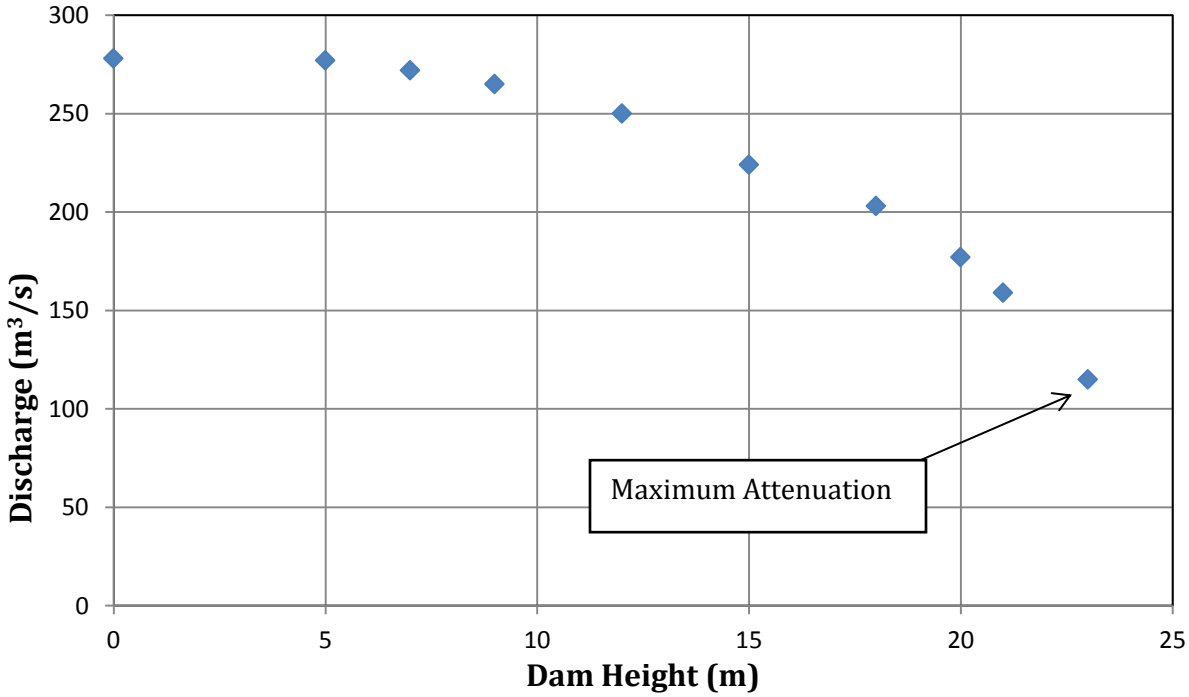

Figure 6.14: 1 hour duration GMP peak outlet discharge vs. dam height

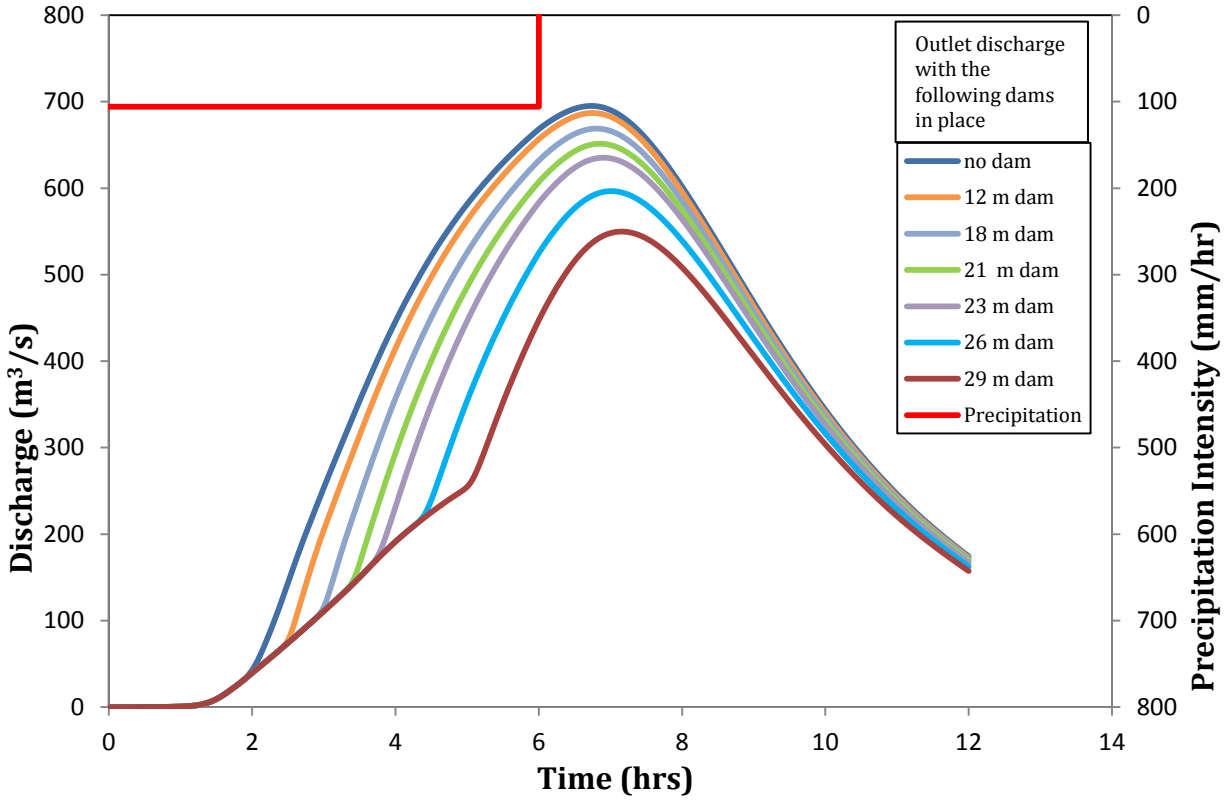

Figure 6.15: 6 hour duration GMP outlet discharge

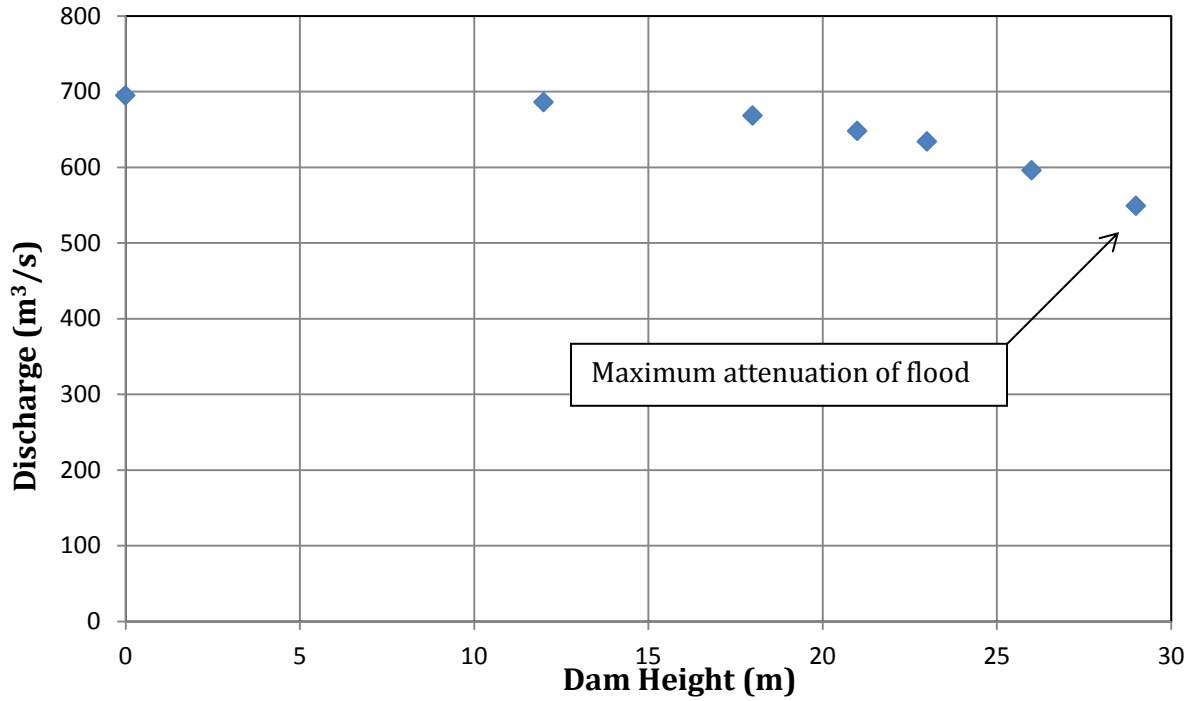

Figure 6.16: 6 hour duration GMP peak outlet discharge vs. dam height

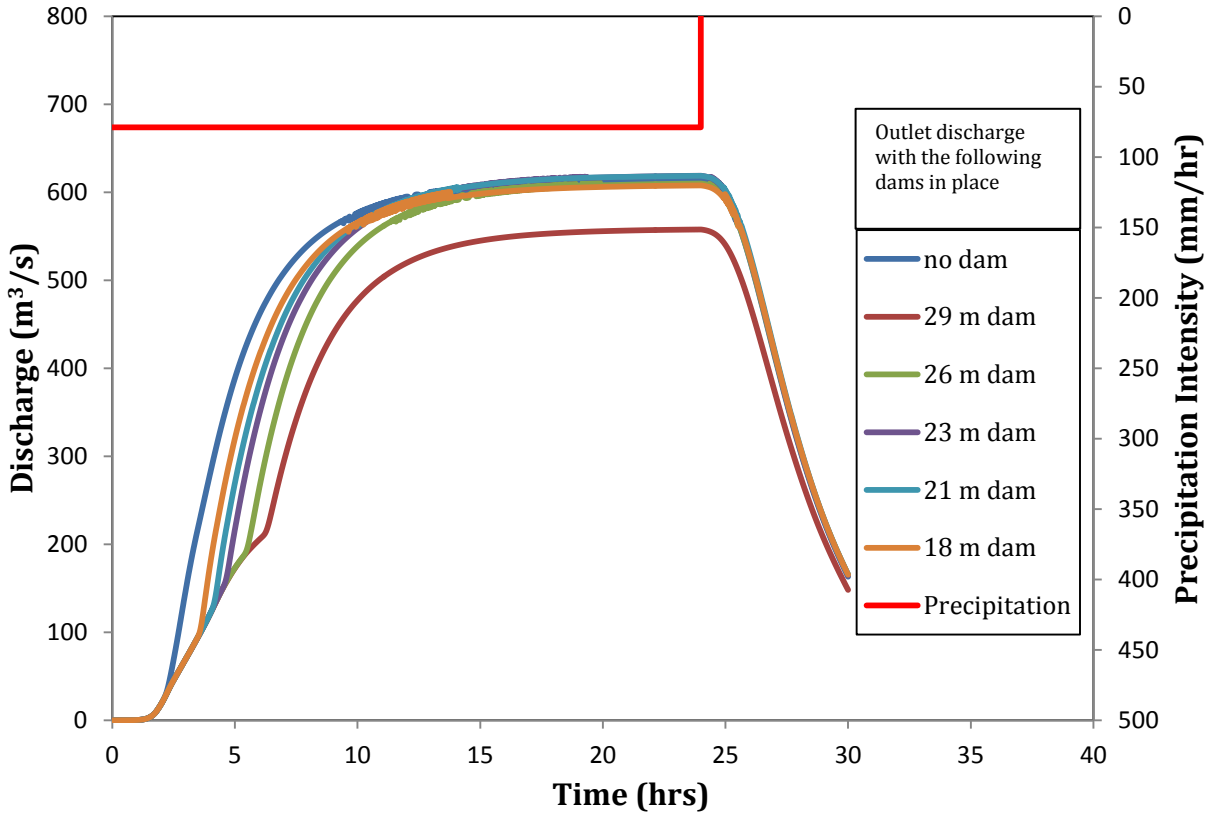

Figure 6.17: 24 hour duration GMP outlet discharge

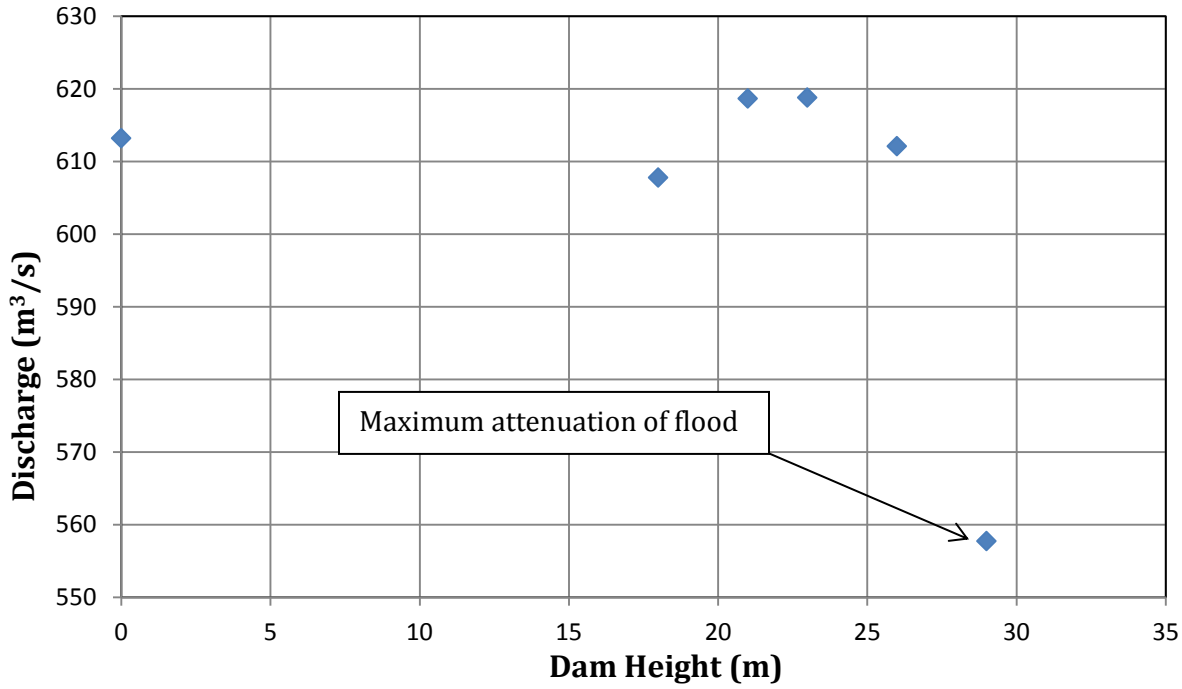

Figure 6.18: 24 hour duration GMP peak outlet discharge vs. dam height

Table 6.2: Summary of GMP simulation results

GMP Event Duration	Precipitation Intensity (mm/hr)	Peak Outlet Discharge Without Dam (m^3/s)	Height of Dam causing maximum attenuation of flood (m)	Peak Outlet Discharge With Dam (m^3/s)	Attenuation (%)
1 hour	203	279	23	115	59
6 hour	106	685	29	545	21
24 hour	79	613	29	557	9

Section 6.4 Discussion of Results

The estimated PMP and GMP events of duration 1, 6, and 24 hours were simulated in the California Gulch watershed. The precipitation was modeled as uniformly distributed over the watershed. The simulated hyetographs were rectangular. Simulations with these precipitation intensities were incorporated with artificial rectangular shaped dams inserted across the main stem channel in California Gulch. The height of these dams ranged from 5 meters to 29 meters as measured from the thalweg of the channel and the width of all of the dams was 30 meters. The created reservoirs were modeled as initially empty, and the initial soil moisture condition was modeled as dry (no recent precipitation). The process of filling the reservoir resulted in attenuation of the outlet hydrograph relative to the outlet hydrograph produced without an upstream reservoir. In some cases the dam was overtopped and a flood pulse was routed through the downstream flood plain to the outlet of the watershed.

The magnitude of the attenuation of the outlet discharge was quantified for each precipitation event and plotted. The results of these simulations, including the maximum attenuation of the outlet hydrographs, are summarized in Tables 6.1 and 6.2. These series of simulations demonstrate and confirm the ability of TREX to model the backwater effect

of dams within a watershed. A process was developed utilizing a GIS program for modifying The DEM of a watershed to represent simple dams across a channel within a watershed. This process can be transferred to other watersheds where dams are proposed or where changes in discharge due to an existing upstream dam are to be studied. This analytical technique will provide a process for estimating downstream flood wave attenuation which could be useful in the implementation of dams and channel conveyance structures downstream of dams.

Chapter VII. Conclusions

Section 7.1 Conclusions about TREX Overtopping Modeling and Flood Routing

Input point source hydrographs of peak discharge up to 50,000 m^3/s were stably routed through the California Gulch watershed showing that flows far surpassing realistic magnitudes can be simulated. Relationships were determined between simulated peak input discharges and stable time steps for Courant numbers between 0.2 and 1.0.

Stable time step and peak outlet discharge data were taken from several TREX rainfall-runoff simulations from other watersheds to compare with California Gulch data. The trend line determined for the multi-watershed rainfall-runoff data fit the data fairly well, implying that stable grid celerity as a function of flood discharge could be somewhat transferable between watersheds. Also this trend line was in relatively good agreement with the CFL trend line from the California Gulch point source simulations showing that point source flood routing can yield basic information about simulation time step stability that could be useful when applied to other types of flood simulations like rainfall-runoff.

The computer modeled routing of a hydrograph through a watershed can be a powerful tool for flood plain management and dam design. In many cases a two-dimensional model provides a more accurate simulation of the flood flow interaction with the flood plain than does a one-dimensional model. A watershed scale two-dimensional model such as TREX can be a very appropriate tool for routing known or modeled flood wave hydrographs through a watershed. The TREX model allows as input a specified hydrograph at a specified location within a watershed. Using this method within TREX to route a dam breach flood provides the benefits of two-dimensional flow inundation of the

floodplain. The distributed parameters within the model also allow for much detail in the characterization of the floodplain. Also, as large discharge event flow data is scarce, calibrating models for these types of events is difficult. A physically based model such as TREX that allows for high resolution detail of the input parameters could be a valid flow estimation tool for events occurring in areas with little or no flow data.

An example scenario was created to simulate the watershed scale effect of a dam breach through the use of the TREX model and empirical dam breach equations. This modeling technique utilizes existing dam failure data and the routing ability of the distributed parameter, two-dimensional TREX model to create simulations of the dam failure process at the watershed scale due to extreme precipitation events. This analysis technique could be useful in floodplain management and planning.

Areal flood mapping was done using TREX and the ESRI ARC suite of GIS tools to quantify the extent of floodplain inundation due to hypothetical flood conditions within the California Gulch watershed, and to exemplify enhanced visualization techniques of the flooding process. The areal distribution and timing of flood plain inundation due to the failure of a proposed or existing dam can be estimated and correlated to dam characteristics such as crest height or to precipitation intensity. Inversely, the crest height of a proposed dam which would be necessary to attenuate a flood wave to the point of not damaging existing infrastructure or buildings could be determined through this analysis technique.

The TREX watershed model successfully simulated large scale (PMP and GMP) precipitation events. The model also successfully simulated geometrically simple dams of a variety of sizes. The results of the simulated dam overtopping events were compiled to

quantify the effect that empty reservoirs can have on downstream discharge. The correlation between dam characteristics, such as crest height, and downstream discharge can be useful. This type of modeling could be quite beneficial as a first order estimation tool for the effectiveness of check dams in flood wave attenuation. If a downstream design maximum allowable discharge was known for a watershed, then the crest height of a dam at a selected location upstream which was necessary to attenuate a flood wave to the allowable discharge could be roughly determined. This analytical technique can be employed for a variety of precipitation events and could be used to correlate a new outlet discharge with storm return period. This technique could be used to help facilitate the processes of dam site location and building material estimation for a proposed dam. Inversely, downstream flooding effects due to the overtopping of an existing dam could be quantified.

References

Abdullah, J. (2013). "Distributed Runoff Simulation of Extreme Monsoon Rainstorms in Malaysia Using Trex." Ph.D dissertation, Colorado State University, Fort Collins, CO.

Altinakar, M. (2008). "Working Group on Dam Issues Related to Floodplain Management, Sub-group on Modeling Tools for Dam Break Analysis." Association of State Floodplain Managers.

Association of State Dam Safety Officials, "Dam Failures and Incidents." Causes of Dam, Failures: 1995 – 2001 <http://www.damsafety.org/news/?p=412f29c8-3fd8-4529-b5c9-8d47364c1f3e> (Nov. 16, 2013).

Bicknell, B.R., Imhoff, J.C., Kittle, J.L. Jr., Donigian, A.S. Jr. and Johanson, R.C. (1997). "Hydrological Simulation Program—Fortran", User's manual for version 11. EPA/600/R-97/ 080. U.S. Environmental Protection Agency (EPA), National Exposure Research Laboratory, Athens, GA.

Brunner, G. W. (2010). "HEC-RAS River Analysis System, Hydraulic Reference Manual, Version 4.1." United States Army Corps of Engineers (USACE), Hydrologic Engineering Center (HEC), Davis, CA.

Crawford, N.H. and Linsley, R. K. (1966). "Digital simulation in hydrology; Stanford Watershed Model IV." Technical Report No. 39, Department of Civil Engineering, Stanford University, Stanford, CA.

DHI. (2005). "MIKE SHE Technical Reference, Version 2005." DHI Water and Environment, Danish Hydraulic Institute, Denmark.

Ewen, J., Parkin, G., and O'Connell, P.E. (2000). "SHETRAN: distributed river basin flow and transport modeling system." *J. of Hydr. Eng.*, 5(3), 250-258.

Feldman, A. D. (2010). "HEC-HMS Hydrologic Modeling System, Technical Reference Manual." USACE, HEC, Davis, CA.

Fread, D. L. and Lewis, J. M. (1998). "NWS FLDWAV Model: Theoretical Description and User Documentation." United Stated Department of Commerce, NWS, NOAA, Silver Springs, Maryland.

Fread, D.L. (1984). "DAMBRK: The NWS Dam-Break Flood Forecasting Model." NWS, NOAA, Silver Springs, MD.

Fread, D.L. (1988), "BREACH: An erosion model for earthen dam failures." NWS, NOAA, Silver Springs, Maryland.

Fread, D.L. (1993), "NWS FLDWAV Model: The Replacement of DAMBRK for Dam-Break Flood Prediction", *Dam Safety '93, Proc. of the 10th Annual ASDSO Conference*, Kansas City, MO, 177-184.

Froehlich, D.C. (1995) "Embankment dam breach parameters revisited." *Proc.of the 1995 ASCE Conf. on Water Resour. Eng.,* San Antonio, TX., 887-891.

Froehlich, D.C. (1995). "Peak Outflow from Breached Embankment Dam." *J. of Water Resour. Planning and Management*, 121(1), 90-97.

Hydrometeorological Report No. 55A, "Probable Maximum Precipitation Estimates - United States Between the Continental Divide and the 103rd Meridian" *Current NWS Probable Maximum Precipitation (PMP) Documents and Related Studies*, <http://www.nws.noaa.gov/oh/hdsc/studies/PMP.html> (Oct. 01 2012).

Jennings, A. H. (1950). "World's greatest observed point rainfalls." *Mon. Wea. Rev.*, 78, 4–5.

Julien, P.Y. (2010). Erosion and Sedimentation. Cambridge University Press, Cambridge, UK.

Julien, P.Y. (2002). River Mechanics. Cambridge University Press, Cambridge, UK.

Julien, P. Y., Saghafian, B. and Ogden, F. L. (1995). "Raster-Based Hydrologic Modeling of Spatially-Varied Surface Runoff." *Water Resour. Bull*., 31(3), 523-536.

Kim, J. (2012). "Hazard Area Mapping During Extreme Rainstorms in South Korean Mountains." Ph.D dissertation, Colorado State University, Fort Collins, CO.

Neitsch, S.L., J.G. Arnold, J.R. Kiniry, R. Srinivasan, and J.R. Williams, (2002). "Soil and Water Assessment Tool – User's Manual – Version 2000." Grassland, Soil and Water Research Laboratory, Agricultural Research Service and Blackland Research Center, Texas Agricultural Experiment Station, Temple, TX.

O'Brien, J. D. (2006) "FLO-2D user's manual, Version 2006.01." FLO Engineering, Nutrioso, AZ.

Pierce, M.W., Thornton, C.I., and Abt, S.R. (2010). "Predicting peak outflow from breached embankment dams." *J. Hydrol. Eng*., 15(5), 338-349.

Schär, Christoph. "The Courant-Friedrichs-Levy (CFL) Stability Criterion." Institut für Atmosphäre und Klima, ETH Zürich, <http://www.iac.ethz.ch/edu/courses/bachelor/vertiefung/numerical_methods_in_environmental_physics/Fol_Ch3_CFL-Criterion.pdf> (Jan. 30, 2014)

Singh, V. P. and Woolhiser, M. (2002). "Mathematical Modeling of Watershed Hydrology." *J. of Hydrologic Eng.*, 7(4), 270-292.

Smith, M. B., Seo, D., Koren, V. I., Reed, S. M., Zhang, Z., Duan, Q., Moreda, F., and Cong, S. (2004). "The distributed model intercomparison project (DMIP): motivation and experiment design." *J. of Hydrol*., 298, 4–26.

Thornton, C. I., Pierce, M. W. and Abt, S. R. (2011). "Enhanced Predictions for Peak Outflow from Breached Embankment Dams." *J. of Hydrol*., 16(1), 81-88.

Velleux, M. L. (2005). "Spatially Distributed Model to Assess Watershed Contaminant Transport and Fate." Ph.D dissertation, Colorado State University, Fort Collins, CO.

Velleux, M. L., England, J. F. Jr. and Julien, P. Y. (2011). "TREX Watershed Modeling Framework User's Manual: Model Theory and Description." HDR-HyroQual, Inc., Mahwah, NJ.

Velleux, M., Takamatsu, M., and Yang, L. (2010). "Literature Review: Comparison of Common Watershed Models for Rainfall, Runoff Sediment Transport, and Contaminant Transport and Fate." HydroQual, Inc., Mahwah, NJ.

Wahl, T. L. (1998). "Dam Safety Research Report: Prediction of Embankment Dam Breach Parameters, A Literature Review and Needs Assessment." U. S. Department of the Interior Bureau of Reclamation Dam Safety Office, Denver, CO.

Wahl, T. L. (2010). "Dam Breach Modeling – An Overview of Analysis Methods." *Joint Federal Interagency Conference on Sedimentation and Hydraulic Modeling*, Las Vegas, NV

Walder, J. S. and O'Connor, J. E. (1997). "Methods for predicting peak discharge of floods caused by failure of natural and constructed earthen dams." *Water Resour. Res.,* 33(10), 2337-2348.

Woolhiser, D.A., Smith, R.E. and Goodrich, D.C. (1990). "KINEROS, A kinematic runoff and erosion model: Documentation and User Manual." United States Department of Agriculture, Agricultural Research Service, ARS-77.

Appendices

Appendix 1.0 Probable Maximum Precipitation Maps

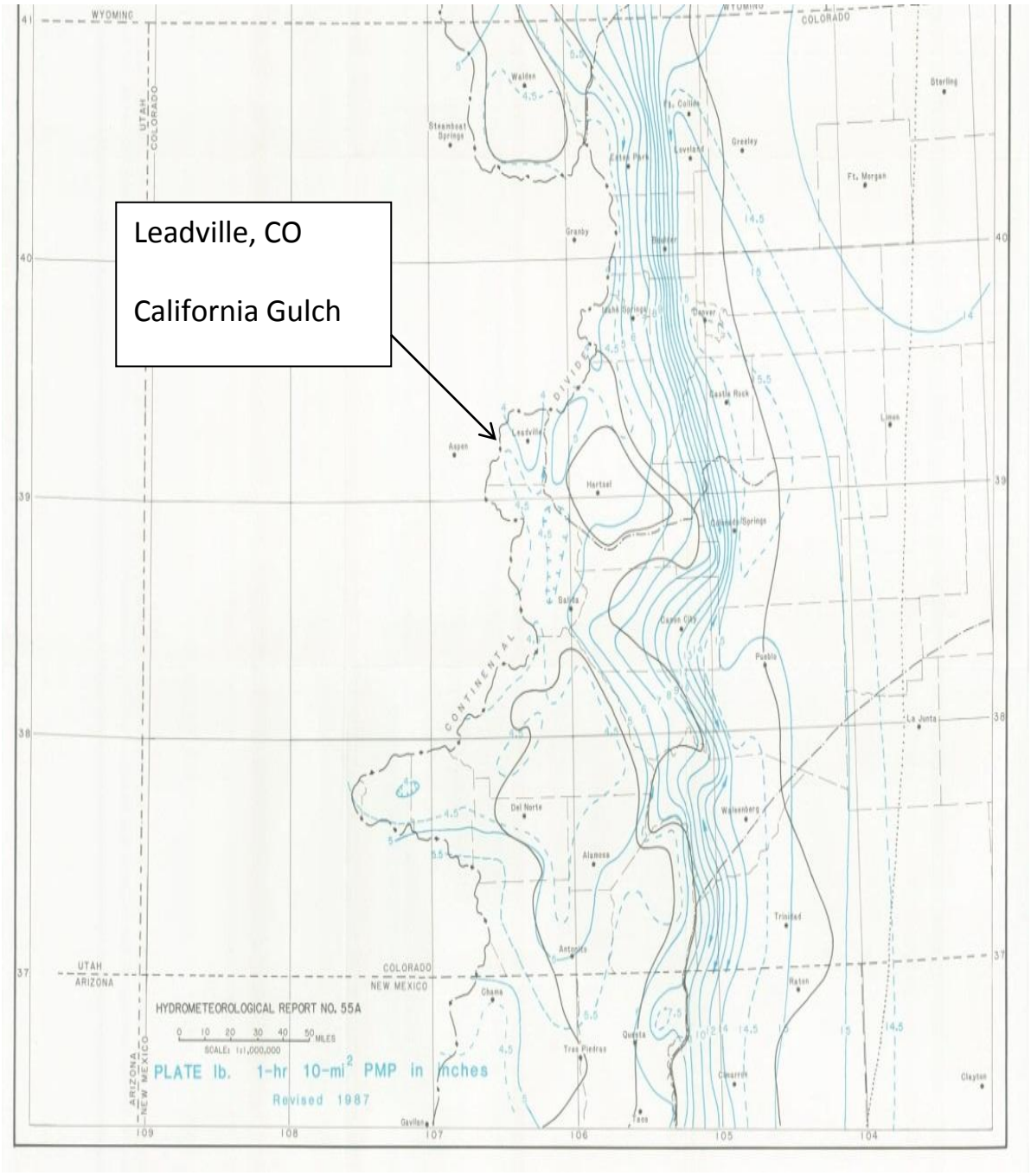

Figure A1.1: 1 hour duration PMP map for California Gulch (http://www.nws.noaa.gov/oh/hdsc/PMP_documents/HMR55A_Plates_I_III.pdf)

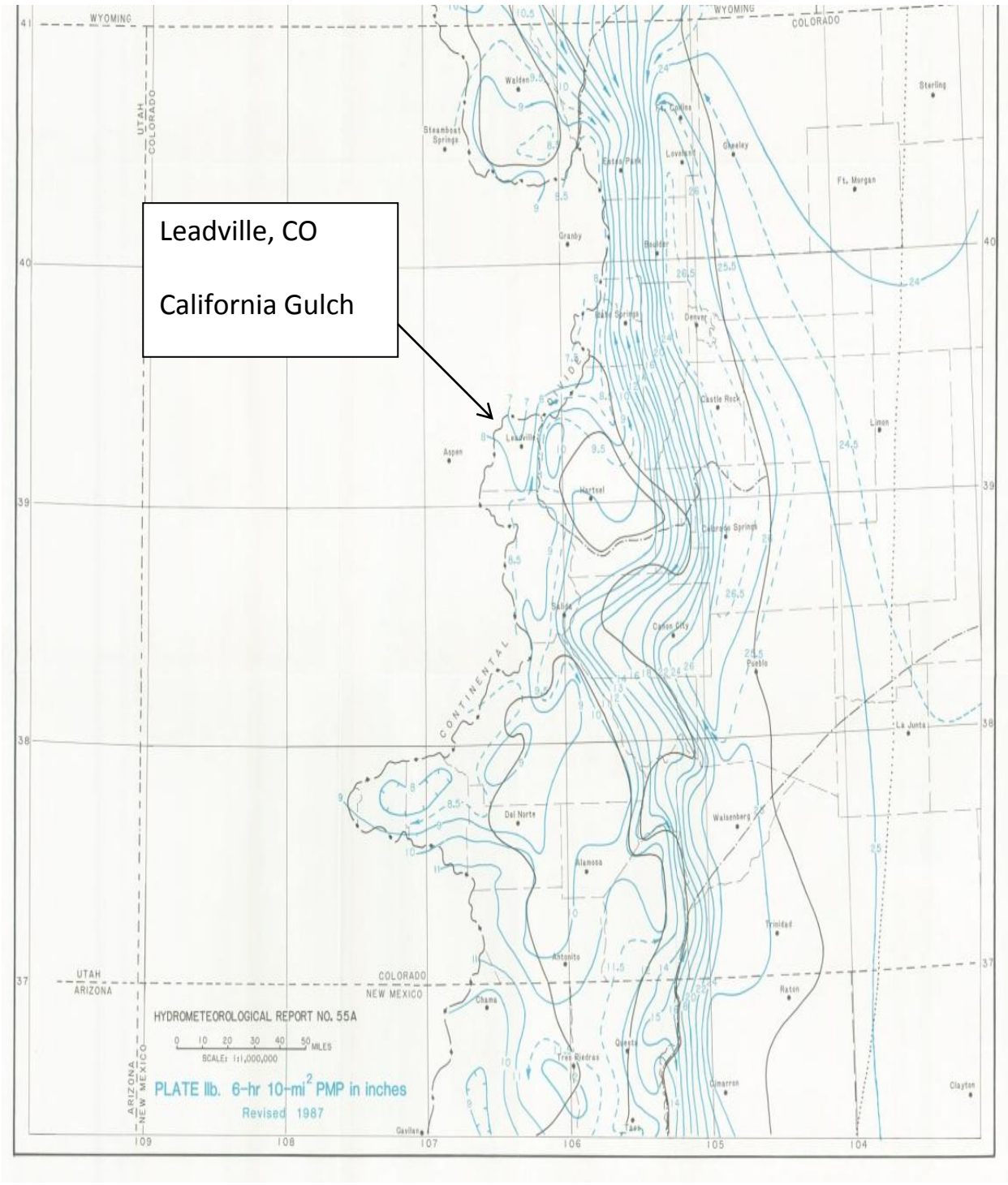

Figure A1.2: 6 hour duration PMP map for California Gulch (http://www.nws.noaa.gov/oh/hdsc/PMP_documents/HMR55A_Plates_I_III.pdf)

Figure A1.3: 24 hour duration PMP map for California Gulch (http://www.nws.noaa.gov/oh/hdsc/PMP_documents/HMR55A_Plates_I_III.pdf)

Appendix 2.0 Comparison of Popular Hydrologic Models

Table A2.1: Hydrologic model inter-comparison (Singh et al. 2002)

Model name/acronym	Author(s) (year)	Remarks
Stanford watershed Model (SWM)/Hydrologic Simulation Package-Fortran IV (HSPF)	Crawford and Linsley (1966), Bicknell et al. (1993)	Continuous, dynamic event or steady-state simulator of hydrologic and hydraulic and water quality processes
Catchment Model (CM)	Dawdy and O'Donnell (1965)	Lumped, event-based runoff model
Tennessee Valley Authority (TVA) Model	Tenn. Valley Authority (1972)	Lumped, event-based runoff model
U.S. Department of Agriculture Hydrograph Laboratory (USDAHL) Model	Holtan and Lopez (1971), Holtan et al. (1974)	Event-based, process-oriented, lumped hydrograph model
U.S. Geological Survey (USGS) Model	Dawdy et al. (1970, 1978)	Process-oriented, continuous/event-based runoff model
Utah State University (USU) Model	Andrews et al. (1978)	Process-oriented, event/continuous streamflow model
Purdue Model	Huggins and Monke (1970)	Process-oriented, physically based, event runoff model
Antecedent Precipitation Index (API) Model	Sittner et al. (1969)	Lumped, river flow forecast model
Hydrologic Engineering Center—Hydrologic Modeling System (HEC-HMS)	Feldman (1981), HEC (1981, 2000)	Physically-based, semidistributed, event-based, runoff model
Streamflow Synthesis and Reservoir regulation (SSARR) Model	Rockwood (1982), U.S. Army Corps of Engineers (1987), Speers (1995)	Lumped, continuous streamflow simulation model
National Weather service-River Forecast System (NWS-RFS)	Burnash et al. (1973a,b), Burnash (1975)	Lumped, continuous river forecast system
University of British Columbia (UBC) Model	Quick and Pipes (1977), Quick (1195)	Process-oriented, lumped parameter, continuous simulation model
Tank Model	Sugawara et al. (1974), Sugawara (1995)	Process-oriented, semidistributed or lumped continuous simulation model
Runoff Routing Model (RORB)	Laurenson (1964), Laurenson and Mein (1993, 1995)	Lumped, event-based runoff simulation model
Agricultural Runoff Model (ARM)	Donigian et al. (1977)	Process-oriented, lumped runoff simulation model
Storm Water Management Model (SWMM)	Metcalf and Eddy et al. (1971), Huber and Dickinson (1988), Huber (1995)	Process-oriented, semidistributed, continuous stormflow model
Xinanjiang Model	Zhao et al. (1980), Zhao and Liu (1195)	Process-oriented, lumped, continuous simulation model
Hydrological Simulation (HBV) Model	Bergstrom (1976, 1992, 1995)	Process-oriented, lumped, continuous streamflow simulation model
Great Lakes Environmental Research Laboratory (GLERL) Model	Croley (1982, 1983)	Physically based, semidistributed continuous simulation model
Pennsylvania State University—Urban Runoff Model (PSU-URM)	Aron and Lakatos (1980)	Lumped, event-based urban runoff model
Chemicals, Runoff, and Erosion from Agricultural Management Systems (CREAMS)	USDA (1980)	Process-oriented, lumped parameter, agricultural runoff and water quality model
Areal Non-point Source Watershed Environment Response Simulation (ANSWERS)	Beasley et al. (1977), Bouraoui et al. (2002)	Event-based or continuous, lumped parameter runoff and sediment yield simulation model
Erosion Productivity Impact Calculator (EPIC) Model	Williams et al. (1984), Williams (1995a,b)	Process-oriented, lumped-parameter, continuous water quantity and quality simulation model
Simulator for Water Resources in Rural Basins (SWRRB)	Williams et al. (1985), Williams (1995a,b)	Process-oriented, semidistributed, runoff and sediment yield simulation model
Simulation of Production and Utilization of Rangelands (SPUR)	Wight and Skiles (1987), Carlson and Thurow (1992), Carlson et al. (1995)	Physically based, lumped parameter ecosystem simulation model
National Hydrology Research Institute (NHRI) Model	Vandenberg (1989)	Physically based, lumped parameter, continuous hydrologic simulation model
Technical Report-20 (TR-20) Model	Soil Conservation Service (1965)	Lumped parameter, event based runoff simulation model

Table A2.2: Hydrologic model inter-comparison continued (Singh et al. 2002)

Model name/acronym	Author(s) (year)	Remarks
Systeme Hydrologique Europeen/Systeme Hydrologique European Sediment (SHE/SHESED)	Abbott et al. (1986a,b), Bathurst et al. (1995)	Physically based, distributed, continuous streamflow and sediment simulation
Institute of Hydrology Distributed Model (IHDM)	Beven et al. (1987), Calver and Wood (1995)	Physically based, distributed, continuous rainfall-runoff modeling system
Physically Based Runoff Production Model (TOPMODEL)	Beven and Kirkby (1976, 1979), Beven (1995)	Physically based, distributed, continuous hydrologic simulation model
Agricultural Non-Point Source Model (AGNPS)	Young et al. (1989, 1995)	Distributed parameter, event-based, water quantity and quality simulation model
Kinematic Runoff and Erosion Model (KINEROS)	Woolhiser et al. (1990), Smith et al. (1995)	Physically based, semidistributed, event-based, runoff and water quality simulation model
Groundwater Loading Effects of Agricultural Management Systems (GLEAMS)	Knisel et al. (1993), Knisel and Williams (1995)	Process-oriented, lumped parameter, event-based water quantity and quality simulation model
Generalized River Modeling Package—Systeme Hydroloque Europeen (MIKE-SHE)	Refsgaard and Storm (1195)	Physically based, distributed, continuous hydrologic and hydraulic simulation model
Simple Lumped Reservoir Parametric (SLURP) Model	Kite (1995)	Process-oriented, distributed, continuous simulation model
Snowmelt Runoff Model (SRM)	Rango (1995)	Lumped, continuous snowmelt-runoff simulation model
THALES	Grayson et al. (1195)	Process-oriented, distributed-parameter, terrain analysis-based, event-based runoff simulation model
Constrained Linear Simulation (CLS)	Natale and Todini (1976a,b, 1977)	Lumped parameter, event-based or continuous runoff simulation model
ARNO (Arno River) Model	Todini (1988a,b, 1996)	Semidistributed, continuous rainfall-runoff simulation model
Waterloo Flood System (WATFLOOD)	Kouwen et al. (1993), Kouwen (2000)	Process-oriented, semidistributed continuous flow simulation model
Topgraphic Kinematic Approximation and Integration (TOPIKAPI) Model	Todini (1995)	Distributed, physically based, continuous rainfall-runoff simulation model
Hydrological (CEQUEAU) Model	Morin et al. (1995, 1998)	Distributed, process-oriented, continuous runoff simulation model
Large Scale Catchment Model (LASCAM)	Sivapalan et al. (1996a,b,c)	Conceptual, semidistributed, large scale, continuous, runoff and water quality simulation model
Mathematical Model of Rainfall-Runoff Transformation System (WISTOO)	Ozga-Zielinska and Brzezinski (1994)	Process-oriented, semidistributed, event-based or continuous simulation model
Rainfall-Runoff (R-R) Model	Kokkonen et al. (1999)	Semidistributed, process-oriented, continuous streamflow simulation model
Soil-Vegetation-Atmosphere Transfer (SVAT) Model	Ma et al. (1999), Ma and Cheng (1998)	Macroscale, lumped parameter, streamflow simulation system
Hydrologic Model System (HMS)	Yu (1996), Yu and Schwartz (1998), Yu et al. (1999)	Physically based, distributed-parameter, continuous hydrologic simulation system
Hydrological Modeling System (ARC/EGMO)	Becker and Pfutzner (1987), Lahmer et al. (1999)	Process-oriented, distributed, continuous simulation system
Macroscale Hydrolgical Model-Land Surface Scheme (MODCOU-ISBA)	Ledoux et al. (1989), Noilhan and Mahfouf (1996)	Macroscale, physically based, distributed, continuous simulation model
Regional-Scale Hydroclimatic Model (RSHM)	Kavas et al. (1998)	Process-oriented, regional scale, continuous hydrologic simulation model
Global Hydrology Model (GHM)	Anderson and Kavvas (2002)	Process-oriented, semidistributed, large scale hydrologic simulation model
Distributed Hydrology Soil Vegetation Model (DHSVM)	Wigmosta et al. (1994)	Distributed, physically based, continuous hydrologic simulation model
Systeme Hydrologique Europeen Transport (SHETRAN)	Ewen et al. (2000)	Physically based, distributed, water quantity and quality simulation model
Cascade two dimensional Model (CASC2D)	Julien and Saghafian (1991), Ogden (1998)	Physically based, distributed, event-based runoff simulation model
Dynamic Watershed Simulation Model (DWSM)	Borah and Bera (2000), Borah et al. (1999)	Process-oriented, event-based, runoff and water quality simulation model
Surface Runoff, Infiltration, River Discharge and Groundwater Flow (SIRG)	Yoo (2002)	Physically based, lumped parameter, event-based streamflow simulation model

Table A2.3: Hydrologic model inter-comparison continued (Singh et al. 2002)

Model name/acronym	Author(s) (year)	Remarks
Modular Kinematic Model for Runoff Simulation (Modular System)	Stephenson (1989) Stephenson and Randell (1999)	Physically based, lumped parameter, event-based runoff simulation model
Watershed Bounded Network Model (WBNM)	Boyd et al. (1979, 1996), Rigby et al. (1991)	Geomorphology-based, lumped parameter, event-based flood simulation model
Geomorphology-Based Hydrology Simulation Model (GBHM)	Yang et al. (1998)	Physically based, distributed, continuous hydrologic simulation model
Predicting Arable Resource Capture in Hostile Environments-The Harvesting of Incident Rainfall in Semi-arid Tropics (PARCHED-THIRST)	Young and Gowing (1996) Wyseure et al. (2002)	Process-oriented, lumped parameter, event-based agro-hydrologic model
Daily Conceptual Rainfall-Runoff Model (HYDROLOG)-Monash Model	Potter and McMahon (1976), Chiew and McMahon (1994)	Lumped, conceptual rainfall-runoff model
Simplified Hydrology Model (SIMHYD)	Chiew et al. (2002)	Conceptual, daily, lumped parameter rainfall-runoff model
Two Parameter Monthly Water Balance Model (TPMWBM)	Guo and Wang (1994)	Process-oriented, lumped parameter, monthly runoff simulation model
The Water and Snow Balance Modeling System (WASMOD)	Xu (1999)	Conceptual, lumped, continuous hydrologic model
Integrated Hydrometeorological Forecasting System (IHFS)	Georgakakos et al. (1999)	Process-oriented, distributed, rainfall and flow forecasting system
Stochastic Event Flood Model (SEFM)	Scaefer and Barker (1999)	Process-oriented, physically based event-based, flood simulation model
Distributed Hydrological Model (HYDROTEL)	Fortin et al. (2001a,b)	Physically based, distributed, continuous hydrologic simulation model
Agricultural Transport Model (ACTMO)	Frere et al. (1975)	Lumped, conceptual, event-based runoff and water quality simulation model
Soil Water Assessment Tool (SWAT)	Arnold et al. (1998)	Distributed, conceptual, continuous simulation model